University of Pisa

BIOS – Research Doctorate School in BIOmolecular Sciences

Course in Biomaterials, XX cycle

Purpose tailoring of bioactive-biocompatible polymers as soluble drug carriers and hydrogels for drug delivery systems

PhD thesis of

Marco Alessandro SUARDI

Tutor: prof. Elisabetta Ranucci.

Co-Tutor: prof. Paolo Ferruti

TABLE OF CONTENT

CHAPTER 1

Introduction:

the concept of polymer therapeutics.

1.1 HISTORICAL PERSPECTIVE

The use of polymers in medicine is not new. Natural polymers have been used as components of herbal remedies for several millennia. The notion of synthetic, water-soluble polymers as macromolecular drugs or components of injectable drug delivery systems has, in contrast, a relatively short history - not surprising given the relative youthfulness of polymer science itself. In fact polymer science was borne only in the 1920s- less than a hundred years ago, thanks to Hermann Staudinger and his contemporaries. Moreover, it wasn't until 1953 that Staudinger was honoured with the first "polymer" Nobel Prize "for his discoveries in the field of macromolecular chemistry". Coincidentally, this is the same year that Watson and Crick published their Nature articles on the structure of DNA (Watson, Crick, 1953). Around this time we saw the beginning of water soluble synthetic polymers as healthcare aids for parenteral administration. During the Second World War synthetic polymeric plasma expanders were widely adopted (e.g.

poly(vinylpyrolidone)) and after few time the first polymer-drug conjugates appeared (e.g. mescaline-N-vinylpyrolidine conjugates with drug attached via non-degradable or enzymatically degradable (gly-leu) side chains (Jatzkewitz, 1955). Biologically active polymeric drugs also started to gain popularity, and divinylether-maleic anhydride copolymer (pyran copolymer) was tested clinically as an anticancer agent in the 1960s. From that moment on, a wide range of polymers - modified polysaccharides, synthetic polypeptides and synthetic polymers - have been successfully transferred into the market as polymeric drugs, giving rise in 1970s to more clearly defined chemical and biological rationale for the design of polymeric drugs, polymer-protein conjugates (Davis, 2002) and polymer-drug conjugates (Ringsdorf, 1975), the so called “polymer therapeutics” family, which will be treated more extensively below.

1.2 CURRENT STATUS

The first poly(ethyleneglycol) (PEG)ylated proteins were approved by regulatory authorities for routine clinical use in the early 1990s: PEG-adenosine deaminase used to treat acute immunodeficiency syndrome and PEG-L-asparaginase to treat acute lymphoblastic leukaemia. At the same time in Japan, a stryene-co-maleic anhydride conjugate of the anticancer protein neocarzinstatin called SMANCS, developed by Maeda and colleagues, was successfully used as a treatment of patients with primary liver cancer (a very difficult disease to treat) and this led to market approval for the treatment of this disease. During his research, Maeda also discovered the passive tumour-targeting phenomenon called the "enhanced permeability and retention effect" (EPR effect). This phenomenon is attributed to two factors: the disorganised pathology of angiogenic tumour vasculature with its discontinuous endothelium leading to hyperpermeability towards circulating macromolecules, and the lack of effective tumour lymphatic drainage, which leads to subsequent macromolecular accumulation. It is now well established that long circulating macromolecules including polymer conjugates, and even polymer-coated liposomes, accumulate

passively in solid tumour tissue by the EPR effect after intravenous administration and can increase tumour concentration many fold (Matsumura et al., 1986; Maeda et al., 2000).

In recent years a wide number of synthetic polymers have been produced for therapeutic aims, including synthetic random copolymer of L-alanine, L-lysine, L-glutamic acid and L-tyrosine (M, = 5000- 11000 g/mol) given subcutaneously to treat multiple sclerosis patients (Teitlebaum et al., 1997) and also those poly(allylamine)s developed clinically as polymeric sequestrants for oral administration to hypercholesterolemic patients (Mandeville et al., 1997). The first synthetic polymer anticancer drug conjugate entered clinical trials in 1994. This was an N-(2-hydroxypropyl)methacrylamide (HPMA) copolymer conjugate of doxorubicin (Duncan, 2003). Since then, five more HPMA copolymer conjugates have progressed into the clinic, and the first conjugate bearing antiangiogenic therapy is now being tested in vivo Anticancer conjugates based on other polymeric carriers including poly(glutamic acid), PEG and polysaccharides are also now in clinical trials.

With growing appreciation of the molecular basis of disease in the late 1980s, the hope of "gene therapy" began to gain momentum. While the viral vectors are still preferred for gene delivery, there has been a continuing hope that polymeric non-viral vectors can become a feasible alternative - i.e. biomimetics delivering DNA safely without the threat of toxicity. Early research used simple polycationic vectors such as poly(L-lysine) and poly(ethyleneimine). Since then a wide variety of complex multicomponent, polymer-based vectors have been designed as gene delivery systems (Pack, 2005). With still some distance to the first polymeric viral vectors as marketed products, there is still much to do.

1.3 THE AIM OF THE PHD WORK

The term "polymer therapeutics" has been adopted to encompass several families of constructs all using water-soluble polymers as components for design polymeric drugs, polymer-drug conjugates,

polymer-protein conjugates, polymeric micelles to which a drug is covalently bound, and those multi-component polyplexes being developed as non-viral vectors.

The main object of this PhD work has been the synthesis, characterization and in some extent application of poly(amidoamine) (PAA) derivatives that can be considered belonging to the polymer therapeutics family. In particular three groups of PAAs have been studied:

- a family of polymeric precursors designed for obtaining polymer conjugates with sulfhydryl containing molecules, both drugs and/or proteins, that will be treated in Chapter 4;
- a family of amphiphilic polymers, composed by hydrophilic PAA backbone with cholesterol pendants, designed to self assemble in water media in nanoparticles capable to transport lipophilic drugs, that will be treated in Chapter 5;
- a special PEG-PAA cationic block co-polymer containing reversibly cross-linkable functions, capable to form polyplexes with "environment sensitive" stability; this work treated in Chapter 6.

Beside this three main objects, a preliminary work concerning kinetic study of Michael polyaddition reaction in organic solvents is presented in Chapter 3, while in Chapter 7 a study concerning liposomes and lipids bilayer deposition on purposely fuctionalized glass surfaces is reported. General features concerning introduced topics will be treated below.

1.3.1 Polymer-drug and polymer-protein conjugates

In the early '70, Ringsdorf identified a model for polymer-drug conjugates (Figure 1.1) that represent still nowadays the starting point for developing a polymeric adducts. In the Ringsdorf's model, a number of drug molecules are bound to a macromolecule through a spacer molecule,

which can incorporate a predetermined breaking point to ensure release of the drug at the site of interest. The polymer conjugate can additionally contain moieties, for example, antibodies or sugar moieties, which target disease related antigens or receptors. In addition, solubilizing groups can be attached to the polymer backbone to modify the bioavailability of the drug–polymer conjugate.

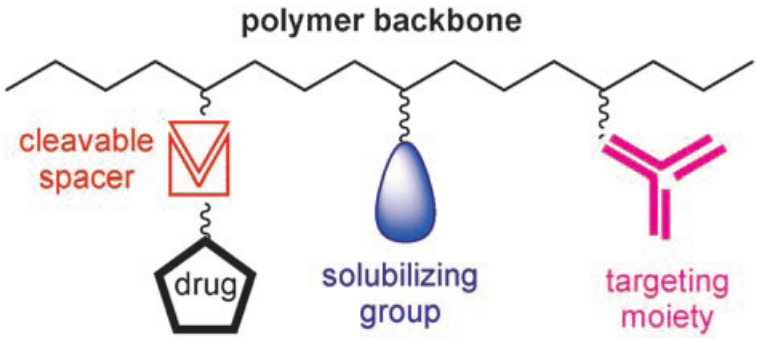

Figure 1.1. Ringsdorf's model for drug-delivery systems based on synthetic polymers.

Macromolecules chosen for the preparation of drug– polymer conjugates should ideally be water-soluble, nontoxic, and nonimmunogenic, as well as degraded and/or eliminated from the organism. Finally, the macromolecular carrier should exhibit suitable functional groups for attaching the respective drug or spacer.

There is a large number of advantages that can be achieved through a polymer conjugation. Some examples worth to be mentioned are:

- stabilization of labile active molecules from chemical and biological degradation
- protection from proteolytic degradation
- reduction of immunogenicity
- decreased antibody recognition
- increased plasma half life
- modification of organ disposition

- drug penetration into selected cell compartments through endocytosis
- enhanced possibilities of drug targeting

Cancer therapy represent one of the fields in which polymer-drug conjugation could bring major advantages. In fact, the possibility to exploit EPR effect constitute another important improvement, since consequent passive tumour targeting lead to enhanced efficacy of drugs with reduced side effects. Several drug–polymer conjugates are being investigated in phase I–III studies at present.

Another important field of research regards polymer-protein conjugation. Therapeutically relevant proteins such as antibodies, cytokines, growth factors, and enzymes are playing an increasing role in the treatment of viral, malignant, and autoimmune diseases. The development and successful application of therapeutic proteins, however, is often impeded by several difficulties, for example, insufficient stability and shelf-life, costly production, immunogenic and allergic potential, as well as poor bioavailability and sensitivity towards proteases. Consequently, frequent administration at an excessively high dose is required to reveal their therapeutic effects in vivo. As a result, homeostasis is destroyed, and unexpected side effects occur. Therefore, there has been a continuing search for improved alternatives. Bioconjugation with water-soluble polymers improves the plasma clearance and body distribution, resulting in increased therapeutic effects and decreased side effects.

As previously discussed, starting from the 1970s several conjugates of polyethylene glycol (PEG) to proteins have been produced. This technique is now well established and is called PEGylation PEGylation increases protein solubility and stability, and hence prolongs plasma half-life, and can reduce protein immunogenicity Although there are other available polymers for protein conjugation such as HPMA copolymers, poly(ethyleneimine) (PEI), linear polyamidoamines, polyvinylpyrrolidone (PVP), polyacrylamide (PAAm), polydimethylacrylamide (PDAAm),

polyvinyl alcohol (PVA), chitosan, dextrin and dextran, PEG is still the most popular option since the clinical value of PEGylation is now well established.

1.3.2 Polymeric micelles

The development of drug nanocarriers for poorly soluble pharmaceuticals is an important task, particularly because large proportions of new drug candidates emerging from highthroughput drug screening initiatives are water-insoluble, but there are some unresolved issues. The therapeutic application of hydrophobic, poorly water-soluble agents is associated with some serious problems, since low watersolubility results in poor absorption and low bioavailability. sometimes associated with complications as embolism and local toxicity. On the other hand, the hydrophobicity and low solubility in water appear to be intrinsic properties of many drugs, since it helps a drug molecule to penetrate a cell membrane and reach important intracellular targets.

To overcome the poor solubility of certain drugs, the use of various micelle forming surfactants in formulations of insoluble drugs is suggested. This is why micelles and nanoparticles, including polymeric ones, represent a promising type of pharmaceutical carriers. Micelles and nanoparticles form colloidal dispersions with a particle size between 5 and 1000 nm. These nanostructure are designed to increase the solubility and bioavailability of poorly soluble pharmaceuticals, therefore they are often composed by special amphiphilic molecules as building blocks.

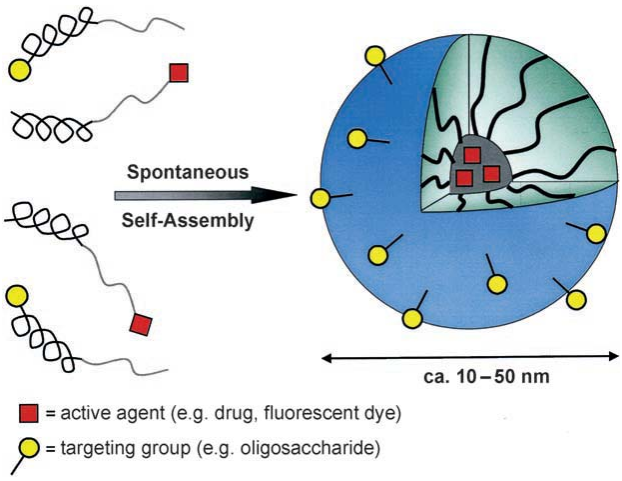

Figure 1.2. Formation and architecture of block-copolymer micelles which spontaneously form by self-assembly in water. The characteristic features are a pronounced core–shell architecture which can be controlled by the individual polymer blocks. Typical examples of block copolymers are PEO-b-PPO, PEO-b-PCl, and PEO-b-PAsp.

Because of their small size (5-100 nm), micelles demonstrate spontaneous penetration into the interstitium in the body compartments with leaky vasculature (tumors and infarcts) by the EPR effect. Specific ligands (eg, antibodies and/or certain sugar moieties) can be attached to the waterexposed termini of hydrophilic blocks. By virtue of their small size and by functionalizing their surface with synthetic polymers and appropriate ligands, nanoparticulate carriers can be targeted to specific cells and locations within the body after intravenous or subcutaneous injection. Such approaches may enhance detection sensitivity in medical imaging, improve therapeutic effectiveness, and decrease side effects. Some of the carriers can be engineered in such a way that they can be activated by changes in the environmental pH, by chemical stimuli, by the application of a rapidly oscillating magnetic field, or by application of an external heat source.

1.3.3 Polyplexes

Viral vectors, bionanoparticles with diameters of 100 nm or less, have long been proven to be the most efficient and stable transgene vectors into the cell and thus are suitable for vaccine and gene

therapy Viruses are able to use the host cell machinery for protein synthesis, and some of them are able to stably insert into the host cell genome and provide a long-term transgene expression in transduced cells. Thus, viral gene carriers possess higher gene transfection efficiency than non viral vectors However, despite some successes in clinic trials, viral vector gene transfer still has some safety issues. The immune response caused by the expression of viral proteins has to be overcome.

For these reasons the use of polymers as synthetic non-viral carriers for introducing nucleic acids into cells appears very appealing. Several diseases could be potentially cured by means of gene therapy, i.e. cancer, Alzheimer disease, arthritis reumatoide and other auto-immune diseases, genetic diseases and syndromes. Moreover gene therapy seems to be very promising to improve in vivo tissue engineering.

Polymers can be generated in large quantities in chemically defined, non-antigenic and non-immunogenic form. A plethora of different chemical structures and polymer sizes may be applied to tailor-made polymers with optimized characteristics for the extracellular delivery of nucleic acid to the target tissue and the subsequent intracellular delivery into the target cells. For the purpose of nucleic acid transfer, polymers have been applied for incorporating nucleic acids into nanoparticles or microspheres. Alternatively, cationic polymers are applied as carriers for complexing gene vectors into polyplexes. Polyplexes form spontaneously upon mixing negatively charged nucleic acid with the polycationic polymer due to electrostatic interaction. This process can be controlled to result in the formation of particles with defined virus-like sizes which efficiently transfect cell cultures and also have shown encouraging gene transfer potential in vivo administration.

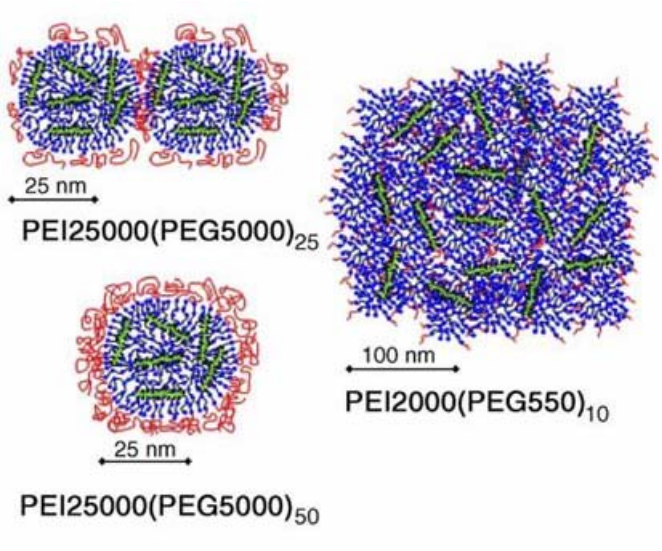

Figure 1.3. three dimensional model of PEI-PEG polyplexes

With first-generation polymeric carriers, gene therapeutic effects have been demonstrated in animals, although modest efficiencies and significant toxicity restrict broader therapeutic application. Key issues for future optimization of polyplexes include improved specificity for the target tissue, enhanced intracellular uptake, and reduced toxicity and immunogenicity. Novel cationic polymers have to be made more biocompatible by reducing their potential for unspecific adverse interactions with the host, and by designing them in a biodegradable form. “Smart” polymers and polymer conjugates are being developed that in a dynamic manner present virus-like delivery functions in the appropriate phase of the gene delivery process.

1.3.4 AFM imaging in the field of drug delivery.

The ability to fully characterise drug systems, to provide drug targeting with high specificity and drug delivery with integrated controlled release are all a major challenge to the pharmaceutical industry. These challenges have, in part, been difficult to meet due to often poor understanding of the physicochemical properties of drug systems.

The family of scanning probe microscopes (SPMs) has revolutionised our ability to characterise and understand the interactions between drug systems and their exposed environments. These microscopes have enabled the study of pharmaceutical devices and drug particles with minimal pre-treatment in both air and liquid at the nanoscale level.

The AFM was invented 1986. The main features of the AFM include its ability to image non-conductive samples (therefore a range of biological and drug particles can be studied) and to measure the surface topography of samples at subnanometer resolution. Most importantly of all for pharmaceuticals the AFM can work under a range of conditions including in air and liquid over a range of temperatures, with minimal sample manipulation and low running costs.

During AFM imaging a sharp probe tip, usually made of silicon (Si) or silicon nitride (Si3N4) located on the underside of a flexible cantilever, raster scans over a sample surface. This motion is achieved using a piezoelectric scanner (Fig. 1). The bend and twist of the cantilever due to the forces of interaction between the tip and sample are monitored via a laser beam that is reflected from the back of the cantilever onto a position sensitive, quadrant photodiode detector. A resolution of few nanometres can be achieved, thus allowing reliable investigation upon nanoscaled systems. AFM is at present, one of the most powerful techniques in nano (bio) technology investigation. Some example of AFM imaging application are reported in the Figures 1.4 and 1.5.

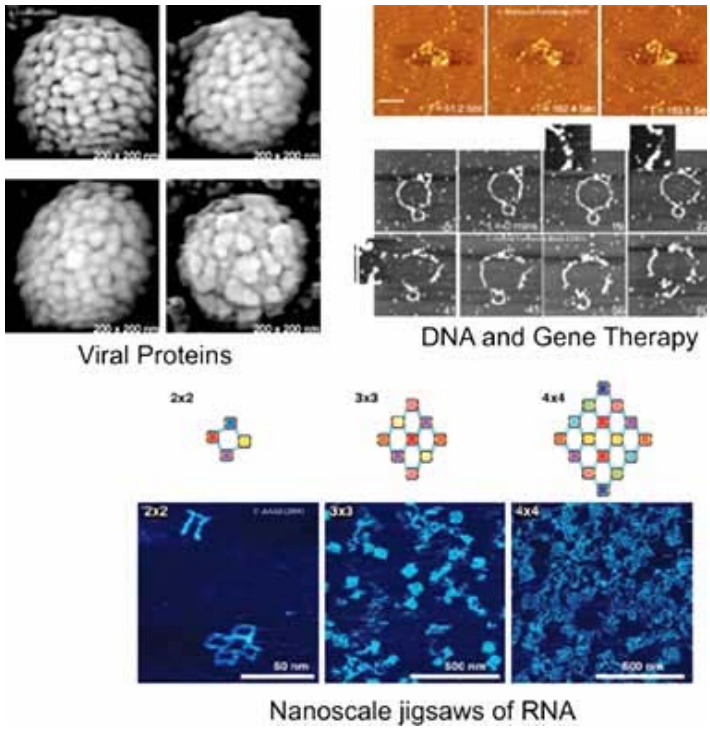

Figure 1.4: Examples of AFM imaging in the fild of biological investigations.

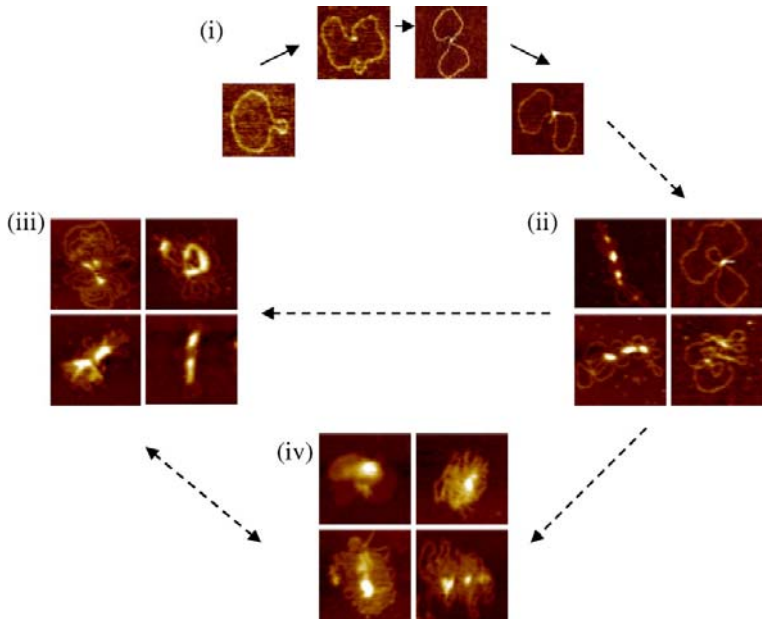

Figure 1.5: AFM study of DNA. Taken from Chim et al., 2006 [Y.T.A. Chim, Direct Nanoscale Visualisation of DNA Systems for Gene Therapy, in School of Pharmacy, LBSA, University of Nottingham, Nottingham, 2006, p. 208]

CHAPTER 2

PAAs, a family of bioactive and biocompatible polymers

2.1 POLY(AMIDOAMINE)S' PROPERTIES

Poly(amidoamine)s (PAAs) represent a family of biodegradable and biocompatible polymers with a recognised potential in the pharmaceutical field (Lin et al., 2007; Lavignac et al, 2005; Griffiths et al., 2004; Richardson et al, 2001). The first extensive studies on PAA synthesis have been published in 1970 (Danusso, Ferruti, 1970) and their chemical properties and biomedical applications reviewed in several instances (Ferruti et al., 2002; Ferruti et al., 1985)

2.1.1 GENERAL SYNTHESIS AND STRUCTURE

PAAs are obtained by stepwise Michael type polyaddition reaction of primary or bis-secondary amines to bisacrylamids. The polymer obtained presents tert-amino and amido groups regularly arranged along the main chain (Scheme 2.1).

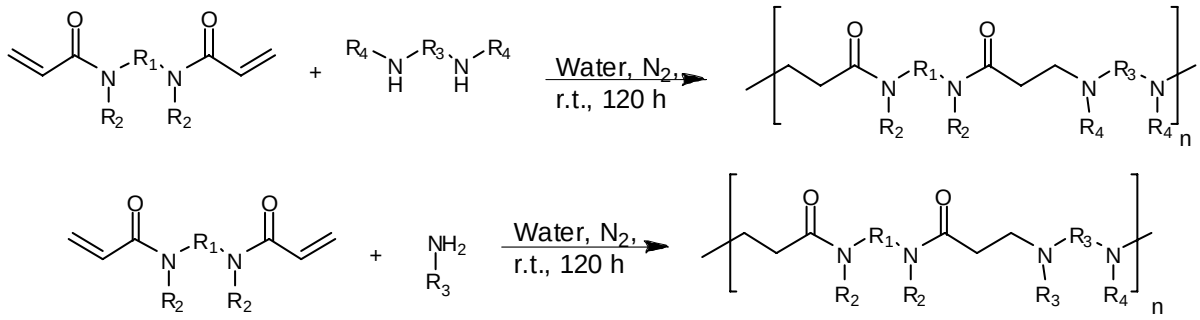

Scheme 2.1: Synthesis of linear PAAs R1, R2, R3, R4 can be any alkyl residues eventually containing carboxyl, amide, ester, ether groups.

The polymerisation reaction takes place in solvents carrying mobile protons, such as water or alcohols, without added catalysts (Scheme 2.2). The number-average and weight-average molecular weights of the PAAs usually range between 5000 – 40000 and 10000 – 70000 respectively, with a polydispersity index around 2 depending on the isolation method.

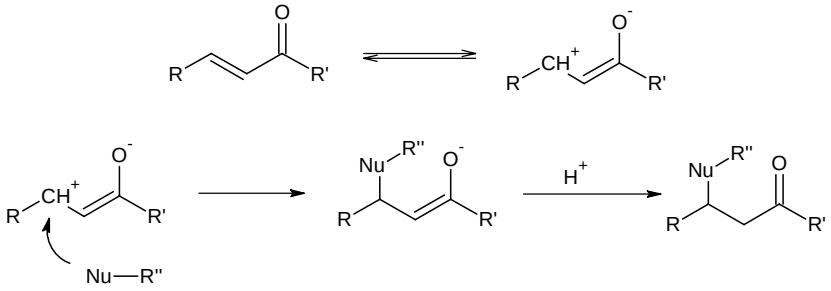

Scheme 2.2: Michael type addition mechanism.

The reaction is considerably influenced by temperature. High temperatures accelerate the polyaddition reaction rate but the resulting polymers showed lower molecular weights because of the larger increase of hydrolysis reaction rate (Ferruti et al, 1994) .

It is possible to obtain amphoteric PAAs using carboxyl containing starting monomers, carboxyl groups not influencing the polyaddition reaction. In this case, a stoichiometric amount of base (inorganic such as lithium or sodium hydroxide, or organic, such as triethylamine) must be added to

the monomer mixture in order to prevent amine protonation by the acid groups. Amphoteric PAAs show remarkable biological properties as will reported later in this chapter.

Non amphoteric PAAs are soluble in water as well as chloroform, lower alcohols, dimethyl sulfoxide and other polar solvents. However, amphoteric PAAs dissolve only in water. The intrinsic viscosities of PAAs in organic solvents or aqueous media usually range from about 0.15 to 1 dl/g. As a rule, PAAs exhibit relatively large hydrodynamic volumes in solution if compared with vinyl polymers of similar molecular weight, indicating a tendency to assume an extended chain conformation in solution

It is possible to obtain cross linked PAAs using polyfunctional monomers, such as bis-primary amines, by totally or partly replace the bis-functional amine monomer during the reaction (Scheme 2.3). The soft hydrogels obtained have been studied as substrate for cell culture but can be also used as synthetic intermediates for special purposes (Ferruti, Caruso et al., 2005; Ferruti, Piras et al, 2005).

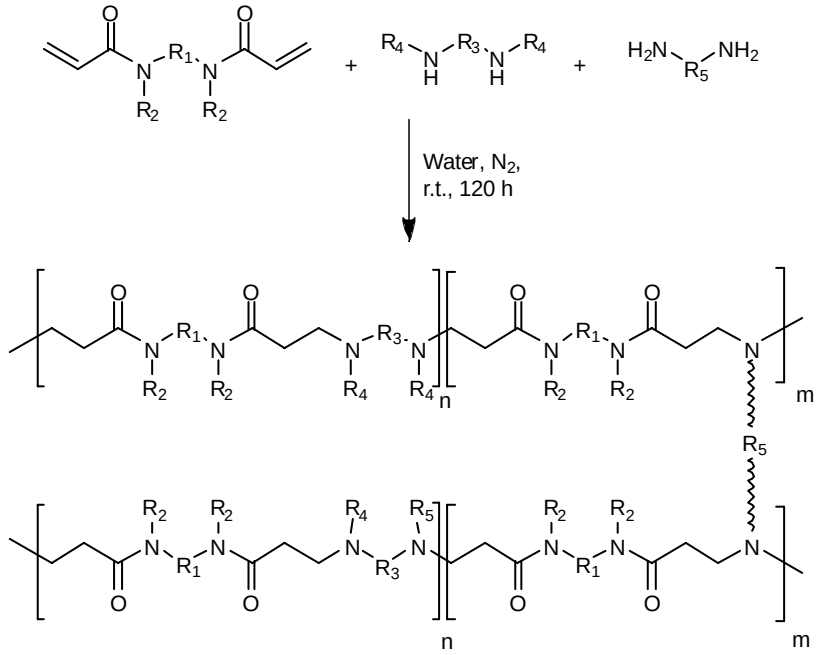

Scheme 2.3: Synthesis of cvalently cross-linked PAAs hydrogels. R1, R2, R3, R4 can be any alkyl residues eventually containing carboxyl, amide, ester, ether groups.

2.1.2 FUNCTIONALISATION OF PAAS

PAAs are inherently highly functional polymers, however, further functionalisation of PAAs may be useful for special purposes. Functional groups not capable of undergoing Michael addition under the conditions of PAA synthesis, for instance hydroxy, tert-amino, allyl, amido and ether groups, do not compete with the polimerisation reaction. Therefore, the introduction of these additional functions in PAAs as side substituents can be simply achieved by using monomers properly functionalised. Chemical groups capable of reacting with activated double bonds under the conditions of PAA synthesis such as SH, NH_2, NHR and PH_2, if unprotected, cannot as a rule be introduced directly as side substituents in PAAs. However, it is possible to obtain these types of functional groups by functionalization of purposely pre-synthesised polymers. Syntheses of PAAs carrying primary amines or sulphidryl containing pendants have been recently published.

2.1.3 DEGRADATION OF PAAS

All PAAs, containing amidic bonds in their main chain, are degradable in aqueous solution. The degradation of several PAAs has been extensively studied by means of viscometric and chromatographic techniques (Ferruti, 2002; Ferruti, 1994). The mechanism of PAA degradation seems to be purely hydrolytic as no vinyl groups, such as those which would have derived from a β-elimination reaction, could be determined. It has been demonstrated that degradation rate of PAAs in aqueous media is strongly influenced by temperature and pH, as well as by the structure of both the amine and amide moieties. Degradation seems not to be affected by the presence of isolated lysosomal enzymes at pH 5.5.

2.1.4 ACID-BASE PROPERTIES OF PAAS

All PAAs contain tert-amino groups in their main chain and therefore can be classified as polyelectrolytes (Richardson et al., 2001; Ferruti et al., 2002). Normally, the values of the

protonation constants (log K) of polyelectrolytes depend on the degree of protonation of the whole macromolecule. They follow the modified Henderson-Hasselbach equation:

$$\log K_i = \log K_i^0 + (n-1)\log\left[\frac{(1-\alpha)}{\alpha}\right] \qquad \text{(Eq 2.1)}$$

where $\log K^0_i$ is the protonation constant of a group present in a completely unionised polymer and α = degree of protonation.

The protonation constants of polyelecrolytes are usually referred to as "apparent" constants, as opposed to the "real" constants of non macromolecular acids and bases. However, in most PAAs the results of the potentiometric titrations are consistent with n values very close to 1. This means, that in PAAs, the tendency of the aminic nitrogen atoms of each repeating unit to assume a proton in practice does not depend on the degree of protonation of the whole macromolecule. Therefore, real or "quasi real" basicity constants can be determined. As a consequence, non ampohoteric PAAs behave as polycations and show the same number of basicity constant than the amino groups present in their repeating unit (Figure 2.1).

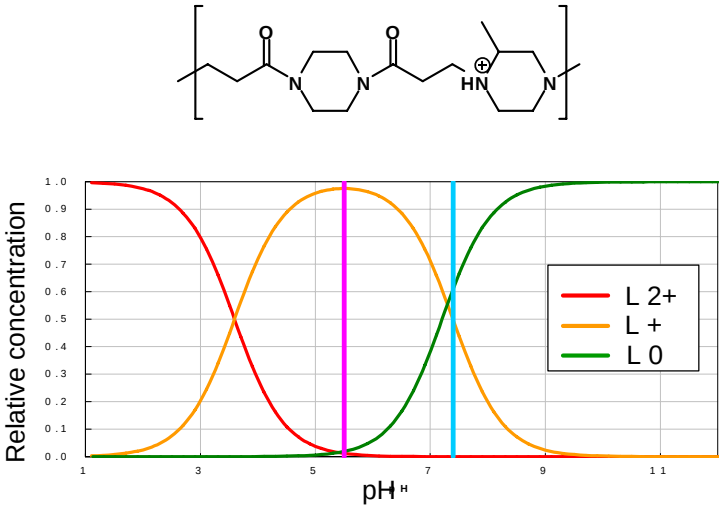

Figure2.1: Protonation profiles the cationic PAA represented above the chart, in which each curve represent relative abundance of different protonation profiles of the repeating units. pH scale is from 1 to 11.

By a proper choice of the starting monomers, the acid and basic strength of the amino and the carboxyl groups can be controlled in such a way that the polymer passes from a prevailingly anionic to a prevailingly cationic state as a consequence of relatively modest pH changes (Figure 2.2).

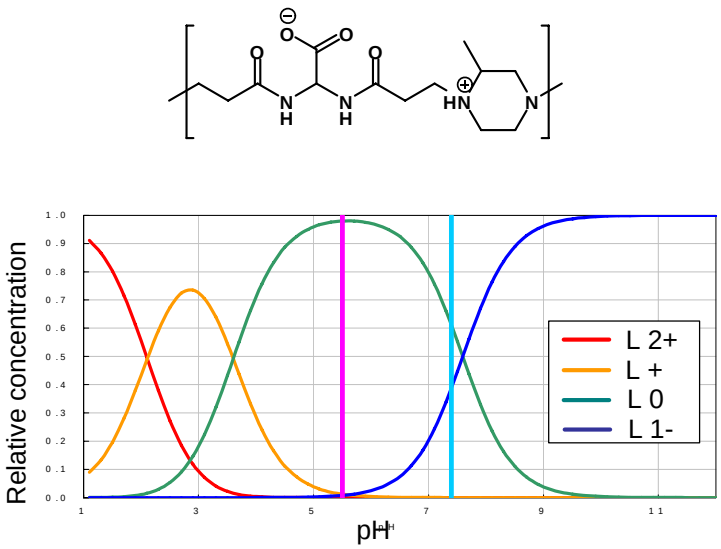

Figure2.2: Protonation profiles the amphoteric PAA represented above the chart, in which each curve represent relative abundance of different protonation profiles of the repeating units. pH scale is from 1 to 11.

2.1.5 BIOLOGICAL PROPERTIES OF PAAS

PAAs are endowed with many interesting properties for using in biological and biomedical applications. Cationic PAAs are usually one or two order or magnitude less cytotoxic (IC_{50} between 0.5 and 3 mg/ml) than other commonly used polycations such as poly-L-lysine and polyethyleneimine (IC_{50} 0.01 mg/ml) but show the same properties in DNA complexing ability. For this reason they can be regarded as potential transfection promoters (Richardson et al., 2001; Lavignac, 2004).

Moreover, amphoteric PAAs are often non-cytotoxic (IC50 above 5 mg/ml, similar to dextrane) and stealth-like: when parenterally administered to living animals, mice or rats, they don't accumulate in liver or kidneys but can circulate for prolonged time in the bloodstream (Franchini et

al., 2006; Ferruti, Franchini et al., 2007) . This property is very important in designing polymer therapeutics for cancer therapy.

PAAs are internalized by cells via the endocytic pathway. In intracellular compartments, where the pH is lowered to first 6.5 (endosomes) then 5.0 (lysosomes), they become prevailingly cationic and display endosomolytic properties.

The degradability of the PAAs is very important as well, in order to allow renal clearance once the polymer has completed his function in the body. The hydrolysis degradation mechanism, completely non-enzimatic, allow a fine tuning of the polymer life in the body. The cytotoxicity of different PAAs degradation products have been also tested, always leading to IC_{50} values similar or larger than the native polymers.

2.2 PAAS AS POLYMER THERAPEUTICS.

2.2.1 RADIOACTIVE LABELLED PAAS

Radioactive labelled PAAs have been obtained by substituting a small amount (4 % on a molar basis) of tyramine (Figure 2.3) for the same amount of aminic monomers. This allows radioiodination by I^{125}.

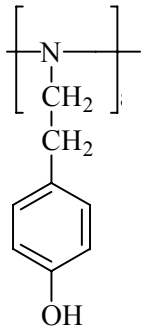

Figure 2.3: Structure of tyramine units in PAA.

2.2.2 FLUORESCENT LABELLED PAAS

A wide choice of fluorescent labels for proteins is commercially available. They usually contain an activated carboxyl group that will couple with the ε-amino groups of L-lysine units of proteins. It is obviously of advantage to introduce primary amino groups as side substituents in PAAs, to render them amenable to the same labelling techniques as proteins. However, the potential interest in polymer therapeutics of PAAs carrying pendant primary amino groups is not limited to that. In fact, they may act as general purpose polymer carriers for carboxylated drugs and will easily yield PAA-protein conjugates by consolidated techniques. The direct introduction of primary amino groups in PAAs by using primary amino-substituted monomers in the polymerisation recipe is not possible under the synthetic conditions normally adopted for PAAs, since all primary amino groups will participate to the polimerisation reaction.

Under non selective conditions primary bis(amine)s usually give crosslinked products on reaction with bis(acrylamide)s, because they react as tetra-functional monomers. To prepare PAAs carrying primary NH_2 groups as side substituents (NH_2-PAAs), a general-purpose synthetic strategy is to use as monomers primary diamines, in which one of the aminic functions has been protected by a group capable of preventing its addition reaction on activated double bonds. The protecting group must be stable under the conditions of PAA synthesis, but easily removable under conditions not affecting PAA stability. A convenient synthesis and discussion about the synthetic considerations have been recently published (Malgesini et al., 2003)

2.2.3 MITOMYCINC-PAA CONJUGATES

PAA-MMC adducts were synthesised from ISA4. After in vitro studies, preliminary experiments were carried out to investigate the efficacy and toxicity of these PAA-MMC conjugates *in vivo*. The PAA-MMC conjugates were equi-active compared to MMC given i.p. route and indeed in this pilot experiment a long term survivor was observed in each group treated with conjugate. It was found that PAA-MMC conjugates were less toxic than free MMC when administered at a MMC-equivalent dose of 5 mg/kg, that is, the maximum tolerated dose of free MMC that can be given to animals.

2.2.4 PLATINATES-PAA CONJUGATES

ISA23 and two other PAAs containing pendant β-cyclodextrins were used to synthesise PAA-platinates by reaction with cisplatin. The conjugates had a content of 8-70 wt % platinum and in vitro at pH 5.5 and pH 7.4 they released low molecular weight platinum species (0 - 20 %/72 h). In vitro the PAA-platinates were generally less toxic than cisplatin towards lung tumour cell lines (IC_{50} for cisplatin was 2-5 μg/ml and 1-130 μg/ml for the PAA-platinates). In *in vivo* experiments the PAA-Pt derivatives were equi-active compared to cisplatin in an i.p. L1210 leukaemia model

thus confirming their ability to liberate biologically active platinum species. Whereas ISA23-platinate was significantly less toxic in vivo than cisplatin, the cyclodextrin-containing PAAs did show significant toxicity on repeated dosing and thus are unsuitable for further development. As regards activity, preliminary experiments have shown that the ISA23-platinum conjugate displayed similar antitumour activity to that reported for other platinum conjugates of similar molecular weight. PAA-platinates have the advantage of good water solubility which is maintained during storage in contrast with other polymer-platinates, which often show reduced solubility after very short times (1-2 weeks).

2.2.5 RICIN- AND GELONIN-PAA CONJUGATES

Plant and bacterial toxins have been widely explored as anticancer agents, particularly in the form of immunotoxins. PAAs ability to mediate intracellular delivery of ribosome-inactivating toxins, in particular ricin and gelonin have been proved (Pattrick et al., 2001). Ricin, derived from *Ricinus communis* beans, is a highly cytotoxic protein when present in the native dimeric form, consisting of an A-chain (RTA) and a B-chain (RTB) linked by a disulphide bridge. RTB is the cell binding moiety which acts to promote binding and endocytosis of RTA. Once inside the cell, RTA is believed to utilize the E-R associated protein degradation pathway (ERAD pathway) and is translocated to the cytosol in a partially unfolded state. Once in the cytosol, RTA refolds and exhibits pharmacological activity by cleavage of the N-glycosidic bond of adenosine nucleoside leading to inhibition of protein synthesis. RTA alone does show some inherent toxicity towards cells but this is a very inefficient process. This effect is greatly reduced compared to the toxicity of the holotoxin. Gelonin toxin does not contain the cell-binding subunit of ricin and is completely non-toxic to intact cells. Cationic membrane interacting PAAs were chosen to investigate their ability to promote intracytoplasmic delivery. They were incubated with B16F10 cells in vitro together with two non permeant toxins: either ricin A-chain (RTA) or gelonin. The relatively non

toxic PAAs (IC_{50} 1.8 mg/ml) restored activity to the inherently inert toxins. The addition of a small quantity of tyramine to the PAA structures designated ISA4 to allow radiolabeling had no effect on their pK_a values. Ricin and RTA displayed IC_{50} values of 0.3 and 1.4 μg/ml, respectively, and gelonin was non-toxic over the range studied. In all further experiments, non-toxic concentrations of RTA (250 ng/ml) and gelonin (1.4 μg/ml) were used. When B16F10 cells were incubated with a combination RTA-PAA conjugates (250 ng/ml), the observed IC_{50} fell to 0.65±0.05 mg/ml.

Similar results were obtained with gelonin.

Cytotoxicity assays were again performed using B16F10 cells but in this case a fixed concentration of ISA4 was combined with increasing concentrations of RTA (0-10 μg/ml). As the PAA concentration increased, less RTA was required to achieve the IC_{50} level. It can be clearly seen that a mixture of this PAA and RTA can be used to promote cytotoxicity to a greater level than seen for the holotoxin at a polymer concentration of 1.5 mg/ml. These observations suggest that specific PAA-toxin combinations warrant further development as novel therapeutics.

2.2.6 MELLITIN-PAA CONJUGATES

Mellitin (MLT) is a peptide of α-helical conformation and it is the main constituent of the venom of the European honey bee (*Apis mellifera*). It is a cationic and it spontaneously associates with natural and artificial membranes. The peptide has a molecular weight of 2860 and it is a typical representative of biologically active peptide drugs with high therapeutic potential. Bee venom has been found to have a marked effect on the immune system, cardiovascular system and it also exhibits anti-tumour activity. Melittin is commonly used in the treatment of arthritic disorders, such as rheumatoid arthritis and osteoarthritis but it has been used as an endosomolytic agent, too. A poly(ethyleneimine) (PEI)–MLT conjugate was used to form polyplexes that increased gene expression in several cell lines. More recently a maleic anhydride derivative of MLT was used to deliver oligonucleotides to the cytosol of Hela cells.

Novel ISA1- and ISA23-like MLT conjugates have been prepared. Both conjugates displayed pH dependent haemolytic activity and ISA1–MLT also enhanced intracellular delivery of the non-permeant toxin gelonin compared to the parent ISA1 polymer. Whilst ISA23–MLT did not deliver gelonin, its lack of haemolytic activity at pH 7.4, and retention of cytotoxicity, suggests it worthy of further evaluation as an anticancer polymer therapeutic (Lavignac et al., 2005).

2.2.7 AGMATINE CONTAINING PAAS

Recently a peptidomimetitc PAA, labeled AGMA1, have been obtained by polyaddition reaction of bis(acrylamido)acetic acid and agmatine (4-aminobutylguanidine) (Annunziata et al, 2007; Franchini et al., 2007; Ferruti, Franchini et al., 2007).

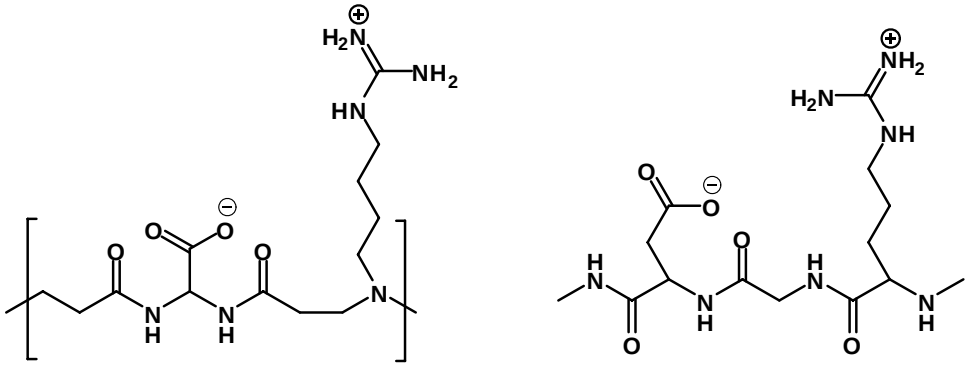

Figure 2.3 : structure of agmatine containing amphoteric PAA (left part) compared to the RGD tripeptide sequence.

Despite the large amount of cationic charge in physiological conditions (55% at pH 7.4 and 945 at pH 5, see Figure 2.5), this amphoteric polymer showed a very low toxicity, probably due to the structural similarities with the tripeptide arginine-glycine-aspartic (RGD sequence). This oligopeptide, in fact, interacts wit a_vb_3 integrins, and it is involved in cell proliferation and adhesion mechanisms.

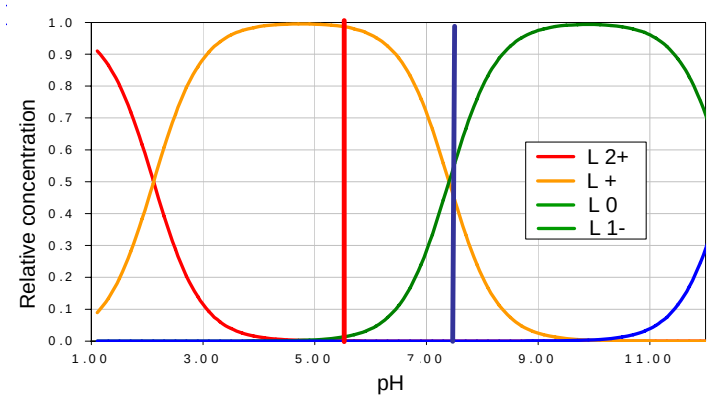

Figure2.5: Protonation profiles of AGMA1, in which each curve represent relative abundance of different protonation profiles of the repeating units. pH scale is from 1 to 11.

Agmatine containing amphoteric polymers have been tested as carriers for drug delivery and as transfection promoters. In vitro assays demonstrated the polymer ability to interact with cell membranes in a non disruptive way and to effectively protect DNA by enzymatic degradation in biological environment and to promote stable gene transfection in living cells. In vivo assays demonstrated a stealth like behavior with passive accumulation in tumour by EPR effect. Agmatine containing PAAs' hydrogels, easily obtained using a polyfunctional amine monomer, are fully cytocompatible and showed also remarkable properties adhesion and proliferation promoters towards several cell lines (Ferruti, Piras et al, 2005).

CHAPTER 3

Kinetic study of PAAs synthesis in organic solvents

3.1 AIM AND RATIONALE OF THE WORK

PAAs are a family of polymers obtained by Michael type polyaddition reaction in which amine and amide groups are regularly arranged along the main chain. Several different fuctional groups are compatible with Michael reaction, such as carboxyl, hydroxyl, allyl, amide or ether groups. This fact represent a clear advantage in PAAs synthesis, since PAAs containing chemical functions as side-substituents can be easily obtained using suitable functionalized monomers. In fact, only a few groups are able to interfere in the polyaddition reaction and, in principle, nearly every aliphatic amine and bisacrylamide can be used as a monomer (Ferruti et al., 2002).

For special purposes, such as hydrophilic-hydrophobic block co-polymer or compatibilisers for drug formulations, PAAs containing hydrophobic moieties can be obtained. This involves the use of water insoluble monomers and, therefore, organic reaction solvents are needed (Malgesini et al,

2003). Pioneering studies previously performed showed that high molecular weight polymers can only be obtained in organic solvents bearing mobile hydrogens, such as alcohols; indeed aprotic solvents give always poor results irrespective of their polarity (Danusso, Ferruti, 1970). In fact, mobile hydrogens play a key role in reaction mechanism of Michael addition, and hydrogen mobility strongly influenced reaction kinetics.

Since systematic comparison studies of the polymerization kinetics of PAAs in water and alcohols were lacking, we performed a comparative study of the kinetics in water, methanol and ethylene glycol of a typical polyaddition reaction, namely that of 2-methylpiperazine (MP) to 1,4-bisacryloylpiperazine (BP). Formamide, was also studied, together with a typical dipolar aprotic solvent, dimethylformamide. With this solvents choice a wide range of several common solvents, often used also in biological field, are taken into account; moreover they represent almost all commonly used solvent classes with respect with their polarity and acid-base properties.

3.2 EXPERIMENTAL PART

3.2.1 Materials.

1,4-Bis(acryloyl)piperazine (BP) was prepared as previously described (Ferrutim 1985); 2,5-dimethylpiperazine (DMP) was commercially available (Aldrich) and was used without further purification. The 2-methylpiperazine (MP) was purchased from Fluka and recrystallized from n-heptane (1 g MP in 20 mL solvent) before use. Its purity was checked just before use by potentiometric titration. The organic solvents were anhydrous analytical grade freshly purchased from Fluka. They were transferred under dry nitrogen by means of syringes. The bottles were opened just before use and their content left over molecular sieve. 0.1M hydrochloric acid solution was purchased from Riedel-de Haen. Water was doubly distilled.

3.2.2Measurements

UV-VIS spectra were run on a Perkin-Elmer Lambda EZ210 spectrometer connected to a PC for data transfer. For all measurements, quartz cells with a 1 cm path length were used. The calibration curves were obtained for each solvent in the analysis of 1,4-bis(acryloyl)piperazine at nine different concentrations; the absorbance at 250 nm fell within the range 0.04-0.9. The solutions were prepared using as solvent 0.1M hydrochloric acid containing 0.05% v/v of the organic solvent used. The data were processed by means of the least square fitting.

3.2.3Model polymerization reactions

A 0.4 M solution of 1,4-bis(acryloyl)piperazine in the appropriate solvent (25 mL) and a 0.4 M solution of 2-methylpiperazine (or 2,5-dimethylpiperazine) in the same solvent (25 mL) were introduced, by means of syringes into a 100 mL one-necked flask, equipped with a silicon rubber stopper and thermostated at 25°C. The reaction mixture was flushed with dry nitrogen and then kept at 25°C without stirring. Aliquots (10 μL) were withdrawn at specific reaction times and the final volume of each adjusted to 20 mL with 0.1 M hydrochloric acid. The UV absorption of each solution was measured against the appropriate blank solution, that is, 0.1 M hydrochloric acid containing 0.05% v/v of organic solvent; the experiments were performed in duplicate.

3.3RESULTS AND DISCUSSION

The aim of this work was the study of the kinetics in different solvents (water, methanol, ethylene glycol, formamide, and dimethyl formamide) of a typical polyaddition reaction leading to a PAA. The model reaction adopted in this study was the polyaddition of MP to BP (Scheme 3.1):

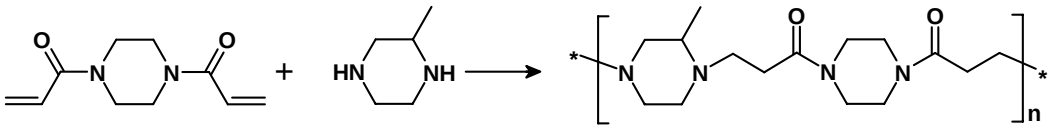

Scheme 3.1. Polyaddition reaction of BP to MP.

This reaction was chosen as model PAA preparation because both the monomers involved, as well as the resultant polymer, are easily soluble in water, lower alcohols and formamide. Perhaps plain piperazine would have been an even better model because it bears two perfectly identical amino groups. Piperazine, however, was discarded because its polymer with BP is soluble only in water and, therefore, in organic solvents precipitation would occur after a short reaction time. Moreover, MP is the amine used as the monomer in the PAAs with particular biomedical interest, some of which, also employ BP as a co-monomer. In addition, in the case of water, also DMP was used in comparison to MP, in order to investigate the effect of the different steric hindrance of the substituents in the α–position to the reactive secondary amine groups on the polyaddition reaction with bisacrylamides.

The reactions were carried out at 25°C (close to the room temperature for the PAA syntheses). The reaction progress was monitored by UV spectroscopy, chosen for its sensitivity, fastness and cheapness, measuring the decrease of the intensity of the absorption band of the conjugated double bonds of BP. The following procedure was invariably adopted. The polymerization reactions were carried out at a 0.2 M concentration in the selected solvent (see Experimental), that is, approximately 1/10 of the reaction concentrations commonly adopted in PAA syntheses. Aliquots (10 μL) of the polymerization solutions were taken at specific time intervals and diluted in 20 mL 0.1 M aqueous hydrochloric acid in order to stop the polymerization reaction and to reach a suitable concentration for UV measurements. The UV spectra of MP, BP and their polyaddition product were, therefore, preliminarily studied in 0.1 M aqueous hydrochloric acid containing 0.05% v/v of organic solvent, in order to verify the influence of the residual solvent on the absorption spectra of reagents and products. The absorption spectra in 0.1 M aqueous hydrochloric acid + 0.05% (v/v) methanol are shown in Figure 3.1.

In all the aqueous mixtures, the absorption spectrum of BP showed a peculiar absorption band with a maximum at 240 nm due to the π-π* transition of the BP conjugate double bond. In this

range, BP spectrum partially interferes with the tail of polymer absorption bands. For this reason, a different wavelength, 250 nm, was chosen for measuring the decrease in BP concentration.

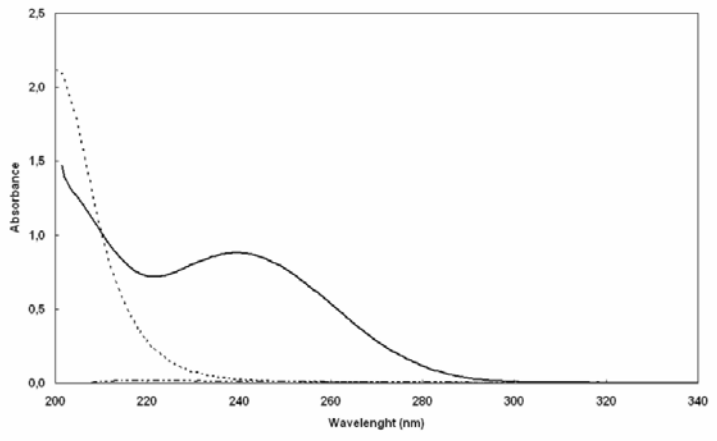

Figure 3.1. Absorption spectra of BP (---), MP (·-·) and the the polyaddition products (···) in 0.1 M aqueous hydrochloric acid + 0.05% (v/v) methanol.

The molar extinction coefficients curves obtained in the different aqueous hydrochloric acid/solvent mixtures, ε, are reported in Table 3.1. The experimentally determined values of ε show slight differences in different aqueous/solvent mixtures, reflecting the different interactions between solvent and BP.

Table 3.1. Molar extinction coefficients ε for bis-acryloylpiperazine[a]

Solvent	**Molar extinction coefficient ($M^{-1}cm^{-1}$)**
Water	10600
Ethylene glycol	12200
Methanol	11400
Formamide	11700
Dimethyl formamide	12400

[a)] In 0.1 M Hydrochloric acid with 0.05% of different organic solvents at 250 nm

3.3.1Determination of the rate constants: steric hindrance effect.

The conversion curves obtained in the polyaddition reaction of BP with MP in the series of solvents listed in Table 1 are shown in Figure 3.2. The reaction proceeds much faster in water and glycol than in methanol, formamide in dimethylformamide, the latter solvents gave the poorest performance.

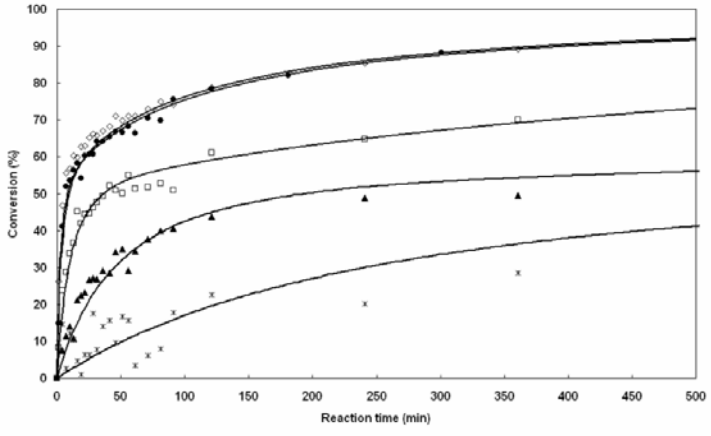

Figure 3.2. Conversion curves of the polyaddition reaction of BP with MP in different solvents [(●) water, (◇) glycol, (□) methanol, (▲) formamide, (∗) dimethyl formamide]. Best fitting curves were obtained using equation (3) and for dimethylformamide equation (4).

We referred to our Previous studies demonstrated that polyaddition reactions involving acrylamides, bis-acrylamides and/or bis-acrylic esters, proceed with a pseudo-second order kinetics (Ranucci, Ferruti, 1991; Ferruti et al, 1998; Emilitri et al., 2005) with the kinetic constants that included the concentration of the catalytic protonic species, when performed in the presence of hydroxyl solvents. Thus, to investigate the kinetic features of the polymerization reactions of BP with MP in different protic solvents, data obtained were substituted in the following equation:

$$\frac{d[BP]}{dt} = -k[BP][MP] \qquad \text{Eq (3.1)}$$

on integration, if the initial reagent concentrations, $[BP]_o$ and $[MP]_o$, are equal, equation (3.2) is obtained:

$$\frac{1}{[BP]} = \frac{1}{[BP]_o} + kt \qquad \text{Eq (3.2)}$$

The results obtained from the experimental data using equation (3.2), are reported in Figure 3.3 (a-*d)*.

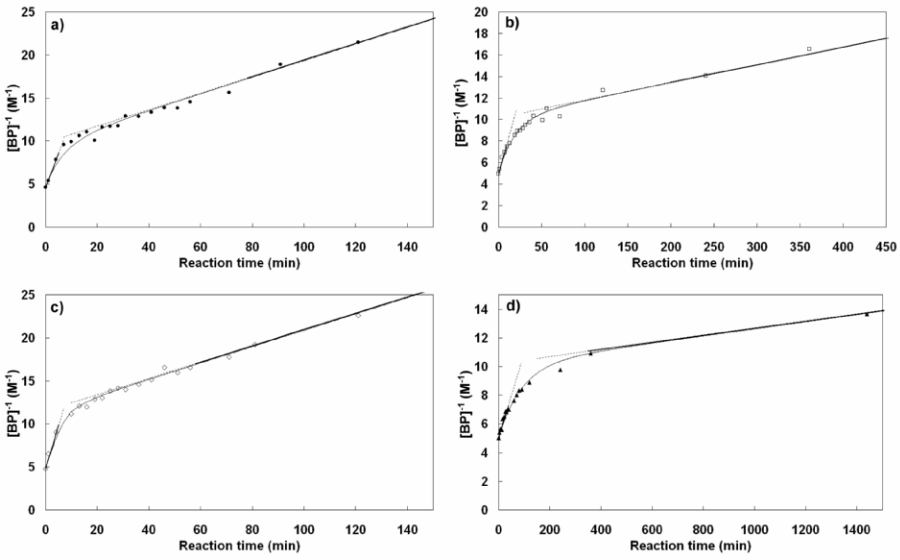

Figure 3.3. Calculated kinetic data using equation (2). Panels (a)-(d): polyaddition reaction of MP to BP in (a) water, (b) methanol, (c) ethylene glycol and (d) formamide. Best fitting curves were obtained using equation (3).

Unexpectedly, the *1/[BP]* versus *t* curves obtained were not linear, but they all diverged at approximately 50% conversion. These facts suggested that the amine groups on MP may not be equivalent, due to the different steric hindrances by the neighbouring groups. To confirm this hypothesis, polymerization reactions were performed in water using 2,5-dimethylpiperazine (DMP) with two equivalent amine groups. A typical conversion curve was obtained (Figure 3.4).

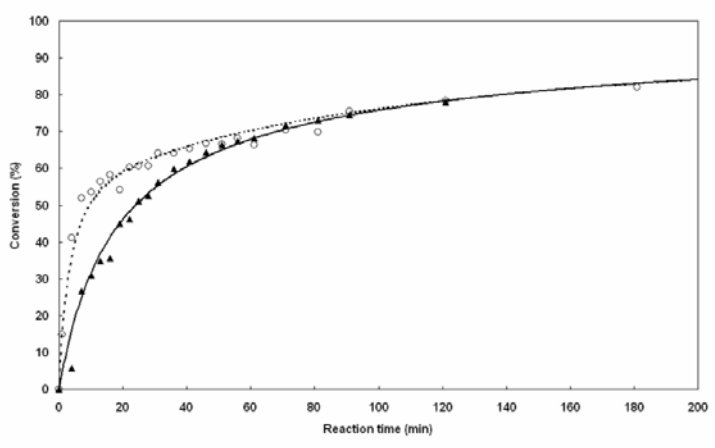

Figure 3.4. Conversion curves of the polyaddition reaction of BP with MP (O) and DMP (▲) in water.

The results obtained from these experimental data using equation (3.2), are reported in Figure 3.5. In this case, the relationship *1/[BP]* versus *t* curve was approximately linear with some deviation in the lower conversion region.

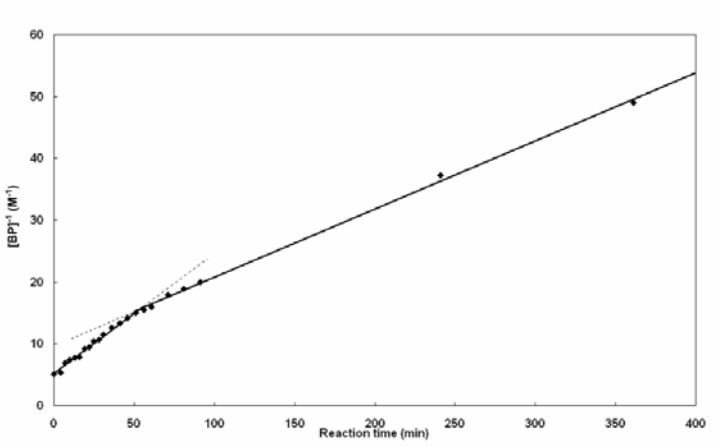

Figure 3.5. Calculated kinetic data using equation (2) for the polyaddition reaction of BP with DMP in water. Best fitting curve were obtained using equation (3).

This was ascribed to a small decrease in reactivity affecting the second amino group of DMP after the first addition step had occurred. The pseudo-second order kinetic constants, k_{DMP}, are reported in Table 3.2.

Table 3.2. Kinetic constants for the polyaddition reaction[a] with 2,5-dimethylpiperazine (DMP)

Solvent	k_1 ($min^{-1}M^{-1}$)	k_2 ($min^{-1}M^{-1}$)
Water	0,804	0,0961
Methanol	0,143	0,0158
Etylene glycol	1,013	0,0946
Formamide	0,042	0,0030
Water - DMP	/	0,0972

a) In 0.1 M Hydrochloric acid with 0.05% of different organic solvents at 250 nm.

These findings suggest that the polyaddition reaction of MP with BP proceeds through two distinct reaction steps, each characterized by a different rate. The first relatively fast step corresponds to the addition of the least hindered amine, while the second to the addition of the most hindered amine.

3.3.2Determination of the rate constants: solvent effect.

For protic solvents, the kinetics constants of the two reaction steps were obtained by determining the slopes of the very initial and the very final segments of the *1/[BP]* versus *t* curves (Figure 3.3), with the assumption that in either regions the reaction of one amino group of MP prevails over the other. Specifically, the faster step, with kinetic constant k_1, occurs in the initial phase of the reaction, while the slower step, with kinetic constant k_2, occurs in the final reaction phase.

The values of the k_1 and k_2 kinetic constants obtained for the different protic solvents are reported in Table 3.2. These values were used to simulate the theoretical conversion curves by numerically integrating the differential equation (3.3)

$$\frac{d[BP]}{dt} = -k_1[BP][MP_1] - k_2[BP][MP_2] \qquad \text{Eq (3.3)}$$

where $[MP_1]$ = concentration of the least hindered amino group and $[MP_2]$ = concentration of the most hindered amino group. The results, reported in Figure 3.3, well fit the experimental data. Moreover, as reported in Table 3.2, the k_2 value calculated for the MP reaction in water (0.0961 $min^{-1}\ M^{-1}$) is very close to the k_{DMP} value (0.0961 $min^{-1}M^{-1}$) in the same solvent thus confirming that steric hindrance influences the second MP reaction step.

The case of dimethylformamide was quite different. In this case, the best fitting curve was obtained by assuming a third order kinetics (Eq. (3.4)), which accounts for the autocatalytic effect of the aminic protons, being the solvent proton catalysis effect negligible. Due to the fact that the reaction rate in dimethylformamide under the conditions adopted is very slow, it was not possible to reach more than 50% conversion and, consequently, to determine the kinetics of the second step. The kinetic constant determined was 0.0142 $min^{-1}M^{-2}$.

$$\frac{d[BP]}{dt} = -k[BP][MP]^2 \qquad \text{Eq (3.4)}$$

A comparison of the kinetic constants obtained in the different solvent systems allowed us to confirm that the proton concentration and solvent polarity are the main factors affecting the reactivity of the system. The pK_a and dipole moment, μ, values for all solvents employed are reported in Table 3.3.

Table 3.3: Pk_a and the dipole moment, (μ) of the solvents used in the BP/MP polyaddition reaction[a)].

Solvent	pK_a	μ (D)
Water	14.00	1.85
Ethylene glycol	15.84	2.2 [b)]
Methanol	16.71	2.87
Formamide	16.80	3.37
Dimethyl formamide	>30	3.24

[a)] Kosuke, 2002; [b)] Li et al., 2002.

It was observed that, in general, the reactivity increased with increasing proton concentration and decreasing solvent polarity. In the case of formamide, a dipolar solvent with an autoprotolysis constant (pK_a = 16.80) which is similar to that for methanol (pK_a = 16.71), the reaction rate is remarkably low. It appears that in the case of formamide, which has a very high dipole moment, the establishing of dipole-dipole interactions between solvent and reactants largely overshadowed the positive effect of proton availability on the reaction rate. In particular, the polarizable acrylic moiety of BP, stabilized by the dipolar solvent, showed a decrease in addition reactivity. The same stabilizing effect may be responsible for the very low reaction rate observed in dimethylformamide, a classical aprotic dipolar solvent, which also had a very low autoprotolysis constant (pK_a >30).

3.4 CONCLUSIONS.

A kinetic study of Michael type polyaddition reaction was performed in different protic and aprotic solvents. It was found that solvent nature play a key role in the behaviour of this reaction, being its kinetic strongly depending on protonation constant and polar dipole of the solvent. In particular the reaction rate increase with increasing the autoprotolisis constant, taking into account the proton catalytic effect, and decrease with increasing the dipole moment, taking into account the stabilization of reactants for dipole-dipole interaction.

Water demonstrated overall the best solvent for Michael type polyaddition reactions, even if alcohols or ethylene glycol appear to be suitable alternatives as reaction media, when water insoluble bisacrylamids or amines are used in PAA synthesis.

CHAPTER 4

Synthesis of new polymeric precursors of PAA-drug or PAA-protein conjugate by disulfide bond

4.1 INTRODUCTION

In recent years a large number of research work is focusing on products in which disulfide bonds are involved. Disulfide bonds represent an important functional group in organic and also inorganic chemistry. They are being largely used for their properties to easily undergo reduction and oxidation and to interact with metal surfaces or complex metal ions. When different disulfides are mixed together, direct disulfide-disulfide exchange reaction occurred until redox equilibrium was reached, and for this property they have been recently considered in molecular dynamic library synthesis (Danieli et al., 2006).

Disulfide bonds play also a key role in biological field. A very wide range of metabolic processes involved disulfide bond formation or reduction, from sugar and lipid metabolism and oxidative phosphorilation, to protein folding and stabilisation, cell signalling, aging, apoptosys, and so on, the major part of which have probably to be discovered (Appfel, 1976; Jordan, Gibbins, 2006).

Moreover, many diseases have been recently associated with redox imbalances, such as AIDS and other immune diseases, Parkinson and Alzheimer syndromes, cancer and many others (Reynolds et al, 2007; Bonomini et al., 2008; Huber, Parzefall, 2007; Wu et al, 2004).

Recent researches demonstrated that cytoplasmic fluids are quite strongly reducing compared to extracellular fluids, such as plasma and other body fluids. As a consequence, disulfide bonds are stable in bloodstream but undergo reduction inside cells and therefore can be regarded as "smart" stimuli-responsive linkages in polymer therapeutic design for intravenous administration (Arpicco et al, 1997; Masuho et al., 1982; Miyata et al., 2005). Several publications reports on disulfides used as cleavable linkers in drug or gene delivery systems (Saito et al., 2003; Lin et al., 2007; Kwok et al., 2003). For these reasons, we decided to synthesise novel linear PAAs bearing pendant 2-ethenyldithiopyridine moieties (PAA-SSPy) as intermediates for the synthesis of new bioactive macromolecular conjugates sensitive to electric stimuli by exchange reaction with thiol-containing active molecules. The strategy adopted consist of a two step synthesis: first a cystamine cross-linked PAA was synthesised, in fact, having cystamine two primiary amine groups, react in polyaddition reaction as tetra-functional monomer, thus generating a hydrophilic tri-dimensional network; second, the hydrogel obtained was de-reticulated by direct disulfide exchange reaction with dipyridyl disulfide (Scheme 4.1).

A linear and soluble PAA with 2-Ethenyldithiopyridine pendants was obtained, that can be regarded as a precursor for thiol containing bioactive molecules conjugates. Ethenyl-dithiopyridine group is in fact extremely reactive towards these reactions for which the driving force is provided by the production of 2-mercaptopyridine that, mostly turning into the tautomeric 2-thiopyridone form, is an excellent leaving group (Bulmus et al., 2003).

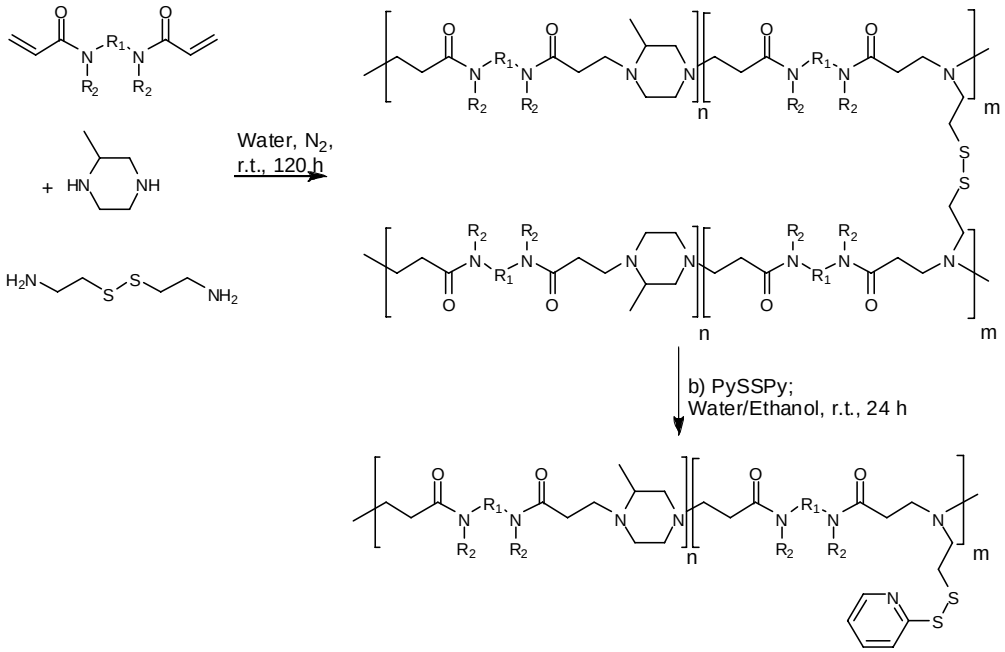

Scheme 4.1: general synthesis of PAAs containing 2-ethenyl dithiopyridine pendants.

4.2 EXPERIMENTAL PART

4.2.1 BAC20-PDEA. In a two necked flask, equipped with nitrogen inlet and stirring bar, BAC (0.134 g, 0.68 mmol), lithium hydroxide (0.034 g, 0.812 mmol) and pyridyl disulfide ethane amine (PDEA, 0.030 mg, 0.135 mmol) were dissolved in water (0.075 ml) under nitrogen. After 24 hours MP (0.054 g, 54.1 mmol) was added and the reactive solution maintained under stirring for 72 hours and then diluted to 50 ml. The solution pH was adjusted to 2.5 by addition of a 1M hydrochloric acid aqueous solution and ultrafiltered over a 3000 nominal cut-off membrane. The product was eventually liophilized. Yield = 60.6%. $\overline{M}_n$ = 7500, $\overline{M}_w$ = 18000, d = 2.4.

NMR of BAC30-SSPy hydrochloride: ^{1}H NMR (D_2O): δ (ppm) = 8.29, 7.71, 7-36, 7.19 (m, mercaptopyridine group, pattern A), 7.98, 7.56, 7.45, 6.92, (m, mercaptopyridine group, pattern B) 5.56 (m, br, NH-C**H**-NH), 2.85-3.62 (m, br, N-C**H**, N-C**H$_2$**, S-C**H$_2$**), 2.70-2.74 (m, br, CO-C**H$_2$**), 1.37 (skeleton, CHC**H$_3$**). UV spectrum (0.6 mg/ml): maxima 252 (0.32), 278 (0.39), 317 (0.41), 350 (shoulder, 0.27). For comparison: PDEA (0.05 mM): 236 (0.29), 310 (0.35); Mercaptopyridine:

(0.06 mM): 272 (0.54), 343 (0.38). After addition of reducing agents no variations occurred in UV absorbance spectrum.

*4.2.2 HG-BP30***.** In a two-necked flask, BP (1.960 g, 10.0 mmol), cystamine di-hydrochloride (0.338 g, 1.5 mmol) and lithium hydroxide monohydrate (0.126 g, 3.0 mmol) were dissolved in water (3.5 mL) under nitrogen. 2-Methylpiperazine (0.701 g, 7.0 mmol) was added under stirring until a homogeneous solution was obtained. After 120 hours the gel obtained was finely ground, extensively washed with water, estracted with acetone, and dried at 30° C and 0.1 tor. Yield = 84%. Swelling: 2.7 (H_2O); 1.8 (EtOH); 2.4 (CH_2Cl_2). $(C_{15}H_{26}N_4O_2)_{0.7\cdot n}(C_{12}H_{20}N_3O_2S)_{0.3\cdot n}$ $(294.4)_{0.7\cdot n}(270.38)_{0.3\cdot n}$: Calcd. C 59.97, H 8.49, N 18.05, O 11.14; S 3.34; Found = C 58.53, H 8.78, N 16.45, O 12.84.

HG-BP20, HG-BP10, HG-BAC30, HG-BAC20 and *HG-BAC10* were prepared following the same procedure described for HG-BP30 (see Table 4.1 for reagents' amounts). The HG-BAC series was treated with ethanol in place of acetone before drying. In all cases, the yields were approximately 85% and the elemental analyses agreed with the theoretical. The swelling degrees were: HG-BP20: 3.7 (H_2O); 2.3 (EtOH); 3.9 (CH_2Cl_2); HG-BP10: 4.2 (H_2O); 3.1 (EtOH); 6.6 (CH_2Cl_2); HG-BAC30: 10.5 (H_2O); HG-BAC20: 21.4 (H_2O); HG-BAC10: 41.8 (H_2O).

Table 4.1: Preparation of cystamine cross-linked PAA hydrogels [a)]

Code	BP (mmol)	BAC (mmol)	Cystamine .2HCl (mmol)	$LiOH.H_2O$ (mmol)	2-methylpiperazine (mmol)
HG-BP10	10.0	-	0.5	1.0	9.0
HG-BP20	10.0	-	1.0	2.0	8.0
HG-BP30	10.0	-	1.5	3.0	7.0
HG-BAC10	-	10.0	0.5	11.0	9.0
HG-BAC20	-	10.0	1.0	12.0	8.0
HG-BAC30	-	10.0	1.5	13.0	7.0

[a)] All hydrogels were prepared in 3.5 mL water.

*4.2.3 BP30-SSPy***.** HG-BP30 (5.00 g, 1.13 mmol disulfide) was soaked in ethanol (30 mL) and 2,2'-dipyridyldisulfide (0.750 g, 3.4 mmol) with catalytic 2-mercaptopyridine were added. The PAA gel dissolved within 5 hours. The reaction mixture was stirred for further 24 hours at r.t. and then diluted to 100 mL with water. Excess 2,2'-dipyridyldisulfide precipitated and was filtered out. The solution pH was then adjusted to 2.5 (HCl) , ultrafiltered through a membrane with nominal cut-off 3000 and liophilized.

BP20-SSPy and *BP10-SSPy* were prepared as BP30-SSPY, using a three-fold molar excess of 2,2'-dipyridyldisulfide with respect to disulfide units.

BP30-SSPy: Yield = 70.4%. Yield of the exchange reaction (from NMR data) = 71.9%. $\overline{M}_n$ = 9500, $\overline{M}_w$ = 32000, d = 3.3.

BP20-SSPy: Yield = 64.9%. Yield of the exchange reaction (from NMR data) = 67.8%. $\overline{M}_n$ = 47000, $\overline{M}_w$ = 190000, d = 4.0.

BP10-SSPy: Yield = 83.4%. Yield of the exchange reaction (from NMR data) = 77.5%. $\overline{M}_n$ = 40000, $\overline{M}_w$ = 130000, d = 3.2.

Polymers of the BP series, as hydrochlorides, were soluble in water, methanol, DMSO, DMF, but insoluble in chloroform, acetone and most organic solvents; as free bases, soluble in DMSO, DMF chloroform and methanol, but insoluble in water, acetone, toluene, ether and ethylacetate.

Complete ^{1}H and ^{13}C NMR characterization in reported in Table 2. The spectra of all samples equally confirmed the proposed structures. UV-Vis absorption spectra: 302, 235

BAC10-SSPy, BAC20-SSPy and *BAC30-SSPy* were prepared by the same procedure, using a 2:1 (v/v) water/ethanol mixture as reaction medium.

BAC30-SSPy: Yield = 69.2%. Yield of the exchange reaction (from NMR data) = 62.7%. $\overline{M}_n$ = 25000, $\overline{M}_w$ = 47000, d = 1.8.

BAC20-SSPy: Yield = 68%. Yield of the exchange reaction (from NMR data) = 66.1%. $\overline{M}_n$ = 44000, $\overline{M}_w$ = 93000, d = 2.1.

BAC10-SSPy: Yield = 85.6%. Yield of the exchange reaction (from NMR data) = 65.3%. $\overline{M}_n$ = 26000, $\overline{M}_w$ = 52000, d = 2.0.

All polymers of the BAC series were in all cases soluble in water, but insoluble in most organic solvents.

NMR of BAC30-SSPy hydrochloride: Complete ^{1}H and ^{13}C NMR characterization in reported in Table 4.2. The spectra of all samples equally confirmed the proposed structures.

Table 4.2. Relevant ^{1}H and ^{13}C chemical shifts (δ) of BP-SSPy and BAC-SSPy hydrochlorides in D_2O. *

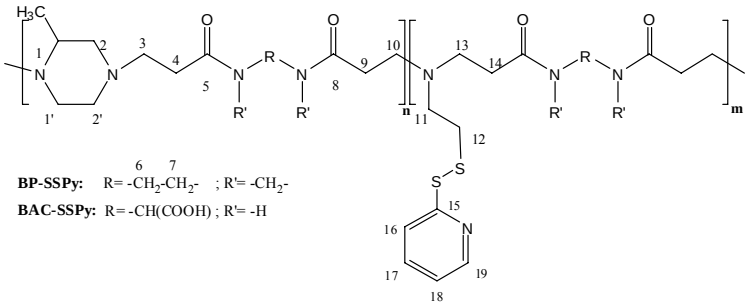

		1	2[a]	1'[a]	2'[a]	Me-1	3	4	5	5'	8	8'	6/6'	7/7'	9	10	11	12	13	14	15
BP-SSPy	**^{1}H**	3.42	2.85;3.40	3.15;3.65	3.00;3.42	1.35	3.18	2.86					3.65	-3.75	2.89	2.18;3.57	2.70;3.58[a]	3.00	3.48	2.98	
	^{13}C	56.35	55.4	48.85	49.6	14.1	52.6	28.2	170.9	170.5	170.6	170.3	44.6 44.8	41.3 41.6	27.7 27.8	48.5	51.9	26.9	50.7	26.8	156.6
BAC-SSPy	**^{1}H**	3.46	2.90;3.46	3.19;3.62	3.10;3.46	1.33	3.14	2.70					5.15	172.8 172.9	2.73	3.22;3.62	3.51	2.83	3.20	2.70	156.8
	^{13}C	56.25	55.1	48.3	49.3	13.9	52.5	30.3	171.6				58.0 58.15		29.8	48.5	51.5	28.7	50.1	31.7	

[a] for ^{1}H resonance: AB system

4.2.4 BAC10-SSNBA was prepared by the same procedure described for BAC10-SSPy but replacing 2,2'-dipyridyldisulfife with 5,5'-dithiobis(2-nitrobenzoic) acid (Ellman's reagent, 0.5g).

NMR of BAC30-SSPy hydrochloride: ^{1}H NMR (D_2O): δ (ppm) = 8.03 (broad, nitrobenzoic residue, -C(NO_2)-C**H**-), 7.67 (broad, nitrobenzoic residue, -C(CO_2H)-C**H**-C(S-)-), 7.60 (m, pyridine, -C(S-)C**H**-CH), 5.56 (m, br, NH-C**H**-NH), 2.85-3.62 (m, br, N-C**H**, N-C**H$_2$**, S-C**H$_2$**), 2.70-2.74 (m, br, CO-C**H$_2$**), 1.37 (skeleton, CHC**H$_3$**).

*4.2.5 BP30-SSG***.** BP30-SSPy hydrochloride (0.3 g, 0.149 mmol SSPy units) was dissolved in 20 mL TRIS buffer under nitrogen pH 8.50 and the solution purged with nitrogen. L-Glutathione reduced (0.0458 g, 0.149 mmol) was added. The solution turned immediately intensely yellow. After 30m a 1 M HCl aqueous solution was addet until pH 2.5 was reached, the solution was diluted with water (300 mL), ultrafiltered and isolated as in the previous cases. Yield = 82.8 %. Reaction yield ≃100%.

$\overline{M}_n$=28 000 $\overline{M}_w$=51 000, d = 1.82. $[\alpha]_D^{25}$= -7.4 deg·dm^{-1}·g^{-1}·cm^3, (c=1 in H_2O). For comparison purposes, L-glutathione reduced $[\alpha]_D^{25}$= –17.2 deg·dm^{-1}·g^{-1}·cm^3, (c=2 in H_2O).

^{1}H NMR (D_2O): δ (ppm) = 8.43 (m, pyridine, N-C**H**-CH), 7.84-7-87 (m, pyridine, N-C-C**H**-C**H**), 7.35 (m, pyridine, N-CH-C**H**), 3.77 (glycine residue, HO-CO-C**H$_2$**-NH), 2.88-3.65 (m, br, CO-C**H$_2$**, N-C**H**, N-C**H$_2$**, S-C**H$_2$**), 2.15 (glutamic acid residue, H_2N-CH-CH_2-C**H$_2$**), 2.09 (glutamic acid residue, H_2N-CH-C**H$_2$**), 1.38 (d, CHC**H$_3$**). ^{13}C NMR (D_2O): δ (ppm) = 170.59-171.11 (, **C**=O), 156.86 (pyridine, N-**C**), 149.76 (pyridine, N-**C**H), 139.24 (pyridine, N-C-CH-**C**H), 122.82 (m, pyridine, N-CH-**C**H), 122.14 (pyridine, N-C-**C**H), 43.33 (glycine residue, HO-CO-**C**H_2-NH), 41.46-56.48 (**C**-N, **C**-S), 31.59 (glutamic acid residues, H_2N-CH-CH_2-C**H$_2$**), 26.94-28.34 (**C**-CO), 26.28 (glutamic acid residue, H_2N-CH-**C**H_2), 14.18 (, CH**C**H_3).

BAC30-SSG was prepared by a similar procedure. Yield = 78.2 %. Reaction yield ≃100%.

$\overline{M}_n$ = 24 900, $\overline{M}_w$ = 42 000, d = 1.69. $[\alpha]_D^{25}$= -5.4 deg·dm^{-1}·g^{-1}·cm^3, (c=1 in H_2O). The NMR spectra were as expected.

4.2.6 BAC30-SSG-UV: BAC30-SSPy hydrochloride (20.0 mg, 12.0 μmol SSPy units) was dissolved in 50 mL 0.1M TRIS buffer pH 8.50 and the solution purged with nitrogen. A quartz cuvette was loaded with a 2 ml aliquot of the polymer solution and closed with a rubber stopper. A L-glutathione reduced solution, obtained dissolving L-glutathione reduced (2.5 mg, 8.1*10^{-3} mmol) in purged TRIS buffer (2 ml), was added in 10,0 μl aliquots with a Hamilton gastight syringe. After each addition, the solution was allowed to equilibrate for 5 minutes and a UV-spectrum was recorded.

4.3 RESULTS AND DISCUSSION

The rationale of this work was to obtain a new family of functionalized PAAs bearing pendant 2-ethenyldithiopyridine moieties, to be used as intermediates in the preparation of smart soluble polymer conjugates sensitive to reductive cleavage.

The first and most logic strategy was the direct co-polymerization of bis(acrylamido)acetic acid (BAC) with 2-methylpiperazine (2MP) and pyridyl disulfide ethane amine (PDEA), that in a single step would lead to the desired product. Following this route, a polymer was obtained as shown by SEC traces, but ^{1}H NMR spectra showed two different signal patterns due to the presence of aromatic rings (confirmed by COSY experiments) and different form the typical pattern of ethenylditiopyridin groups. UV-Vis absorption spectrum again confirmed what shown by NMR spectrum. Moreover, after addition of glutathione reduced, no change in the spectrum occurred, thus indicating an important decomposition of ethenyldithiopyridine groups during the reaction, probably due to the strong basicity, and affecting final product reactivity.

For this reason a different synthetic route was chosen, consisting in two synthetic steps: cystamine cross-linked PAA networks were first prepared (Scheme 4.1a) and then converted into linear soluble PAAs bearing activated disulfide pendants by exchange reaction of the cross-linking cystamine moieties with 2,2'-dithiodipyridine (Scheme 4.1b).

Six different cross-linked PAA samples were obtained by reacting bis(acryloyl)piperazine BP (HG-BP10, HG-BP20 and HG-BP30) or BAC (HG-BAC10, HG-BAC20 and HG-BAC30) with 2-methylpiperazine as co-monomer and three different amounts of cystamine as cross-linker. More precisely, in HG-BP10 and HG-BAC10 the amount of the amine hydrogens of cystamine over the total number of amine hydrogens was 10%, whereas in HG-BP20 and HG-BAC20 this amount was 20%, and in HG-BP30 and HG-BAC30 30%. The molar ratios of the reagents used in each preparation are reported in Table 4.1. The choice of the two different bisacryl amides lead us to obtain two PAA families with different ionic behaviour, a purely polycationic (BP series) and an amphoteric PAA (BAC series).

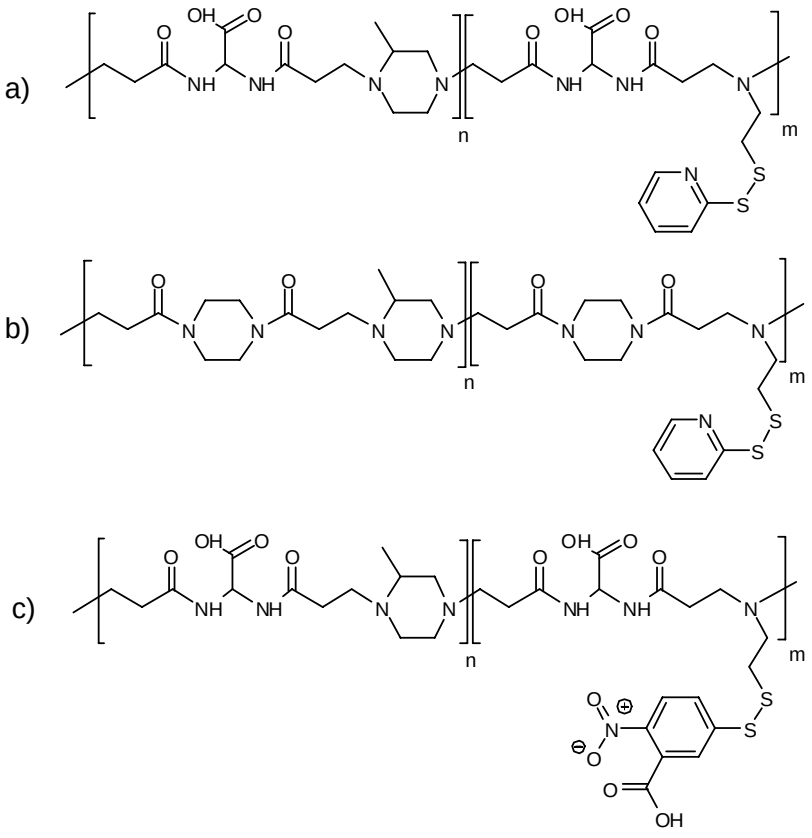

Figure4.1: general structure of PAAs containing reactive pendants towards thiol exchange reaction; a) BAC-SSPy; b) BP-SSPy; c) BAC-SSNBA. For n:m ratio see text.

The exchange reactions were performed on finely ground PAA networks swollen in ethanol (HG-BP series) or in 2:1 (v/v) water/ethanol mixture (HG-BAC series) under slightly alkaline conditions (pH 8.5-9 after dilution with water) and in the presence of a catalytic amount of 2-mercaptopyridine. A 3:1 excess 2,2'-dipirydyldisulfide with respect to cystamine moieties was employed in all cases. The reaction mixture turned to a clear homogeneous solution in few hours, the dissolution time largely depending on the particle size of the hydrogels. The reaction was then allowed to proceed for further 24 hours. The final products were purified by ultrafiltration and recovered by lyophilization, invariably leading to linear soluble polymers (Figure 4.1, a and b).

Similar results were obtained by substituting 5,5'-dithiobis(2-nitrobenzoic acid) (Ellman's reagent) for 2,2'-dipyridyldisulfide (Figure 4.1, c). The properties of the resultant products were on the most the same.

The molecular weights of the linear PAAs obtained, BP10-SSPy, BP20-SSPy, BP30-SSPy BAC10-SSPy BAC20-SSPy and BAC30-SSPy, were of the same order as those of most "traditional" PAAs. This chemically proves that all the four hydrogens of cystamine participate in the polyaddition reaction notwhistanding the chemical constrains of a cross-linked network.

Solubility tests showed that the solubility properties of dithiopyridyl-functionalized PAAs based on BAC are similar to those of the un-functionalized polymer. By contrast, functionalized BP-based PAAs are insoluble in water whereas still soluble in aqueous acids.

All dithiopyridyl-containing PAAs were fully characterized by NMR spectroscopy. Disulfide exchange reaction yields were calculated by the integral ratio of the signals at 1-1.5 ppm (assigned to the methyl group of 2-methylpiperazine residue) and at 7.3 ppm (referred to the proton β to the

nitrogen of pyridyl disulfide moiety). The ^{1}H spectrum of BP10-SSPy is reported in Figure 4.2 as typical example.

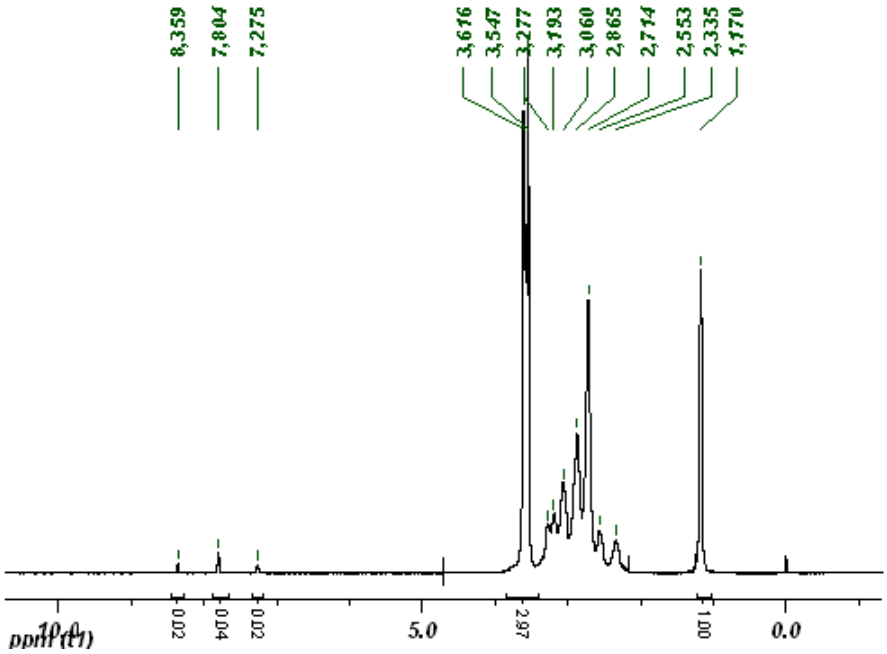

Figure 4.2: ^{1}H spectrum of BP10-SSPy. Integral ratio between 2MP methyl signal (1.17 ppm) and pyridyl moieties signals (8.36, 7.80, 7.28 ppm) is used to calculate reaction yield and degree of functionalisation for each PAA-SSPy product.

The number of pyridyl groups found in the polymers was always somewhat lower than expected; the figures reported in the Experimental part as "yield of the exchange reaction" refer to the ratio between the found and the expected dithiopyridyl content. However, it is unlikely that the exchange reaction was really incomplete, since the starting hydrogels were in all cases completely solubilized long before the reaction was stopped. This behaviour could be ascribed, instead, to possible elimination of some highly functionalized low molecular weight fractions during ultrafiltration. In all cases, for simplify reading, the soluble exchange products are labelled according to the functionalization degree of the parent hydrogels.

Ethenyl dithiopyridine groups reactivity was ascertained by means of reaction with a model oligo peptide containing a thiol group, namely glutathione reduced. The reaction was performed in deoxygenated aqueous solution, with a slight basic catalysis, with an equimolar amount of the

peptide with respect to the molar amount of polymer pendants (Scheme 4.2). After addition of glutathione reactive solution turned immediately to a yellow colour, due to the presence of mercaptopyridine, and the reaction was allowed to proceed for 30 minutes. After purification, the NMR spectra of the resultant products (BP30-SSG and BAC30-SSG) showed the presence of L-glutathione diagnostic carbon atom resonance peaks at 26.13, 53.87, 59.84, 172.44, 173.59 and 174.80 ppm and, in parallel, the disappearance of the aromatic protons of pyridine. As expected, both BAC30-SSG and its BP-deriving counterpart BP30-SSG showed optical rotation power.

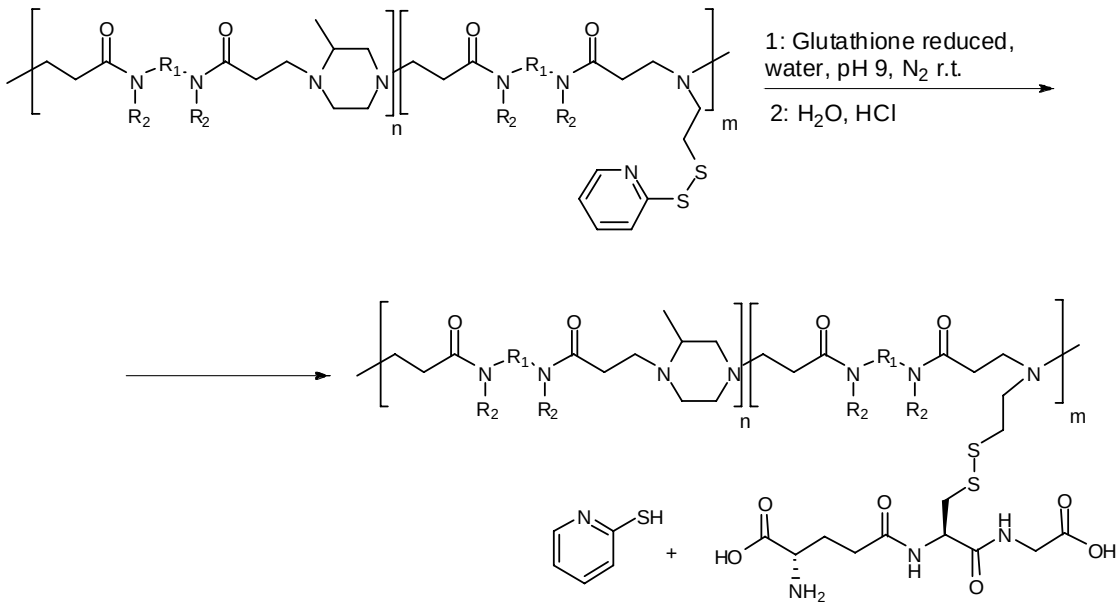

Scheme 4.2: exchange reaction between grutathione reduced and PAAs ethenyl dithiopyridine pendants.

A special reaction was monitored by UV-Vis spectroscopy. Spectra were recorded after the addition of small aliquots of glutathione reduced to the polymer solution and their superimposition is reported in Figure 3. The dark blue line represents the spectrum of the polymer solution at the beginning of the reaction: the peak at 302 nm and the shoulder at 235 nm are ascribed to the linked mercapto-pyridine, beeing polymer backbone absorbing at 220 nm.

During the exchange reaction, a strong bathochromic effect is observed due to the formation of free mercapto-pyridine. The reaction was very fast and quantitative, non further changes occurring after the 5 minutes necessary to obtain a homogeneous solution. This finding confirmed that ethenyldithiopyridinegroups reactivity is not affected by insertion in the PAAs chain.

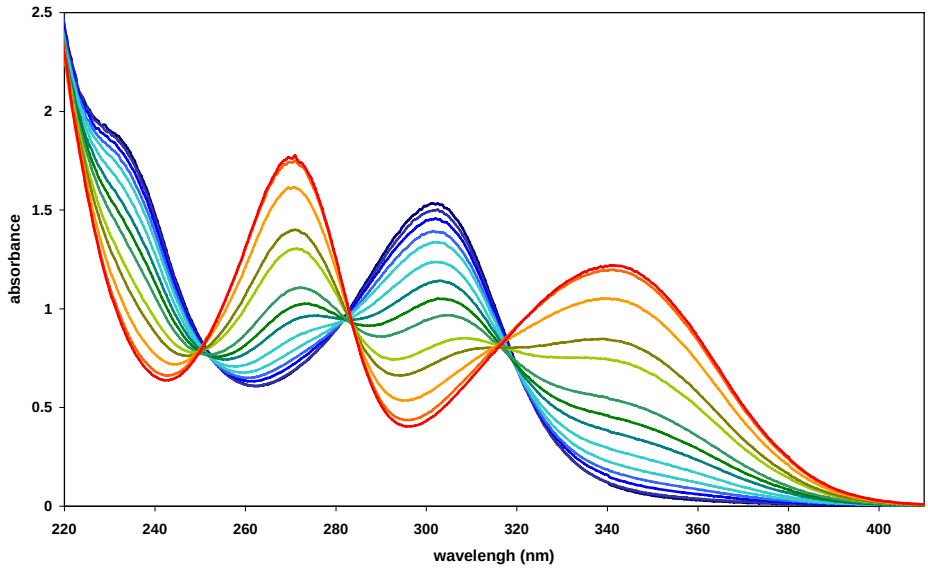

Figure 4.3: Overlap of UV-Vis absorption spectra collected during ehchange reation between glutathione reduced and BAC30-SSPy. Dark blue line represents the spectrum registered at the beginning of the reaction, red line the one registered at the end

When an equimolar amount of glutathione reduced was added, the typical absorption spectrum of mercapto-pyridine, with maxima at 343 and 265 nm, (red line) was observed and no further change occurred to the absorption spectrum if more reducing agent was added. UV determined final concentration of mercaptopyridine was in good agreement with the expected.

4.4 CONCLUSIONS

In this work, cystamine was used as cross-linking agent for obtaining families of PAA hydrogels with different structure and various amount of disulfide containing cross-linkers. These hydrogels

react with symmetrical activated aromatic disulfides, such as 2,2'-dipyridyl disulfide, yielding linear PAA carrying as side substituents activated disulfides. This functional groups can enter under mild conditions into exchange reactions with thiols, including thiol-containing peptides such as L-glutathione reduced, producing conjugates with disulfide bonds, that are stable in bloodstream and easily reduced inside cells. For these reasons PAA-SSPy can be regarded as important synthetic intermediates for "smart" PAA conjugates of biologically active molecules, peptides or proteins containing either original or artificially introduced SH groups.

Applications of this polymeric precursor and synthetic strategy are reported in the following chapters.

CHAPTER 5

Synthesis of nano-structured PAA-Cholesterol conjugates

5.1 INTRODUCTION

In the last years, increasing attention have been paid by chemistry and pharmacology research in the field of drug delivery systems. Poor solubility of drug is one of the most limiting problem in new drugs application. Hydrophilic-hydrophobic compounds, among which block co-polymer or polymer conjugates, are regarded as promising structure in view of their use in drug delivery. In fact, in aqueous environment these molecules self assemble into nano- or micro-particles in which the lipophilic part tend to segregate into domains, capable of remarkable payloads of hydrophobic molecules which solubility resulted enhanced of several times. A general review concerning polymeric nanoparticles is reported in Chapter 1.

Among amphiphilic polymers, increasing attention has been recently paid to cholesterol conjugates of hydrophilic polymers; cholesterol is one of the most common membrane sterols and

plays a relevant role in living organism metabolism and in particular in self-association of molecules in biological environments. A wide range of hydrophilic polymers, such as natural or modified polysaccharides, poly(ester-amine), poly-l-lysine, polyethyleneimine, acryl and vinyl polymers, have been used to obtain hydrophilic-hydrophobic conjugates that exhibit a strong tendency to self-association even at low cholesterol contents and have been studied as gene transfection agents, promoters of intracellular delivery of proteins, carriers of lipophilic anticancer drugs and scaffolds for tissue engineering (Yusa et al., 2000; Xu et al., 2005; Sugimoto et al., 2005; Wang et al., 2006; Iwasaki et al., 2006; Wang et al., 2007; Matsusaki et al., 2005; Akiyiama et al., 2007; Morimoto et al., 2005; Akiyoshi et al., 1997; Akiyoshi et al., 1997).

In the present part of this work, we report on preparation, NMR and morphological characterization and preliminary cytotoxicity evaluation of new PAA-cholesterol conjugates, in which the cholesterol pendants are linked to the polymer backbone through redox-sensitive disulphide bonds. These PAA-cholesterol conjugates have been obtained using the polymeric precursors which synthesis is reported in the previous chapter, and are expected to self assemble in aqueous media into hydrophilic/hydrophobic nanoaggregates or nanogels, characterized by strong hydration of the outer shell due to the highly hydrophilic nature of the PAA portion and endowed with a significant loading capability of lipophilic drugs in the hydrophobic domains. They are also expected to retain the same behavior of the parent polymers in the biological environment, as low cytotoxicity, ability to promote intracellular trafficking of bioactive molecules, and, in the case, stealth-like properties, since in the biological fluids only the hydrophilic polymer chain is exposed. The linkage between cholesterol and PAA chain is obtained by means of redox sensitive disulfide bonds. After internalization, these PAA-cholesterol conjugates are expected to be rapidly dissolve, releasing a drug payload, if present.

5.2 EXPERIMENTAL PART

5.2.1 Instruments.

All NMR experiments were performed on a Bruker Avance 500 spectrometer, operating at 500.13 MHz (^{1}H) and at 125.62 MHz (^{13}C). All deuterated solvents were purchased from Aldrich.

For all other instruments see Appendix 2: Common materials and methods.

5.2.2 Materials

Cell line 3T3/BALB-c Clone A31 mouse embryo fibroblasts (CCL163) was obtained from the American Type Culture Collection (ATCC) and propagated as indicated by the supplier. Dulbecco's Modified Eagles Medium (DMEM), 0.01 M pH 7.4 phosphate buffer saline without Ca^{2+} and Mg^{2+} (PBS), Calf serum (CS), trypsine/EDTA, glutamine, and antibiotics (penicillin/streptomycin) were purchased from GIBCO Brl. Cell proliferation reagent WST-1 was purchased from Roche Diagnostic. Tissue culture grade disposable plastics were obtained from Corning Costar.

5.2.3 Synthesis of PAA-SSChol.

All polyamidoamine-cholesterol conjugates were prepared according to a similar procedure. As model reaction, only BP-SSChol2 synthesis is reported. Parent polymers used in PAA-SSChol syntheses, namely BP-SSPy1, BP-SSPy2, BAC-SSPy1, BAC-SSPy2, were prepared following the procedure described in Chapter 4. Two different compositions for each polymer series in term of initial cystamine content were investigated, leading to the final polymers structures described below.

BP-SSPy2 hydrochloride (1.005 g, 2.6 mmol repeating units, 0.43 mmol SSPy units) and thiocholesterol (0.191 g, 0.47 mmol) were introduced in a two necked flask, equipped with magnetic stirring, and purged with nitrogen. De-oxygenated chloroform/methanol=9/1 mixture (60 mL) and triethylamine (0.3 mL, 2.6 mmol) were added and the solids allowed to dissolve under

nitrogen. The solution turned yellow in few minutes, the reaction mixture was allowed to react for further 15 hours, then the organic solution was poured in water (50 ml). The solution pH was adjusted to 2.5 adding 1M HCl aqueous solution and a emulsion was obtained. The suspension was concentrated to 40 mL by evaporation *in vacuo*, then water (50 mL) was added. The final aqueous suspension was extracted with diethylether (2 x 200 mL) and then dialyzed with a 12,000 nominal cut-off tube against a 80/20 v/v water/methanol mixture till complete disappearance of mercaptopyridine (UV monitored). The ultrafiltered suspension was eventually lyophilized.

BP-SSChol1 was prepared following the procedure described above. BAC-SSChol1 and BAC-SSChol2 were prepared following the same procedure but using 1/1 water/chloroform emulsion as reaction medium in place of methanol/chloroform mixture. Reagent thiocholesterol amount was always 1.1 mol per mol of ethenyl dithiopyridine units of the starting polymer.

BP-SSChol1: yield = 60%. Cholesterol content: 7.8% w/w (calculated on the basis of the parent polymer functionalization, BP-SSPy1). Elemental analysis: found = C 52.3, H 10.1, N 14.9, S 1.35; calculated = C 58.4, H 8.0, N 14.5, S 1.3. IR (cm^{-1}): 3422 (amide N-H stretching), 2928-2858 (C-H stretching), 1637, broad (amide C=O stretching), 1439-1385 (CH2 (bending), 1221 (amine C-N stretching), 1016 (CH bending). $[\alpha]_D^{25}$ = -1.4 $deg \cdot dm^{-1} \cdot g^{-1} \cdot cm^3$ (for comparison, thiocholesterol $[\alpha]_D^{25}$ = -23 $deg \cdot dm^{-1} \cdot g^{-1} \cdot cm^3$). As free base: soluble in chloroform, dichloromethane, methanol, dimethylsulfoxide, insoluble in water. As hydrochloride salt: insoluble in organic solvents, in aqueous solution formed suspensions.

BP-SSChol2: yield = 62%. Cholesterol content: 16.4% w/w. Elemental analysis: found = C 51.7, H 9.4, N 13.4, S 3.16; calculated = C 62.2, H 7.9, N 12.1, S 2.6. $[\alpha]_D^{25}$ = -2.7 $deg \cdot dm^{-1} \cdot g^{-1} \cdot cm^3$. Solubility as BP-SSChol1. As for the PAA bearing ethenyldithiocholesterol pendants, only BP-SSChol2 was considered, performing the integration between the methyl carbon of the

methylpiperazine ring and one of methyl signals of the cholesterol moiety; the observed values confirmed the n:m ratios of the starting material.

BAC-SSChol1: yield = 61%. Cholesterol content: 7.3% w/w. Elemental analysis: found = C 50.6 H 8.2, N 16.7, S 0.9; calculated = C 48.2, H 7.1, N 15.7, S 0.9. IR (cm^{-1}): 3416 (amide NH stretching), 3281 (carboxylic acid OH stretching), 2967-2828 (CH stretching), 1650-1621, broad (amide and carboxylic C=O stretching), 1519 (amide NH bending), 1454-1385 (CH2 bending), 1129 (amine C-N stretching), 1134 (CH bending). Solubility: insoluble in water and in organic solvents; in aqueous solution formed suspensions.

BAC-SSChol2: yield = 62%. Cholesterol content: 13.1% w/w. Elemental analysis: found = C 50.7, H 8.2, N 17.1, S 2.2; calculated = C 50.2, H 7.3, N 14.3, S 2.0. Solubility as BAC-SSChol1.

Complete ^{1}H and ^{13}CNMR characterization of the two series of polymers is reported in Table 5.1.

Table 5.1. Relevant ^{1}H and ^{13}C chemical shifts (δ) of PAA-cholesterol derivatives.*

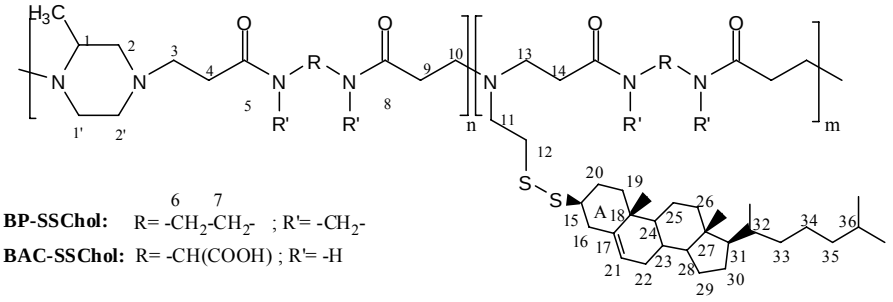

BP-SSChol: R= -CH_2-CH_2- ; R'= -CH_2-

BAC-SSChol: R= -CH(COOH) ; R'= -H

		1	2 [a]	1'/2'	3	4	5/8	6/6'	7/7'	9	10 [a]	15	16	17	18	19 [a]	20 [a]	21	22 [a]	23	24
BP-SSChol	**^{1}H**	2.70	2.50;3.00	3.15-3.40	2.90	2.60		3.50	3.50	2.70	2.92;3.30	2.65	2.30			1.80;2.00	1.95;1.60	5.35	1.45;1.90	1.37	0.92
	^{13}C	52.8	57.3	50.5	52.8	29.3	169.0	45.0;45.2	41.3;41.5	28.4	48.2	49.95	38.9	141.0	36.7	39.6	28.9	121.7	31.8	31.8	50.1

		25	26 [a]	27	28	29 [a]	30 [a]	31	32	33 [a]	34 [a]	35 [a]	36	Me-1	Me-18	Me-27	Me-32	Me-36
	^{1}H	1.45	1.80;2.00		0.90	0.95;1.50	1.20;1.80	1.00	1.50	1.00;1.30	1.05;1.25	1.10;1.20	1.50	1.30	0.97	0.65	0.92	0.83;0.835
	^{13}C	20.9	39.4	42.2	56.7	24.2	28.2	56.1	36.1	36.1	23.8	39.3	27.9	15.0	19.2	11.8	18.6	22.5;22.7

				3.10;3.46																	
				49.3								15	16	17	18	19	20 [a]	21	22 [a]	23	24
BAC-SSChol	**^{1}H**	3.46	2.90;3.46	3.19;3.62	3.14	2.70		5.40				2.62	2.30			1.80-2.00	2.00;1.55	5.40	1.50;2.00	1.50	0.95
	^{13}C	56.25	55.1	48.3	52.5	30.3	172.0	58.0		172.0		50.3	39.1	141.7	36.8	39.95	29.1	121.2	31.9	31.9	50.7

		25	26	27	28	29 [a]	30 [a]	31	32	33 [a]	34	35	36	Me-1	Me-18	Me-27	Me-32	Me-36	**11**	**12**
	^{1}H	1.50	2.00		0.90	0.95;1.50	1.25.1.83	1.00	1.40	0.95;1.20	1.20	1.5	1.55	1.44	1.00	0.70	0.90	0.85		
	^{13}C	21.0	39.8	42.3	56.8	24.3	28.2	56.2	35.8	36.2	23.8	39.3	28.0	15.0	19.3	11.9	18.7	22.6;22.8	**44.2**	**29.7**

[a] for ^{1}H resonance: AB system

*BP-SSChol in $CDCl_3/CD_3OD$ (95:5 ratio) as solvent (HR NMR),BAC-SSChol hydrochloride in D_2O (HR NMR) and BAC-SSChol swelled in $CDCl_3$ (HRMAS NMR). See the text for major explications

5.2.4 Loading capacity.

The uptake ability towards hydrophobic substances was estimated by measuring the amount of azobenzene and estradiol dissolved into the hydrophobic core of the PAA-SSChol nanoparticles samples. The hydrophobic substance (1.5 mg) was added to the polymer solution (1.5 mg polymer in 1.5 mL of water), adjusted to pH 7.4 in PBS 0.01N, in presence of a small amount of methanol (15 μL). After 48 hours the volume was firstly reduced under vacuum to remove methanol, then restored to 1.5 mL with water and the suspension filtered with a 0.45 μm pore size filter to remove the undissolved hydrophobic molecule. Methanol was added to the filtered solution in an equal volume and absorption intensity was measured by UV-Vis spectroscopy at 430 nm for azobenzene and 280 nm for estradiol. A similar sample without polymer was prepared as a blank and the hydrophobic molecule absorption subtracted to the polymer sample ones. The amount of hydrophobic substance was determined with a pre-prepared analytical curve.

5.2.5 Biological evaluations.

Cell Line. Cytoxocity evaluations of the investigated materials were carried out using the 3T3/BALB-c Clone A31 cell line. Cells were grown in DMEM containing 10% CS, 4 mM of glutamine, and 100 U/mL:100 *í*g/mL penicillin:streptomycin (complete DMEM).

Subculturing. A 25 mL flask containing exponentially growing 3T3 cells was observed under and inverted microscope for cell confluence. The complete DMEM media was then removed, and cells were rinsed for a few min with PBS. The buffer solution was removed, and cells were incubated with 0.5 mL of trypsin/EDTA solution at 37 °C in 5% CO_2 incubator for 5 min or until the monolayer started to detach from the flask. Cells were suspended in an appropriate volume of DMEM and plated at a split ratio of 1:6 or 1:10 in a 75 mL flask.

For routine culturing and evaluation of morphology, cells were analyzed under an inverted microscope Nikon Eclipse TE2000-U.

Determination of IC50 of Polymeric Materials. The IC_{50} (50% inhibitory concentration, that is the material concentration at which 50% of cell death in respect to the control is observed) of the investigated polymers was evaluated by exposing cells for 24 h to DMEM containing different polymer concentrations (1 to 10 mg/ml). At the end of the exposure time, cells were incubated with WST-1 cell proliferation reagent for the quantitative evaluation of cell proliferation.

Cell Proliferation Assay. Quantitative proliferation was assayed by using the cell proliferation reagent WST-1 and by following the protocol indicated by the manufacturer. Briefly, cells were allowed to proliferate in DMEM containing different concentration of polymeric materials and then incubated or 4 h with an appropriate volume of WST-1 tetrazolium salts. Formazan production was detected at 450 nm, with 620 nm as reference wavelength using an ELISA microplate reader (Biorad).

5.3 RESULTS AND DISCUSSION

The new PAA-cholesterol conjugates were obtained by thiol-exchange reaction of thiocholesterol with PAA precursors bearing ethenyldithiopyridyl pendants (PAA-SSPy). Four PAAs where chosen as precursors, two purely cationic (BP-SSPy1 and BP-SSPy2) and two amphoteric (BAC-SSPy1 and BAC-SSPy2). They were prepared by employing 1,4-bisacryloylpiperazine (BP) and 2,2-bisacrylamidaocetic acid (BAC), respectively, as bisacrylamide monomers.

5.3.1 Synthesis of PAA-SSChol.

Different PAA-cholesterol conjugates were obtained by thiol exchange reaction of thiocholesterol with the ethenyl dithiopyridine units of BP-SSPy and BAC-SSPy precursors, which syntheses an characterization have been previously developed and studied. Full discussion is reported in Chapter 4: “Synthesis of new polymeric precursors of PAA-drug or PAA-protein conjugate by disulfide

bond". We decided to use both polymer series in order to have a comparison between cholesterol conjugates of both cationic and amphoteric PAAs.

In the case of BP-SSPy polymers (Scheme 5.1), the thiol exchange reaction was performed in a 1:9 (v/v) methanol/chloroform, where both reactants were soluble, whereas in the case of BAC-SSPy (Scheme 5.2) the reaction was performed in a chloroform/water slurry, thiocholesterol residing in the former solvent and BAC-SSPy in the latter.

The thiol exchange reactions went to high yields in the presence of triethylamine as basic catalyst. Stronger inorganic bases lead invariably to undesired side reactions and were therefore discarded as catalysts. When the reaction was complete, water was added to the reaction mixtures and the raw products were acidified to pH 3.5 with dilute hydrochloric acid. The organic solvents were then stripped under vacuum, the resultant suspension extracted with diethyl ether to eliminate excess thiocholesterol, and eventually dialyzed against an 80:20 water:methanol mixture until the complete disappearance of the 2-mercaptopyridine byproduct (UV monitoring). Purified products were obtained in yields higher than 60%.

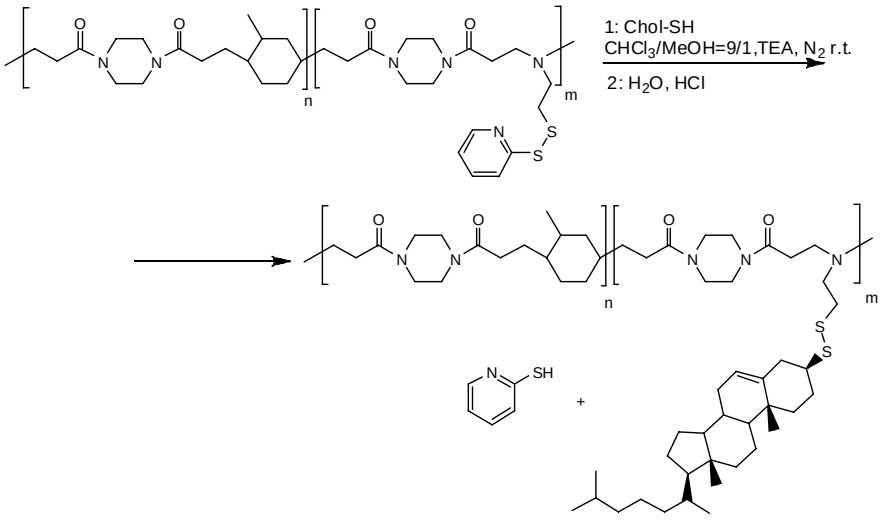

Scheme 5.1: BP-SSChol syntesis.

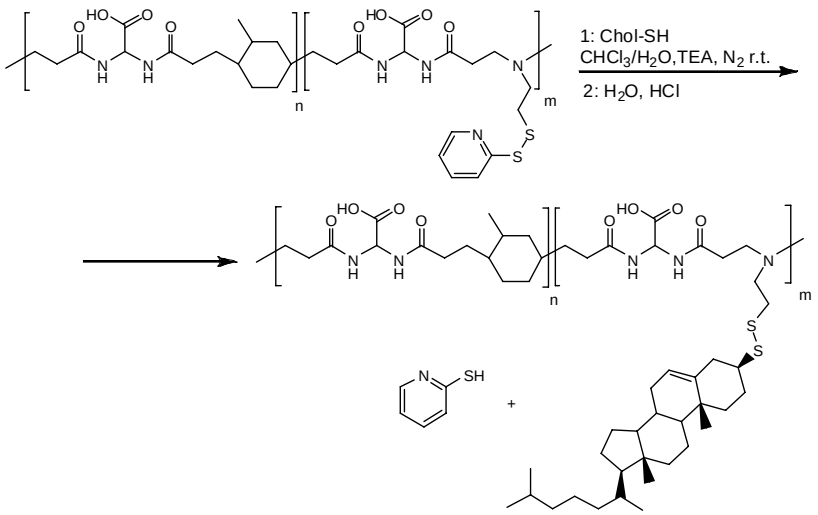

Scheme 5.2: BAC-SSChol syntesis.

All product formed stable cloudy suspensions in water. The polymers of the BP series, as hydrochlorides, were insoluble in chloroform, dichloromethane, methanol and dimethylsulfoxide, whereas, as free bases, showed good solubility in some organic solvents, such as methanol and chloroform. As a consequence, it was possible to perform Specific Optical Rotation measurements and NMR analyses of these products in solution. Indeed, these products showed Specific Optical Rotation ability revealing the presence of chiral moieties linked to the otherwise non-chiral polymer chain. The conjugates of the BAC series were insoluble in organic solvents in all conditions.

The IR spectra of all products showed the presence of carbonyl, amino and amido groups. The absence of peaks due to aromatic compounds confirmed that reaction proceeded to completeness and 2-mercaptopyridine was completely eliminated. Elemental analyses were as expected. In particular the agreement between the found and calculated nitrogen and sulfur percentage was excellent.

5.3.2 NMR characterization

BP-SSChol NMR characterization of this amphiphilic polymers represented an interesting challenge. ^{1}H and ^{13}C NMR spectra of BP series polymer, soluble in organic solvents as free base, were first recorded in DCl_3/CD_3OD 9/1 and the chemical shift assignments were reported in Table

5.1. The assignments relative to the cholesteryl moieties were obtained by comparison with the spectral data of the starting thiocholesterol. All proton and carbon resonances were very similar to the thiocholesterol's ones with the exception of those belonging to the A ring, in which the thiol group was replaced by a disulphide function. In particular, the C-15, C-16, and C-20 resonances, observed in the ^{13}C spectrum of thiocholesterol, at 39.7, 44.2 and 34.0 ppm, respectively, were shifted at 49.9, 38.4 and 28.9 ppm, respectively (Figure 1,a). These chemical shift changes suggested the presence of cholesteryl moieties bound to the main backbone with a disulphide linkage. Remarkably, the lines of cholesterol resonances were sharp in both ^{1}H and ^{13}C spectra in $CDCl_3$ (Figure5.1,a and 5.2,a) whereas those of the PAA backbone much broader. This behavior, never observed in the case of the BP-SSPy parents, was ascribed to the tendency of BP-SSChol to undergo phase association. The hypothesis is that in $CDCl_3$ the hydrophilic PAA portion of the conjugates partially segregates giving rise to a reversed-micellar structure. This reduces mobility giving rise to line broadening.

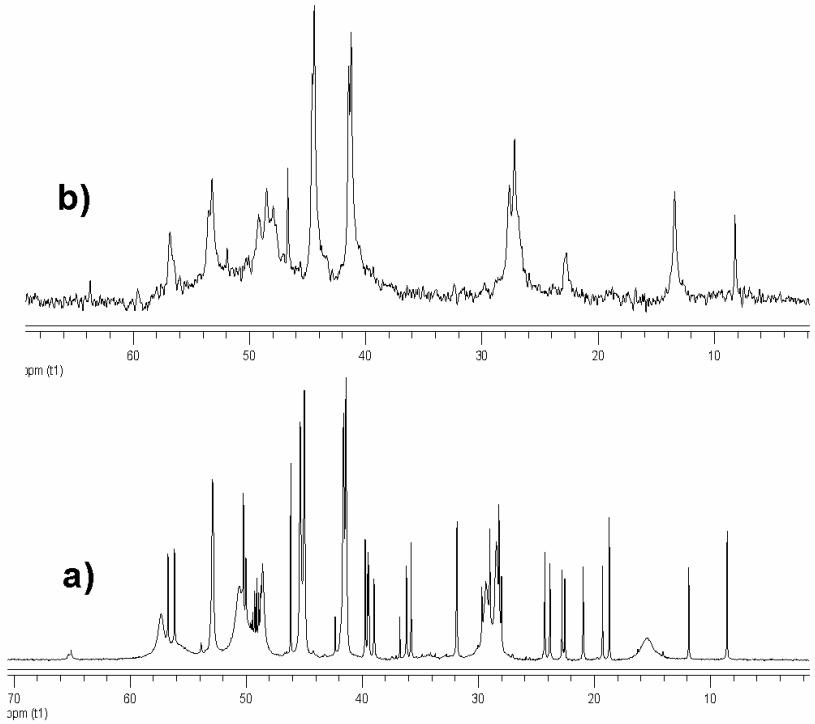

Figure 5.1: ^{13}C spectra of BP-SSChol2 in a) $CDCl_3$ an b) D_2O.

This hypothesis was confirmed by the observation of an analogous, but exactly reversed behavior in D_2O, in which both proton (Figure 5.2,b) and carbon (Figure 5.1,b)spectra of BP-SSChol hydrochloride revealed only PAA backbone's signals, thus indicating the complete loss of mobility of cholesteryl residues.

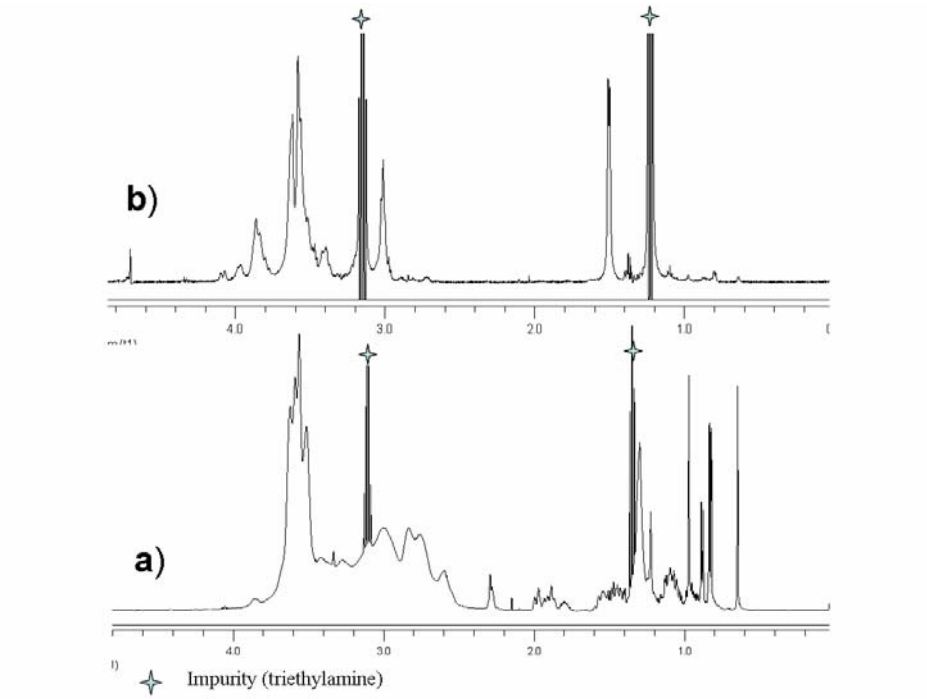

Figure 5.2 ^{1}H spectra of BP-SSChol2 in a) $CDCl_3$ an b) D_2O. ✦Impurity (TEA)

The obvious explanantion is that BP-SSChol conjugates undergo phase segregation of insoluble cholesteryl domains while water soluble PAA segments completely dissolve in D_2O.

BAC-SSChol. Since these conjugates are not soluble in organic solvents, but only swell in $CDCl_3$, the HRMAS technique was used to perform the NMR study. Interestingly, the resulting NMR spectra showed exclusively signals ascribable to the cholesterol residues and the ethylendithionyl bridges. The ^{1}H and ^{13}C assignments reported in Table 1 were indeed in agreement with the chemical shift values previously found for the cholesteryl moiety of BP-SSChol. In addition, it was possible to recognize the C-11 and C-12 signals of the ethylendithionyl segment at 44.2 and 29.7 ppm, respectively. (Figure 5.3,a).

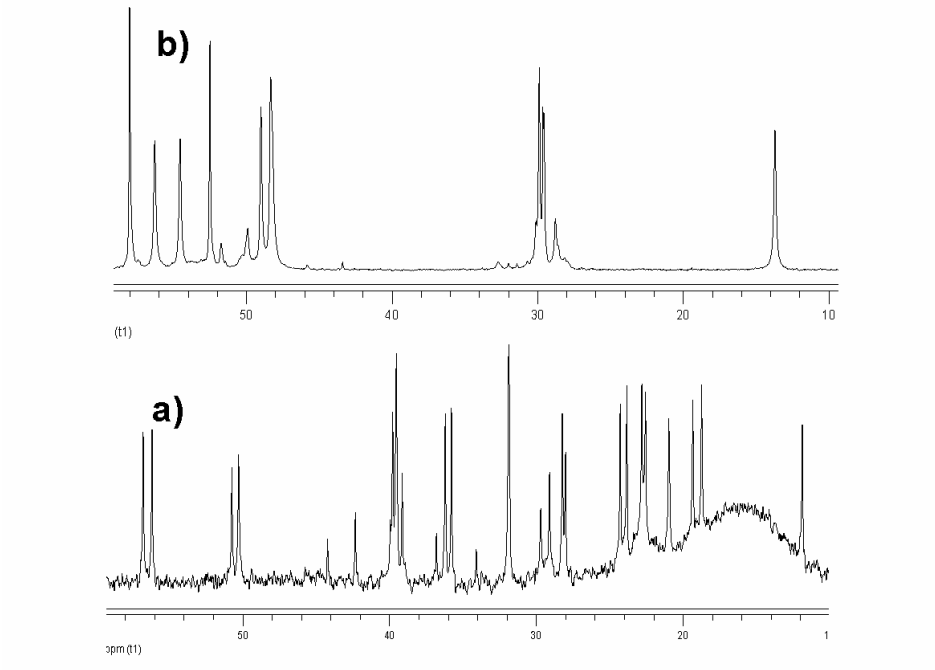

Figure 5.3: ^{13}C spectra of BAC-SSChol2 in a) $CDCl_3$ an b) D_2O.

In contrast, the spectra of BAC-SSChol hydrochloride conjugates, which give stable dispersions in D_2O, revealed only PAA backbone's resonances, in agreement with the previously reported BAC-SSPy's assignments (Figure 5.3,b and 5.4,b). Therefore, the chemical shifts reported in Table 5.1 are referred to the spectra of BAC-SSChol swelled in $CDCl_3$ (HRMAS), for the cholesterol residue, and to BAC-SSChol hydrochloride in D_2O, for the polymer the backbone.

This result points to the conclusion that, as in the case of BP-SSChol conjugates, even in BAC-SSChol ones hydrophobic cholesteryl units segregate from D_2O into insoluble lipophilic domains, which completely lose their mobility and are therefore not revealed by NMR spectroscopy.

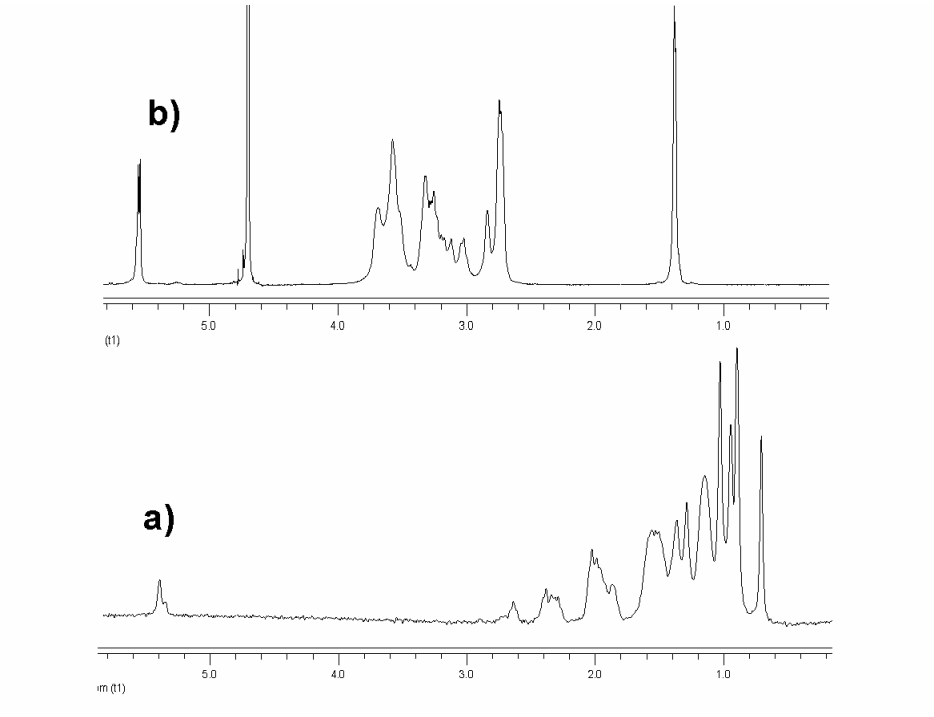

Figure 5.4: ^{1}H spectra of BAC-SSChol2 in a) $CDCl_3$ an b) D_2O.

5.3.3 Morphological characterization.

The dimensions of PAA-cholesterol nanoaggregates in aqueous media were determined by Dynamic Light Scattering (DLS) and their morphological analyses performed by Transmission Electron Microscopy (TEM).

Each sample was routinely filtered through 1 and 0.45 μm porosity filters, prior to DLS and TEM analyses respectively. Filtrate solutions invariably showed, upon drying, a nearly quantitative recovery of the initial sample.

Since PAAs carry ionizable groups, DLS analyses were performed at two different pHs, namely pH 3 and 7.4, in order to evaluate pH-mediated conformational changes. Data obtained, averaged over measurements performed in triplicate are reported in Table 5.2.

All PAA-cholesterol conjugates were found to self-assemble in nanoparticles with narrow monomodal diameter distributions ranging between 100 and 300 nm. It may be observed that BP-

based nanoparticles exhibited invariably larger dimensions than BAC-based nanoparticles with similar cholesterol content, probably due to the lower hydrophilicity of the BP-based PAA backbone, which reduces dispersion ability and leads to a larger aggregates. Moreover, BP-based nanoparticles undergo a considerable increase in diameter as the solution pH increases. This result may also be ascribed to the larger nanoparticle aggregation related to the decrease in the net positive charge, hence in hydrophilicity, occurring in the polymer backbone of BP-based PAAs.

Table 5.2: DLS Analyses of PAA-SSChol conjugates.

Sample	pH 3		pH 7.4	
	D[a] (nm)	SD[b] (nm)	D (nm)	SD (nm)
BP-SSChol1	157	2.8	241	15.9
BP-SSChol2	186	6.5	261	21.4
BAC-SSChol2	106	3.7	122	6.5
BAC-SSChol1	109	3.1	117	6.4

[a] D = diameter of the most frequent particle fraction.

[b] SD = standard deviation from D value.

TEM imaging experiments, performed on dried samples prepared by means of a negative staining technique, lead invariably to results similar to those reported in Figure 5.5, referring to a BAC-SSChol2 sample.

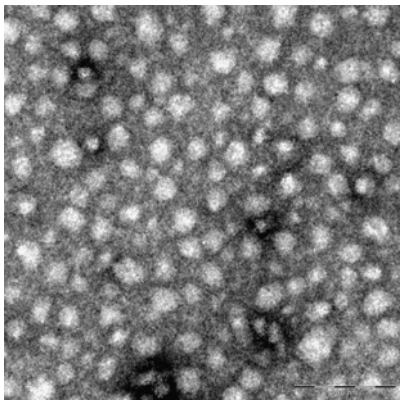

Figure 5.5: TEM image of BAC-SSChol2 nanoparticles obtained with negative staining technique.

Homogeneous round-shaped nanoparticles were revealed, characterized by a quite regular diameter distribution centered around 40 nm. As expected, nanoparticles' diameter determined by TEM in the dry state was invariably approximately 3 times smaller than those obtained by DLS in aqueous media. This finding confirms the large water absorption ability of PAA-cholesterol conjugates, ascribed to their amphiphilic nature. These may be therefore defined as true nanohydrogels, characterized by a water absorbing PAA matrix and insoluble cholesteryl domains as physical cross-links.

5.3.4 Evaluation of uptake ability of PAA-cholesterol conjugates towards hydrophobic substances.

The uptake ability of PAA-cholesterol towards two different hydrophobic probes, namely azobenzene and estradiol, was estimated by measuring the amount of probe "solubilized" by the conjugates by means of UV measurements, in comparison with the amount solubilized by plain water and aqueous PAA solutions. Azobenzene was chosen due to its high lipophilicity and its strong absorbance of UV light, that made it easy to detect its concentration even in very dilute solutions. Estradiol was instead chosen for its structure affinity with cholesterol, which was expected to increase the uptake ability. The amount of azobenzene and estradiol uptaken by each PAA-cholesterol sample is reported in Table 5.3.

The uptake ability ranged between 9 and 20% of the polymer conjugates on a weight to weight basis. It may be observed that a good proportional relationship exists between the amount of hydrophobic probes "solubilized" and the amount of cholesterol moieties in the conjugate. This gives clear indication that lipophilic probes were absorbed in the hydrophobic cholesterol domains. Moreover, the observed uptake ability of the PAA-cholesterol conjugates was comparable to what

elsewhere reported with other amphiphilic polymers, even if with different lipophilic probes (wang, et al., 2005; Iwasaki, Akiyoshi, 2006; Wang et al., 2007).

Table 5.3: Evaluation of uptake ability of hydrophobic substances for PAA-SSChol conjugates.

Sample	Azobenzene/ PAA-SSChol (mg/g)	Azobenzene/ cholesterol[a] (w/w)	Estradiol/ PAA-SSChol (mg/g)	Estradiol/ cholesterol[a] (w/w)
BAC-SSChol1	131	1.8	90	1.3
BAC-SSChol2	288	1.8	124	0.8
BP-SSChol1	94	1.1	129	1.5
BP-SSChol2	210	1.3	189	1.1

[a] weight ratio of the lipophilic probe versus cholesterol contained in the polymer conjugate.

5.3.5 Biological evaluations

The cytoxocity (cellular compatibility) of PAA-cholesterol conjugates was assessed by in vitro cytotoxicity assays performed against 3T3/BALB-c Clone A31 cell lines. Cells were incubated for 24 hours with the polymer solutions and then analyzed for viability with WST-1 tetrazolium salt, which allows for the quantitative evaluation of metabolically active cells. The resulting IC_{50} values, namely BP-SSChol1: 1.5, BP-SSChol2: 3, BAC-SSChol1: >10; BAC-SSChol2: 3 mg/ml, point to the conclusion that all PAA-cholesterol conjugates exhibit, on the whole, low cytotoxicity, especially in the case of BAC-SSChol1 (IC_{50}>10). Apparently, in the two series of polymers, the cholesterol content acts in the opposite way, in that higher contents decrease cytotoxicty of BP-based conjugates, whereas decreases that of the BAC-based ones. However, it is not possible to draw straightforward conclusions regarding the effect of cholesterol content on cytotoxicitiy, since it affects the polymers' state in aqueous systems and it was not possible to screen out this factor.

5.4 CONCLUSIONS

This present chapter reports on a particular application of the research line concerning disulfide based PAAs conjugates, opened with the previous reported work. Thiocholesterol was successfully linked to PAA through ethenyl dithiopyridine pendants and two different families of PAAs, one cationic and one amphoteric were obtained. Both polymer showed remarkable amphiphlic properties and in water formed stable nanoparticles suspensions. Preliminary test on dimensional pH sensitive changes ,suggest for these nanoparticles a inner structure similar to physically cross-linked nano-hydrogels. Hydrophobic cholesterol domains demonstrate capable of considerable lypophilic molecules payloads; moreover preliminary cytotoxicity assays demonstrate a good cytocompatibility. Further studies are ongoing to confirm preliminary results shown and to demonstrate, as we expect, a massive release of drug in presence of reducing agents, after cleavage of disulfide links between cholesterol and polymer, and consequent nanoparticle dissolution. At present, these novel PAA-cholesterol conjugates appear very promising for applications in the field of polymer therapeutics.

CHAPTER 6

Synthesis of cross linked polyplexes for applications in gene delivery

6.1 INTRODUCTION

Gene therapy strategies have been proposed for a vast and diverse range of disorders for which current available treatments are deemed unsatisfactory. Such a research interest to explore a variety of methodologies for the achievement of effective DNA delivery and subsequent expression. A major branch of investigation has focussed on a pharmaceutical approach through the development of nonviral vectors. Within this field, cationic polymers, such as poly(L-lysine) (PLL), have demonstrated efficient condensation of DNA (Kwoh et al., 1999). Systems based on poly(ethylenimine) (PEI) (Boussif et al., 1995), poly(amidoamine) (PAMAM) dendrimers (Kukowska-Latallo et al., 1996), linear PAAs (Jones et al, 2000; Richardson et al., 2001; Ferruti, Franchini et al., 2007) and polymethacrylate-based systems (Van de Weitering et al., 1997), have shown significant promise. Non-viral vectors hold several advantages over modified viruses employed for gene delivery purposes, such as of improved and more predictable safety, higher

DNA carrying capacity and, therefore, increased versatility, more straightforward production and better quality control. Nevertheless, their efficiency is currently lagging far behind that of viral systems. This perhaps should not surprise when taking into account the barriers that exist to the successful delivery of an exogenous sequence of DNA to the nucleus of a target cell and that viruses have evolved to perform such a role (Pouton, Seymour, 1998). It seems that, in all likelihood, a successful nonviral system will require a number of distinct elements, each with a specialist role in the realisation of this goal. Having identified a number of promising cationic polymer candidates, attention has now shifted to their incorporation in multicomponent systems in order to improve their efficacy (Wu et al, 1994; Zhou et al., 1994; Dashg et al., 2000).

The stability of the polymer/DNA complex in serum is a key area of investigation. Particulate systems are rapidly cleared from the circulation by the reticuloendothelial system following parenteral administration, resulting from a range of interactions with serum components, including the complement system (Stolnik et al., 1994) and subsequent phagocytosis. Moreover, the interaction with serum components, together with high dilution, can also affect particle stability and contribute to polyplexes disruption. Thus, the delivery system can be eliminated before it reaches its intended target cell population. A potential solution to this problem is the formation of a steric barrier around particles, as it has been demonstrated with nanoparticulate drug delivery systems by the inclusion of hydrophilic polymers, such as poly(ethylene glycol) (PEG). This PEG layer greatly reduces the adsorption of serum components to the particle surfaces, reducing uptake by the mononuclear phagocytes thus increasing the circulating life of the delivery system (Gref et al., 1994). Furthermore, these hydrophilic polymers can also prevent interparticulate aggregation, improving the colloidal stability of systems. This approach can also be applied to DNA vectors, and a number of researchers have explored the formation and polyfection performance of DNA complexes with co-polymers of varying architecture formed from cationic and hydrophilic polymer segments (Choi et al., 1999; Toncheva et al., 1998; Nguyen et al., 2000).

On the other hand, the major barriers for non-viral gene delivery are believed to be inefficiencies in endosomal escape of the polyplexes that avoid the lysosomal degradation pathway, or in unpacking of DNA from the polyplexes that can enable transcription (Shaffer et al., 2000; Hill et al., 1999).

In past years several linear PAAs have been studied as cationic polymers for DNA delivery. Previous findings established a number of structures that exhibited favourable biocompatibility, in vitro polyfection performance and DNA-condensing properties (Danusso, Ferruti, 1970; Ferruti, Ranucci, 1991). In particular the PAA obtained by reaction of methylene-bis(acrylamide) and N,N'-dimethyl ethylenediamine was identified as the best transfection promoter. In further studies a tri-block co-polymer has been synthesised by addition of two PEG chains on both PAA ends and several formulations have been tested to identify the best ratio between the polycationic polymer and the hydrophilic one, in order to obtain less cytotoxic nanoparticles with increased colloidal stability and retained transfection efficiency in vitro (Bignotti et al., 1994; Rackstraw et al., 2002).

Recently much attention is focusing on disulphide linkages for their importance in biological fields. The presence of the disulphide linkages could increase stability of polyplexes in bloodstream increseang also the biodegradability of the polymers by reductive cleavage in the intracellular environment. Polyplexes obtained resulted more prone to release DNA once internalized inside cells, and enhanced gene expression, as well as a lower cytotoxicity profile of the polymers are obtained (Miyata et al., 2004; Oupicky et al., 2002; Read et al., 2005; Gosselin et al., 2001 and 2002). In recent research it has been demonstrated that disulphide containing PAAs behave as powerful transfection promoters with a very low toxicity (Lin et al, 2006; Christensen et al., 2006; Lin et al., 2007; Lin et al., 2008).

The aim of this work was to increase polyplexes stability using novel PEG-PAA based block co-polymers, capable to form, during polyplexes formation, smart disulphide bridges between different polymer chains. The particles obtained are expected to be resistant to enzymatic degradation as well

as to high dilution and high salt concentration, such as in the bloodstream, but undergo reduction and consequent loss of stability in presence of reducing agents, such as inside cells, thus favouring, in principle, DNA endosomal escape and full explotation of transfection ability.

6.2 EXPERIMENTAL PART

6.2.1 *Materials*

Homo poly(MBA-DMEDA), 30K, amino terminated.(CP1)

MBA (1.54 g, 10.0 mmol) was added in small portions to an aqueous solution of DMEDA (0.88 g, 10.0 mmol in 3.5 ml of water) under nitrogen. The mixture was allowed to react for three days under stirring. Subsequently the solution pH was adjusted to 2.5 with a 1 M aqueous HCl, the solution was ultrafiltered through a membrane with a molecular weight cut off 3000 and eventually freeze dried. Product was characterized by SEC and NMR spectroscopy. $\overline{M}_n$: 27000, $\overline{M}_w$: 42000; Yield: 2.6 g, 93%. ^{1}H NMR (d_6-DMSO): 2.25 (s, 6H, C**H$_3$**N); 2.39 (t, 4H, CO-CH$_2$-C**H$_2$**-N); 2.51 (s, 4H, N-C**H$_2$**-C**H$_2$**-N), 2.66 (t, CO-C**H$_2$**-, 4H); 4.56 (m, broad, NH-C**H$_2$**-NH, 2H), 8.82 (t, broad, N**H**, 2H**).**

Trityl-DMEDA[31] (**1**)

N,N'-Dimethylethylenediamine (19.37 ml, 0.18 mol) was dissolved in dichloromethane (DCM, 75 ml) under stirring in nitrogen atmosphere and the solution cooled to 5°C. Triphenylmethyl chloride (5 g, 0.018 mol) was added in small portions. After the addition was completed, the solution was allowed to react at room temperature for 4 hours. During this time the reaction was monitored by TLC (eluent chloroform:ethanol=8:2), then another aliquot of DCM (50 ml) was added and the solution washed several times with water (50 ml) until neutral pH of the aqueous phase was reached. The organic layer was dried over anhydrous sodium sulphate and the solvent evaporated under reduced pressure. A pale yellow viscous oil was obtained in an almost

quantitative yield. TLC of the product showed a single spot (R.f. 0.54). ^{1}H NMR (CD_3OD): 7.52 (t, benzene ring, 3H), 7.28 (t, benzene ring, 6H), 7.18 (t, benzene ring, 3H), 2.85 (t, CH_3-NH-C**H**$_2$-, 2H), 2.39 (s, C**H**$_3$-NH-CH_2, 3H), 2.31 (t, CH_3-N(Trit)-C**H**$_2$, 2H), 2.10 (s, C**H**$_3$-N-Trit, 3H).

Trityl DMEDA-MBA adduct (**2**)

MBA (55.0 g, 0.35 mmol) was dissolved in methanol (400 ml), (**1)** (5.9 g, 0.017 mol) was added in portions and the mixture was allowed to react for 20 hours at room temperature in the dark. The completion of the reaction was monitored by TLC (eluent $CHCl_3$/MeOH=9:1), then methanol was removed under reduced pressure, the crude product dissolved in chloroform (500 ml) and the organic solution washed several times with water until complete disappearance of MBA trace, as revealed by TLC. The organic layer was dried over anhydrous sodium sulphate and the solvent evaporated under reduced pressure. A pale yellow solid was obtained in an almost quantitative yield. TLC of the product showed a single spot (R.f. 0.7; for comparison MBA R.f. 0.5, Trityl-DMEDA R.f. 0.61). 1H NMR ($CDCl_3$): 7.51 (t, benzene ring, 3H), 7.29 (t, benzene ring, 6H), 7.18 (t, benzene ring, 3H), 6.25, 6.02, 5.68 (m, terminus double bond, 3H), 4.53 (t, broad, -NH-C**H**$_2$-NH-, 2H), 2.77, 2.62, 2.36, 2.31 (m, C**H**$_2$-N(CH_3)-C**H**$_2$-, 8H), 2.39 (s, C**H**$_3$-NH-CH_2, 3H), 2.23 (s, C**H**$_3$-N-(CH_2-)$_2$, 3H), 2.10 (s, C**H**$_3$-N(Trit)-CH_2, 3H).

MBA-DMEDA adduct (**3**)

(**2**) was added in portions to a 1 M HCl aqueous solution (100 ml). The thick suspension formed was left stirring for 1 hour, diluted with water (50 ml) and subsequently washed several times with DCM (6 x 50 ml) to eliminate triphenylcarbinol from the aqueous phase. The organic phase was separated, extracted with water (4 x 50 ml) and the combined aqueous phases eventually freeze dried. A white solid was obtained in an almost quantitative yield (5.6 g, 96 %). 1H NMR (D_2O):

N-tert-Butyloxycarbonyl Cystamine Hydrochloride[32] (**4**)

TEA (19.8 g, 0.190 mol) was added to a dry methanol solution (250 ml) of cystamine bis-hydrochloride (15.0 g, 0.066 mol), and the solution stirred for 15 min at room temperature. Di-tert-butyldicarbonate (14.5 g, 0.066 mmol) was added and the stirring maintained for an additional 3 h, monitoring the reaction progress by TLC (eluent: chloroform/ isopropyl alcohol 1:1, Rf product: 0.25). The solvent was then evaporated, and a 1 M KH_2PO_4 aqueous solution (350 ml, pH 4.2) was added. The aqueous phase was extracted with diethyl ether (3 x 100 ml) to remove N,N'-di-tert-butyloxycarbonyl cystamine, then brought to pH 9 with 3 M NaOH, and extracted with ethyl acetate (6 x 150 ml). The combined organic phases were dried over anhydrous sodium sulphate and evaporated to dryness. The residue was dissolved in water (150 ml) at pH 4 (HCl). The clear solution obtained was freeze-dried and N-tert-butyloxycarbonyl-cystamine isolated as hydrochloride (9.6 g, 75%).

1H NMR (D2O): 1.30 (s, Boc C**H**$_3$, 9H), 2.72 (t, C**H**$_2$-S, 2H), 2.83 (t, C**H**$_2$-S, 2H), 3.21–3.31 (m, 4H, NH_3^+-C**H**$_2$ and CONH-C**H**$_2$).

Mono-piperazine terminated mono-methoxy-PEG750[33] (**5**)

Mono-methoxy-PEG750 (20 mmol, 15g) was introduced in two necked round bottom flask equipped with stirring bar, vacuum/nitrogen inlet and a glass stopper. PEG was melted under gentle warming, purged and kept under nitrogen. Chloroform (50 ml) was added and PEG allowed to dissolve. A three fold excess CDI (9.72 g, 60 mmol) was subsequently added in small portions, after 1 hour, unreacted CDI was quenched by addition of water (5 ml) and the organic phase was washed with brine (4 x 30 ml). The organic layer was dried over anhydrous sodium sulphate, a three fold excess piperazine (5.17 g, 60 mmol) was added and the solution maintained under stirring for 1 hour. The organic solution was washed again with brine until neutral pH of the washing liquor was reached. It was subsequently dried over anhydrous sodium sulphate and the solvent evaporated

under reduced pressure. The crude pale yellow oily product was kept under vacuum for several days until a waxy substance was obtained in quantitative yield.

^{1}H NMR (D_2O): 2.71 (t, broad, 4H, C**H$_2$**-NH-C**H$_2$**, piperazine), 3.30 (s, 3H, O-C**H$_3$**, PEG terminus), 3.38 (broad, 4H, C**H$_2$**-N(CO)-C**H$_2$**, piperazine), 3.5-3.8 (m, broad, 60 H, C**H$_2$**O-C**H$_2$**, PEG chain), 4.17 (broad, 2H, CO-O-C**H$_2$**, PEG).

MBA terminated PEG750 (**6**)

In a two necked flask, MBA (4,52 g, 0.029 mol) was dissolved under nitrogen in methanol (50 ml) at 40° C. (**5**) (2.6 g, 0.003 mol) was dissolved in methanol (5 ml) and added to the MBA solution. The reactive mixture was allowed to react for 2 days. The solution was cooled to r.t., water (40 ml) was added and the organic solvent evaporated under reduced pressure. The aqueous phase was extracted with chloroform (3 x 25 ml). The organic phases were collected and washed with water (3 x 25 ml) and dried over anhydrous sodium sulphate. The solvent was eventually evaporated under reduced pressure to obtain a waxy solid in almost quantitative yield. 1H NMR (D2O): 6.21, 5.77 (vinyl terminus, 3H), 4.61 (-NH-C**H$_2$**-NH-, 2H), 3.67 (-O-C**H$_2$**-PEG chain, 60 H), 3.35 (C**H$_3$**-O-PEG terminus, 3H), 2.46 (-N-C**H$_2$**-C**H$_2$**-CO-, 4H).

PEG-MBA-(cyst-m-Boc) (**7**)

In a two necked flask, (**4**) (6.2 g, 24.5 mmol) was dissolved under nitrogen in water/methanol 7/3 mixture (40 ml) at r.t and lithium hydroxide monohydrate was added up to pH 10. (**6**) (5.0 g, 4.9 mmol) was dissolved in the same solvent (20 ml) and added. The reactive mixture was allowed to react for 4 days. Then water (50 ml) was added and the organic solvent evaporated under reduced pressure. The aqueous phase was washed with ethyl acetate (1 x 40 ml, then 4 x 25 ml) and eventually freeze dried. A white waxy solid was obtained in an almost quantitative yield. No trace of unreacted cystamine-m-Boc could be detected in TLC. ^{1}H NMR (D_2O): 6.18, 5.72 (vinyl

terminus, 0.4 H), 4.61, 4.48 (-NH-C**H**$_2$-NH-,α to vinyl 0.26 H, γ to cystamine residue 1.74 H), 3.67 (-O-C**H**$_2$-PEG chain, 60 H), 3.35 (C**H**$_3$-O- PEG terminus, 3H), 2.81-2.41 (-N-C**H**$_2$-C**H**$_2$-CO-, N-C**H**$_2$-C**H**$_2$-S-, 14.5 H), 1.36 (C**H**$_3$- t-Boc, 7.5 H). Trace of residual double bonds (13%) could be observed in ^{1}H NMR spectrum. Reaction yield: 87%

PEG-(MBA-(Cyst-m-Boc))$_2$ (**8**)

(**8**) was obtained through a two step procedure;

Step1). The same procedure to obtain compound (**6**) was followed but using (**7**) (5.0 g, 3.9 mmol) instead of (**5**) and MBA (6.0 g, 39.0 mmol) and solvent in proportion. Product was purified as described. No trace of residual MBA was detected in the final product that was used in the following step.

Step 2). The same procedure to obtain compound (**7**) was followed but using the product obtained in the previous step instead of (**6**) and (**4**) (5.6 g, 19.5 mmol) and solvent in proportion. Product was purified as described.

(**8**) was obtained in a 91% overall yield (6.0 g). ^{1}H NMR (D_2O): 4.48 (reacted -NH-C**H**$_2$-NH-, 3 H), 3.62 (-O-C**H**$_2$-PEG chain, 60 H), 3.35 (C**H**$_3$-O- PEG terminus, 3H),2.81-2.41 (-N-C**H**$_2$-C**H**$_2$-CO-, N-C**H**$_2$-C**H**$_2$-S-, 25 H), 1.36 (C**H**$_3$- t-Boc, 13.5 H). No trace of residual double bonds could be observed in ^{1}H NMR spectrum, even if the ratio between integrals was not completely in accordance with the expected.

PEG-(SH)$_2$-poly(MBA-DMEDA) (**9**)

(**3**) (2.5 g, 7.9 mmol) was dissolved under nitrogen in water (3 ml) and lithium hydroxide mono hydrate was added until pH 10 was reached. (**8**) (0.13 g, 0.079 mmol) was then added and the reaction left under stirring for 120 hours. A 1M HCl aqueous solution was subsequently added until

pH 4 was reached, the solution was ultrafiltered through 5000 nominal cut-off membrane and eventually freeze dried. A white solid was obtained in 74% yield (1.9 g).

CP02

(**9**) (1 g, 0.08 mmol of cystamine pendants) was dissolved in water (10 ml) and pH adjusted to 8.5 with 1M NaOH solution. The polymer solution was deoxygenated with bubbling nitrogen for 2 hours, then DTT (36 mg, 0.24 mmol) was added and the solution left under nitrogen for two hours. Then 1M aqueous HCl was added to reach pH 2, and the solution was ultrafiltered through a 5000 nominal cut off membrane with deoxygenated water. The product was eventually freeze dried.

Mono-piperazine terminated mono-methoxy-PEG2000[33] (**10**)

The same procedure to obtain (**5**) but using mono-methoxy-PEG2000 (10g, 5 mmol) instead of mono-methoxy-PEG750. The product was purified according to the procedure described and a waxy solid was obtained in quantitative yield.

^{1}H NMR (D_2O): 2.71 (t, broad, C**H$_2$**-NH-C**H$_2$**, piperazine, 4H), 3.30 (s, O-C**H$_3$**, PEG terminus, 3H), 3.38 (broad, C**H$_2$**-N(CO)-C**H$_2$**, piperazine, 4H), 3.5-3.8 (m, broad, C**H$_2$**O-C**H$_2$**, PEG chain, 120 H), 4.17 (broad, CO-O-C**H$_2$**, PEG, 2H).

Poly(MBA-DMEDA), 10K, amino terminated. (**11**)

MBA (1.54 g, 10.0 mmol) was added in small portions to an aqueous solution of DMEDA (0.902 g, 10.25 mmol in 3.5 ml of water) under nitrogen. The mixture was allowed to react for three days. Subsequently the solution pH was adjusted to 2.5 with a 1 M aqueous HCl and the solution was eventually freeze dried without any further purification. Product was characterized by SEC and NMR spectroscopy.

Yield: quantitative. $\overline{M}_n$: 11600; $\overline{M}_w$: 28000. ^{1}H NMR (d6-DMSO): 2.25 (s, 6H, C**H$_3$**N); 2.39 (t, 4H, CO-CH$_2$-C**H$_2$**-N); 2.51 (s, 4H, N-C**H$_2$**-C**H$_2$**-N), 2.66 (t, 4H, CO-C**H$_2$**-); 4.56 (m, broad, 2H, NH-C**H$_2$**-NH), 8.82 (t, broad, 2H, N**H).**

(PEG-(SH)$_4$)$_2$-poly(MBA-DMEDA) (**13**)

In a two-necked flask, MBA (0.308 g, 2.0 mmol), cystamine-m-Boc (0.460 g, 1.6 mmol) and TEA (0.160 g, 0.220 ml, 1.6 mmol) were dissolved in ethylene glycol (2 ml) under nitrogen flow. The reaction was monitored by TLC (eluent: chloroform/ isopropyl alcohol 1:1, Cyst-mBoc Rf: 0.25). After the reaction was complete the crude (**12**) obtained was diluted with ethylene glycol (4 ml), (**10**) (0.42 g, 0.2 mmol) and (**11**) (1.2 g, 0.2 mmol) were added. The mixture was allowed to react for 7 days, then diluted in water (100 ml). A 1 M HCl aqueous solution was added until pH 4 was reached and the final solution dialysed against water (5 x 1L) in a 3500 nominal cut off dialysis tube. The purified product was eventually lyophilized. Yield: 1.25 g, 52%.

^{1}H NMR (D$_2$O): 1,41 (s, O-C-(C**H$_3$**)$_3$, cyst-m-Boc), 2,57 (s, N-C**H$_3$**, PAA-block), 2,61 (m, CO-CH$_2$-C**H$_2$**-N, PAA-block), 3,07 (s, N-C**H$_2$**-C**H$_2$**-N, PAA-block), 3.11 (m, CO-C**H$_2$**-CH$_2$-N, PAA-block), 3,67 (s, O-C**H$_2$**-C**H$_2$**-O, PEG-block), 4.57 (s, NH-C**H$_2$**-NH, PAA-block), 6.22 (d, CH=C**H$_2$**, terminus)

Integral ratios between different signals are as expected. A reaction yield of 72 % is calculated on the basis of the signal referred to the unreacted double bond (6.22 ppm).

CP03

(**13**) (1 g, 0.5 mmol of cystamine pendants) was dissolved in water (10 ml) and pH adjusted to 8 with 1M NaOH solution. The polymer solution was deoxygenated with bubbling nitrogen for 2 hours, then DTT (0.385 g, 2.5 mmol) was added and the solution left under nitrogen for two hours.

Then 1M aqueous HCl was added to reach pH 2, and the solution was ultrafiltered through a 5000 Mw nominal cut off membrane with deoxygenated water. Product was eventually freeze dried.

Poly(MBA-DMEDA-co-ethenyl-dithio pyridine) (XLP)

In a two-necked flask cystamine di-hydrochloride (1.22 g, 5.4 mmol), lithium hydroxide monohydrate (0.45 g, 10.8 mmol) and DMEDA (2.00 g, 22.7 mmol) were dissolved in water (11 ml) under nitrogen flow. MBA (5.00 g, 32.4 mmol), was then added under stirring until a homogeneous solution was obtained. Stirring was stopped and the solution allowed to react for 120 hours. The transparent gel obtained was finely ground and soaked in ethanol solution (35 ml), and 2,2'-dipyridyldisulphide (3.60 g, 16.0 mmol) with few milligrams of 2-mercaptopyridine were added. The reaction mixture, completely dissolved within few hours, was maintained under stirring at room temperature for overall 24 hours, then diluted to 150 ml with water to precipitate the excess 2,2'-dipyridyldisulphide, which was filtered off. The pH of the filtered solution was adjusted to 2.5 with a 1 M aqueous HCl. The polymer was fractioned by ultrafiltration between 10000 and 5000 nominal cutoff membranes and eventually freeze dried.

Yield: 0.73 g. ^{1}H NMR (D_2O): 2,71 (m, CO-CH_2-C**H$_2$**-N, 4H), 2.77 (s, N-C**H$_3$**, 6H), 3.35 (m, CO-C**H$_2$**-CH_2-N, 4H), 3.46 (s, N-C**H$_2$**-C**H$_2$**-N, 4H), 4.57 (s, NH-C**H$_2$**-NH, 2H), 7.27 (m, pyridine, N-CH-C**H**, 1H), 7.67-7-77 (m, pyridine, N-C-C**H**-C**H**, 2H), 8.38 (m, pyridine, N-C**H**-CH, 1H).

DNA

For electrophoretic retardation, plasmid gWIZLuc, containing the firefly luciferase gene was supplied as a 5mg/ml solution by Aldevron (South Fargo, ND) and diluted with water without any further purification to obtain a working solution of 1 mg/ml.

For DLS analyses and polyplexes formation with semi-automatic mixing apparatus, single stranded salmon sperm DNA was supplied by Aldrich and dissolved in water without any further purification to obtain a working solution of 1 mg/ml.

6.2.2 Methods

Preparation of complexes

Complexes were routinely prepared by the addition of a single aliquot of polymer or polymers mixture solution to a 0.05 mg/ml DNA solution, in the required amounts to produce complexes of the desired polymer repeating unit/DNA nucleotide ratio (RU/DNA ratio). The amount of polymer required to produce complexes of a given polymer RU/DNA ratio was calculated according to the following:

$$Polymer\ amount = \frac{Polymer\_RU\_Mw}{DNA\_RU\_Mw} \text{ x } RU/DNA\ ratio \text{ x } DNA\ amount \qquad \text{Eq. (6.1)}$$

The DNA RU molecular weight was taken as 308, for the mean Mr of a DNA nucleotide. The RU molecular weight of the p(MBA-DMEDA) cationic homopolymer was 315 for the dihydrochloride salts; for polymers containing PEG chains or ethenyldithiopyridine units, only MBA-DMEDA RU were taken into account as DNA complexing.

More details on polymer mixture composition and addition order to DNA solution are reported in the results and discussion section.

Hydrodynamic particle size determination

Samples were prepared according to the procedure described above. The z-average particle sizes, polydispersity and light scattering intensity were determined by dynamic light scattering using a Viscotek 802 DLS at 25°C, data analized with Omnisize 2.0 software, Correlator resolution 256 channel.

Transmission Electron Microscopy

Samples were prepared according to the procedure described above. One drop of each sample was placed onto copper grids coated with Pioloform resin (Taab Laboratory Equipment, Reading, UK) and excess liquid blotted using filter paper. After air drying grids were floated on a drop of uranyl acetate staining solution (4% w/v in 50/50 v/v EtOH/H_2O) for 15 min, after which they were washed once in 50% v/v EtOH and twice in purified water, followed by air drying. Grids were analyzed using a JEOL JEM-1010 transmission electron microscope (Jeol, Welwyn Garden City, UK) operating at a voltage of 80 kV. Micrographs were taken at various magnifications with a Kodak Megaplus digital camera 1.6i using the Analysis 3.0 software package.

Gel electrophoresis

Gel electrophoresis was used to observe complex stability and protection from nuclease degradation. Complexes were formed adding the required amounts of polymer to plasmid (2 μg) in PBS with 5 mM $MgCl_2$ (16 μl), followed by incubation at room temperature for 30 min. A DNase I solution (1 μl of 10 μg/ml, containing 4.4 activity units) was added and samples were incubated for 60 min and then cooled to 0°C. A solution of poly(4-styrenesulfonic acid-*co*-maleic acid) sodium salt solution (1 μl of 10 mg/ml) was added to displace polycation. Gel loading buffer consisting of a solution of bromophenol blue (0.25% w/v) in 40% (w/v) sucrose (2 μl) was added. Then samples (9 μl) were loaded onto a 0.8% agarose gel in TAE buffer containing 1 μg/ml ethidium bromide, and developed electrophoretically over 60 min at 70 V, with TAE as running buffer. The gels were photographed on a UV transilluminator to visualise DNA, prior to polymer detection. Gels were stained for polymer using a solution of brilliant blue R250 (1% w/v) in a 50:10:40 mixture of methanol/glacial acetic acid/water for 1 hour. Destaining was achieved using a 10:10:80 methanol/glacial acetic acid/water mixture overnight.

Diluted Bovine pancreatic RNase-Free Deoxyribonuclease I (DNase I), FPLC pure, 1000units were purchased from GE Healthcare Life sciences; agarose was purchased from VWR International Ltd. (Lutterworth, Leicestershire).

Ultrafiltration tests

Polyplexes stability to dilution was proved by ultrafiltration tests. Samples (40 μl) were prepared according to the procedure described, loaded into centrifugal filter Microcon YM-100 with a nominal cut off of 100 k, diluted with water (360 μl) and centrifuged (500 G). The dilution-centrifugation procedure was repeated twice; retained and filtrate solutions were recovered and eventually analyzed with TEM and DLS.

6.3 RESULTS

In this work a novel formulation to obtain suitable DNA-PAA complexes for gene delivery applications has been studied. Two different PAA based block co-polymers (labelled CP2 and CP3) were synthesised and subsequently formulated with another PAA based polymer in which ethenyl dithiopyridine pendants were present (labelled XLP).

The PAA main structure was obtained by polyaddition reaction of MBA and DMEDA, leading to a polymer that demonstrated remarkable DNA complexing properties even if with a non negligible cytotoxicity. According to previous findings and publications, a PEG chain was bound to one or both ends of PAA macromolecule in order to increase colloidal stability of the polyplexes.

A short PAA block containing 2 or 4 sulphidryl pendants was inserted between poly(MBA-DMEDA) and PEG chains in order to further increase polyplexes stability in case of high dilution or elevated ionic strength. Thiol pendants are supposed to react with XLP during the formulation of polyplexes, in order to create a stabilizing network between the PAA-DNA complex and the

surrounding PEG shell. Polyplexes obtained with a homo poly(MBA-DMEDA) (CP1) were used in all case for comparison.

6.3.1 Synthesis.

The PAA homopolymer methylene-bis(scrylamide) co-N,N'-dimethylethylenediamine (CP1) was synthesised according to a well established procedure.

XLP polymer synthesis has been performed according to a procedure developed during the first two years of this PhD course and reported in Chapter 3. XLP structure is reported in Figure 6.1.

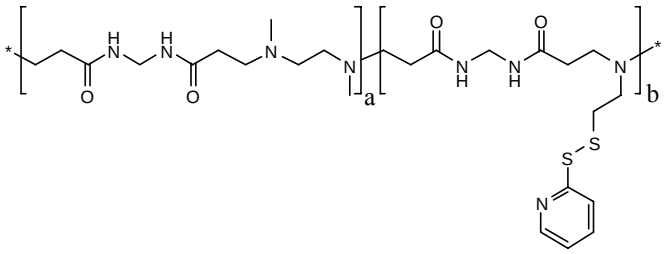

Figure 6.1: structure of XLP

CP2 and CP3 instead were obtained following two different reaction strategies: CP2 was synthesised by a stepwise procedure, to better control the polymer architecture; CP3 was obtained by a tri-block addition procedure. In the CP2 synthesis (Scheme 6.1), a piperazine terminated PEG (**5**) was synthesised, followed by addition of first MBA (**6**)and second mono-protected cystamine (**7**), each step followed by extraction in order to obtain a pure product. Both reactions was performed with a large excess of MBA and m-Boc-Ccystamine respectively in order to limit double PEG chains coupling reaction. The entire MBA and m-Boc-cystamine addition procedure was repeated twice. The amino terminating product (**8**) was eventually used as terminator in a polyaddition reaction with a purposely synthesised mono-adduct of MBA to DMEDA (**3**)**.**

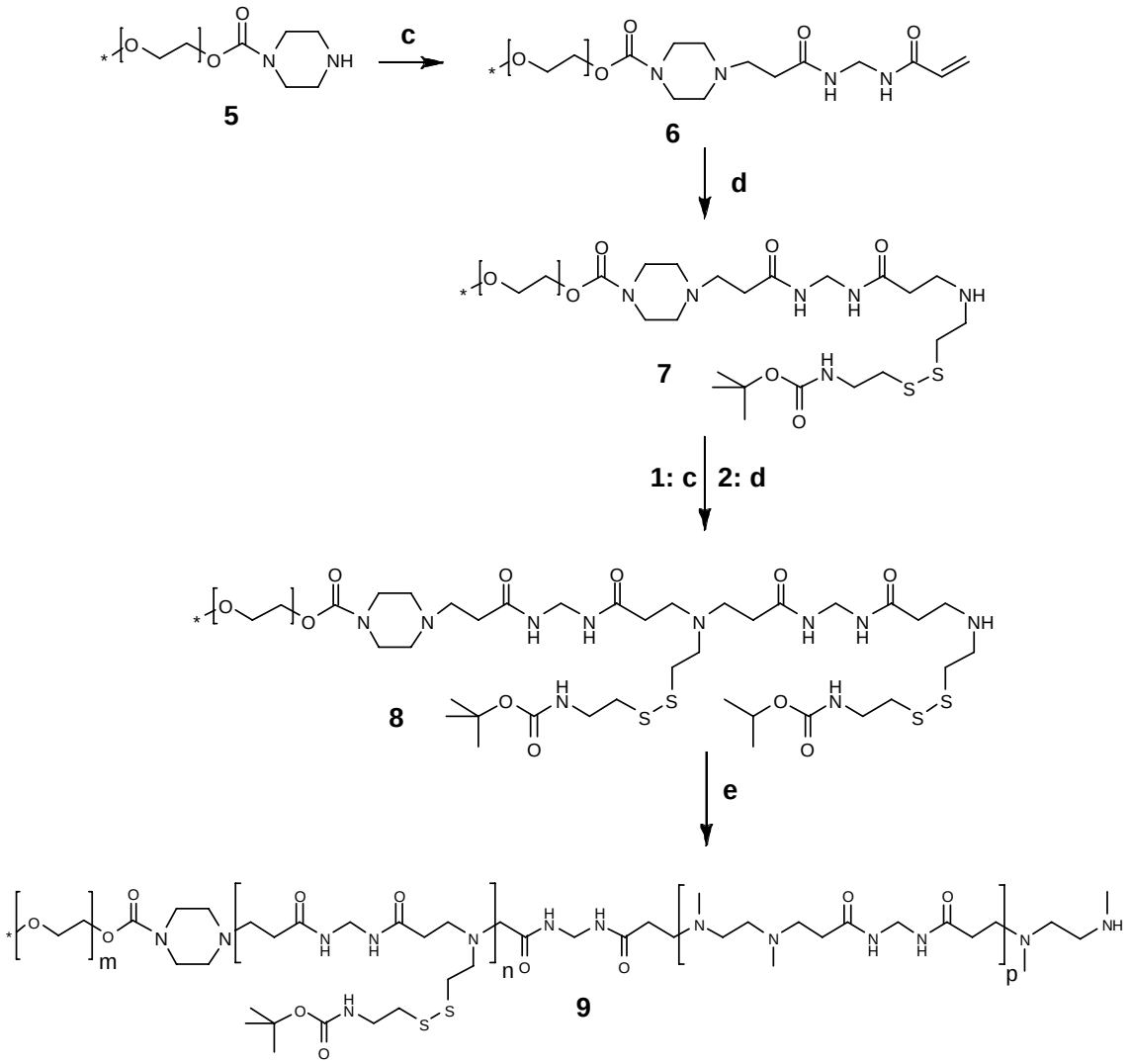

Scheme 6.1: Synthesis of (**9**). reaction conditions: c) methylene-bis(acrylamide) (excess), methanol, r.t, 48h; d) N-Boc-cystamine (excess), water/methanol 7/3, r.t., 100 h; e) (**3)**, water, 120 h.

Intermediate (**3**) have been obtained by addition of MBA to a mono-N-trityl protected DMEDA (**1**), followed by deprotection in HCl solution (Scheme 6.2).

Despite the careful synthetic procedure, the final product showed a reduced amount of cystamine residues compared to the expected one, probably because of a non complete addition reaction of m-Boc-cystamine.

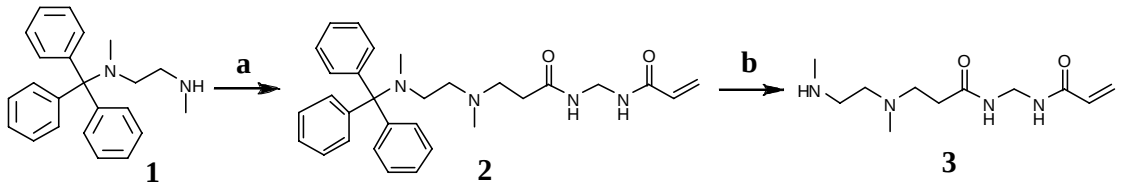

Scheme 6.2: synthesis of AB type MBA-DMEDA monomer. Reaction conditions: a) MBA (excess), methanol, r.t., 20 h; b) 1M HCl

In the preparation of CP3, each block was synthesised separately. Amine-terminating PEG with 2k $\overline{M}_n$ (**10**) and poly MBA-DMEDA terminating with secondary amine groups (**11**) after synthesis were isolated and subsequently added to a oligo MBA-(N-Boc-cystamine) terminating with acrylamido groups. Since N-Boc-cystamine was scarcely soluble in water, ethylene glycol was used as solvent in order not to reduce reaction rate. In fact in previous research we have demonstrated the effectiveness of ethylene glycol in Michael polyaddition reaction (see Chapter 3 for more details) The three blocks were allowed to react for several days because of the relatively low concentration of reactive functions. The polymer obtained was ultrafiltered and eventually freeze dried (Scheme 6.3).

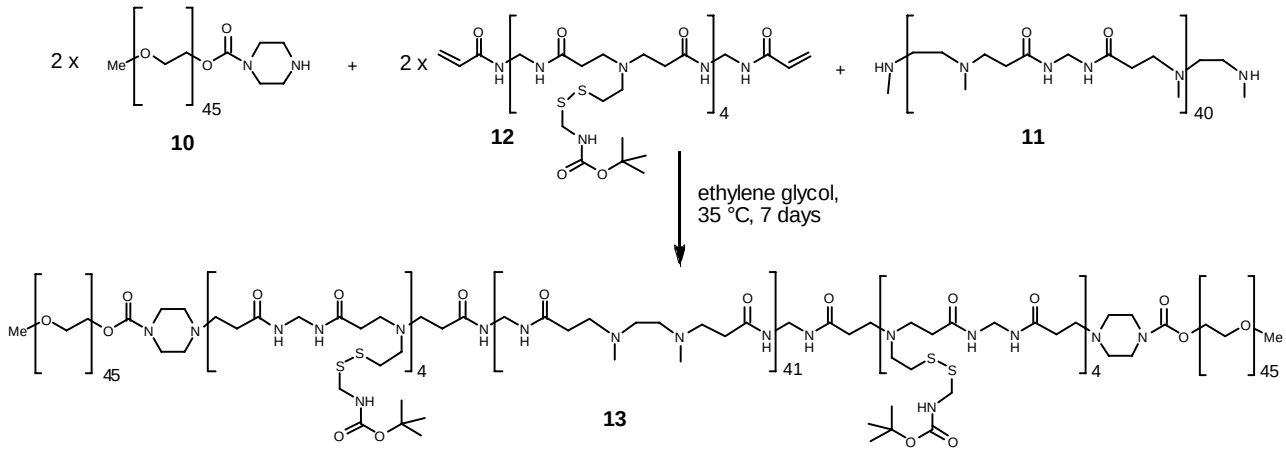

Scheme 6.3: synthesis of CP3

SEC traces and NMR spectra confirmed the expected mean structures. PEG 750 and 2000 block were coupled with a 25000 and 10000 $\overline{M}_n$ PAA ones in the syntheses of CP2 and CP3 respectively, in order to test two different ratios between PEG and cationic polymer.

6.3.2 CP1 based polyplexes

DLS analyses, gel electrophoresis retardation and DNA enzymatic degradation tests were performed on 0.5:1, 1:1, 5:1 polymer:DNA comlpexes, in order to have a reliable comparison with modified polyplexes. Each formulation was prepared in NaCl 0.15, 0.3 or 0.6 mM solutions to evaluate the complex stability and behaviour in the presence of high salt concentration.

Gel electrophoresis retardation showed that CP1 was very effective in DNA complexation (Figure 6.2). Even with the lowest polymer:DNA ratio (0.5:1) a complete DNA compexation occurred and no traces of free DNA or of free polymer were detectable. For every other composition excess CP1 was observed in the stained gel. A certain increase of brightness in the holes could be observed with the increase of NaCl concentration. This was probably due to complexes loosening as a consequence of increased ionic strength that allowed a stronger interaction between ethidium bromide and double stranded DNA.

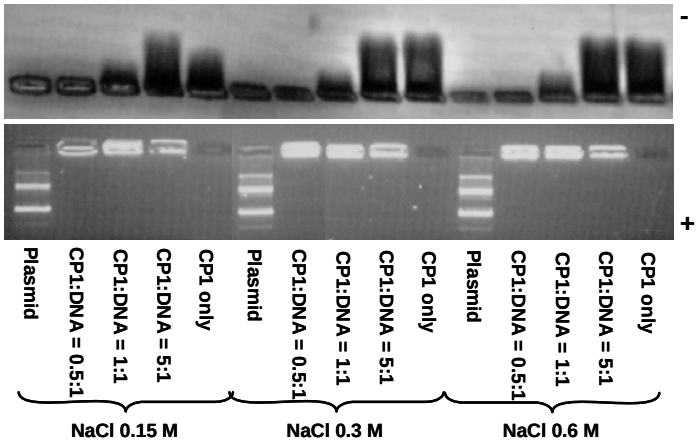

Figure 6.2: Gel electrophoretic retardation of gWIZLuc plasmid by CP1. The lower halves of the gel image shows DNA migration as viewed under UV light; the upper halves are stained for polymer. The anode and cathode are marked + and -, respectively.

A similar result was obtained by DLS analyses: a slight decrease in size is observed with the increase of CP1:DNA ratio while large increase in size was observed with increasing salt concentration, in particular between 0.15 and 0.3 mM salt concentrations. As expected, an increase

in the ionic strength of the solution produced a weakening of the interaction between anionic DNA and cationic CP1, thus leading to an increase of complexes dimension (Figure 6.3).

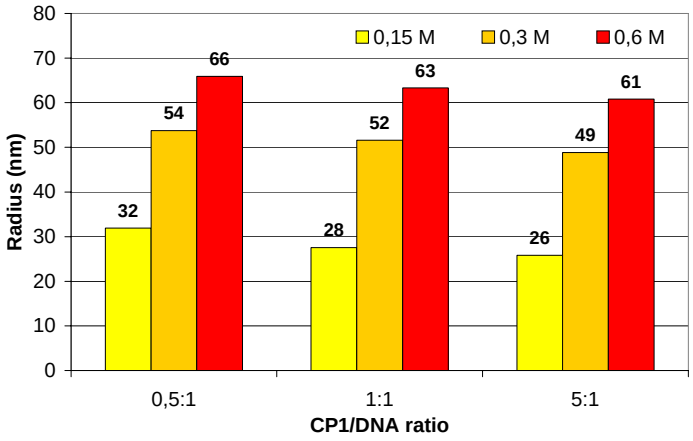

Figure 6.3: DLS analyses of polyplexes obtained by salmon sperm DNA and CP1, in solution with different concentration of NaCl.

This phenomenon was confirmed by the enzymatic degradation test, performed only on polyplexes with CP1:DNA 5:1 ratio: in 10 minutes of incubation with DNase I only DNA was degraded, differently from complexes (Figure 6.4). Only after 60 minutes some degradation occurred to complexed DNA, and complete degradation only in the presence of 0.6 M NaCl. (Figure 6.5)

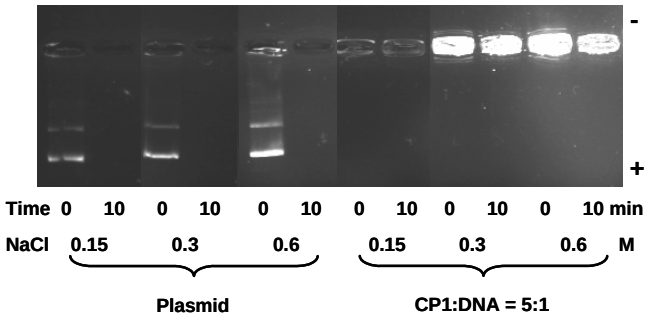

Figure 6.4. Gel electrophoretic retardation of gWIZLuc plasmid by CP1 in solutions with different concentrations of NaCl. The anode and cathode are marked + and -, respectively.

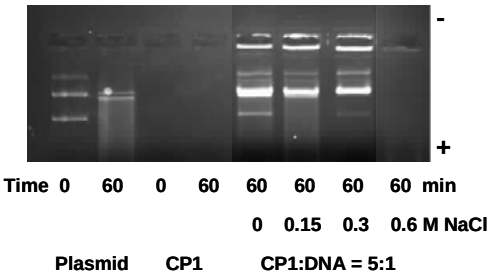

Figure 6.5. Gel electrophoretic retardation of gWIZLuc plasmid by CP1 in solutions with different concentrations of NaCl. The anode and cathode are marked + and -, respectively.

6.3.3 CP2 based polyplexes

This second group of polyplexes was obtained by formulation of CP2 and XLP with DNA. Four different ratios between CP2 and XLP were used, namely 0.2:1, 0.6:1, 0.8:1, 1:1 and 1.4:1, defined on the basis of previous findings [Hill et al., 1999]. Each CP2-XLP composition was combined with DNA according to the same ratios used with CP1.

DLS data obtained for each sample are reported in Table 6.1.

Table 6.1. Salmon sperm DNA and CP2 polyplexes dimensions

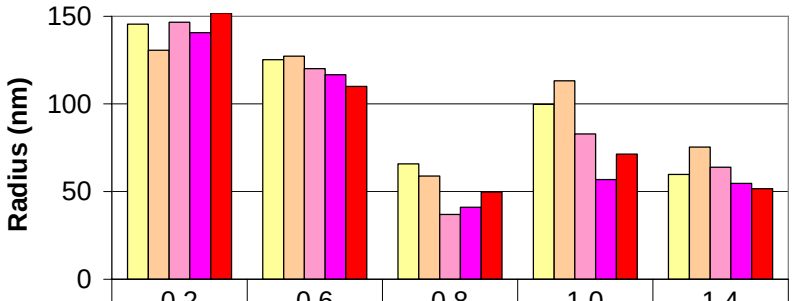

	0,2	0,6	0,8	1,0	1,4
PAA:DNA 1	145,6	125,3	65,8	99,7	59,8
PAA:DNA 1,25	130,7	127,3	58,8	113,2	75,4
PAA:DNA 1,5	146,7	120,2	37,0	82,9	63,9
PAA:DNA 1,75	140,8	116,7	41,1	56,8	54,7
PAA:DNA	151,9	110,0	49,8	71,4	51,6

CP2/XLP ratio

They showed a general decrease in size with increasing the amount of XLP in the formulation, with a minimum around 0.8:1 CP2:XLP ratio. No relevant differences were observed varying the ratio between polymer and DNA in formulations with the lowest amount of XLP, while for 1:1 and 1.4:1 CP2:XLP ratios polyplexes undergo relevant variations, in both cases with a maximum around 1.25:1 polymer: DNA ratio.

TEM images of the two samples with PAA/DNA ratio 1.75:1, and 0.6:1 and 0.8:1 CP2:XLP ratio, as they appeared to be more promising,. Round shaped nanoparticles are shown in Figure 6.6, with a mean diameter around 35 nm. No relevant differences between the two samples were noticed.

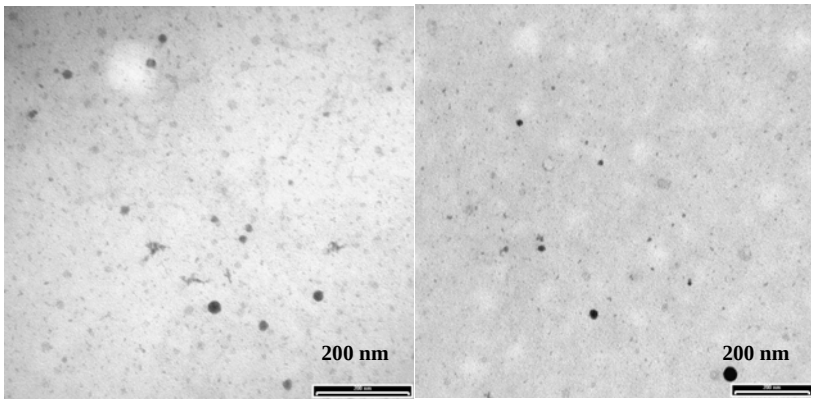

Figure 6.6. TEM images of salmon sperm DNA-CP2 polyplexes, with 1.75 PAA:DNA ratio. On the left: 0.6:1 XLP:CP2; on the right: 0.8:1 XLP:CP2

When the samples are treated with Na_2SO_4 (that was demonstrated to be more effective in polyplexes destabilization than NaCl even at low concentrations), the best result in term of dimension stability was obtained with 0.6:1 XLP:CP2 ratio, at any PAA:DNA ratio (Figure 6.7).

DNA enzimatic degradation test was performed again on samples with 0.6:1 and 0.8:1 ratio between XLP and CP2, followed by gel retardation. DNA and complex with CP1 were added for comparison. While after 10 minutes incubation with DNase I, DNA was completely degraded and no degradation was detectable for CP1 complexes, all the other samples showed some extent of DNA degradation (Figure 6.8). It has to point out that while CP1 was in large excess with respect to

DNA, in CP2-XLP formulations DNA was in stoichiometric amount. Anyway, the fact that DNA was displaced from the complexes by the presence of poly(styrene-4-sulfonic-*co*-maleic)acid, clearly indicate that no effective cross-linking was achieved with this formulation.

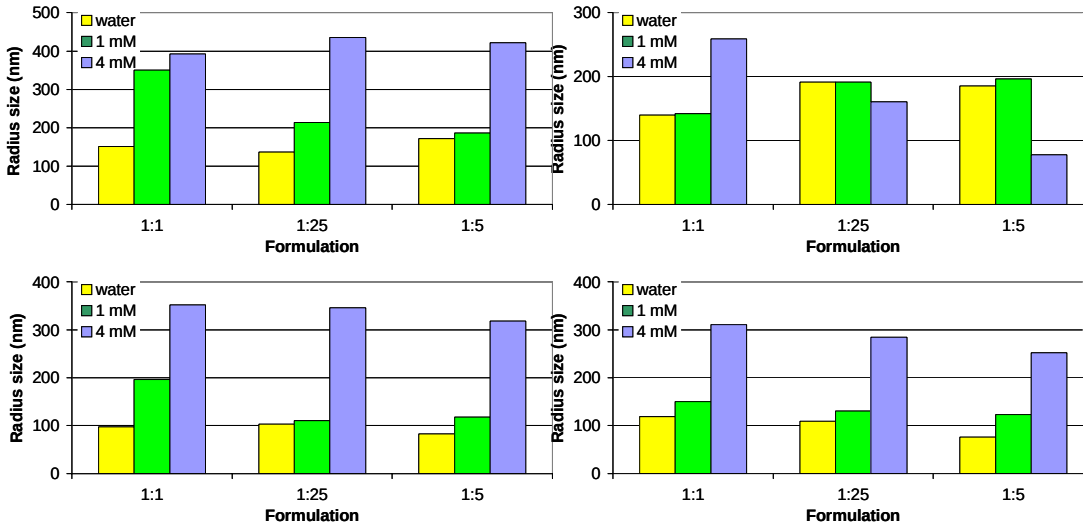

Figure 6.7: DLS analyses of salmon sperm DNA -CP1polyplexes, in solution with different concentration of Na_2SO_4. For each panel: on x axis DNA:PAA ratio; on top left: XLP:CP2=0.2:1; on top right: XLP:CP2= 0.6:1; on bottom left: XLP:CP2=0.8:1; on bottom right: XLP:CP2= 1.4:1.

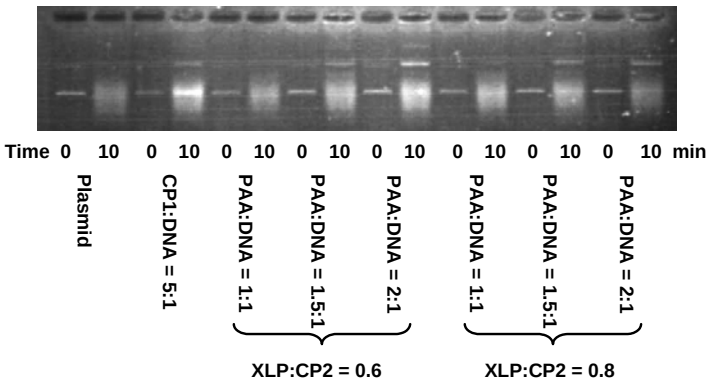

Figure 6.8. Gel electrophoretic retardation of gWIZLuc plasmid by CP1 in solutions with different concentrations of NaCl. The anode and cathode are marked + and -, respectively.

6.3.4 CP3 based polyplexes

On the basis of the results obtained with CP2, a new polymer with longer PEG chains, shorter PAA chain, and increased number of sulfidryl pendants was synthesised to enhance complexes resistance to dilution at high salt concentration. Complexes were formed with higher XLP:CP ratios, namely 2:1 and 3:1, in order to achieve suitable SH:SSPy groups and PEG:PAA ratios. PAA:DNA ratios were maintained. Two different addition orders of the components were followed: in formulation 1 (F1) XLP was added to DNA, then CP3 to the complexes; in formulation 2 (F2) XLP was added to CP, then polymer mixture to DNA solution. Both formulations gave rise to suitable polyplexes with diameters ranging from 65 to 95 nm, with the exception of F1 formulations when using 1:1 PAA:DNA ratio. DLS analyses of the polyplexes are reported in Table 6.2.

No relevant differences between the samples were evidenced by TEM imaging, as shown in Figure 6.9.

Table 6.2. DLS analyses of salmon sperm DNA and CP3 polyplexes.

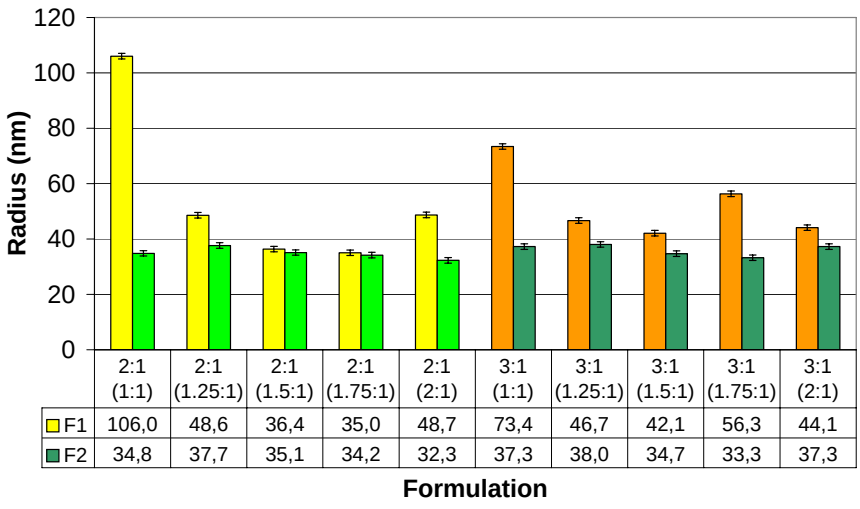

	2:1 (1:1)	2:1 (1.25:1)	2:1 (1.5:1)	2:1 (1.75:1)	2:1 (2:1)	3:1 (1:1)	3:1 (1.25:1)	3:1 (1.5:1)	3:1 (1.75:1)	3:1 (2:1)
F1	106,0	48,6	36,4	35,0	48,7	73,4	46,7	42,1	56,3	44,1
F2	34,8	37,7	35,1	34,2	32,3	37,3	38,0	34,7	33,3	37,3

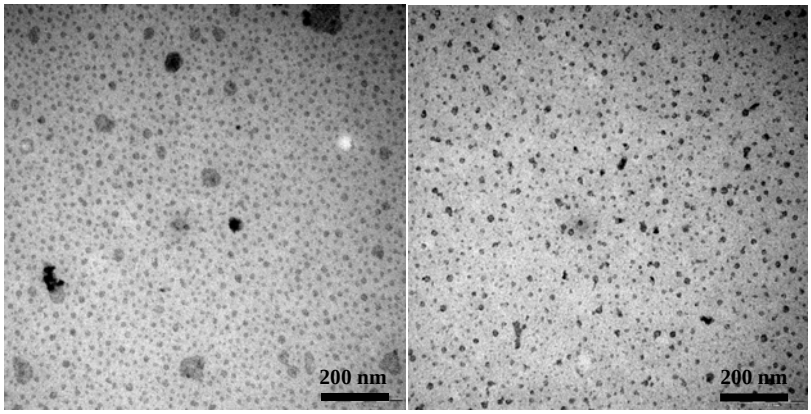

Figure 6.9. TEM images of salmon sperm DNA-CP3 polyplexes, with 1.25 PAA:DNA ratio. On the left: 2:1 XLP:CP3 ratio; on the right: 3:1 XLP:CP3

When sodium sulphate was added to the samples up to 4 and 10 mM concentrations, invariably large increase in size was observed, about three fold ratio. Anyway, samples produced with formulation 2 showed the smaller increase in size. Results of DLS analyses were reported in Table 6.3 and 6.4.

Table 6.3. DLS analyses of salmon sperm DNA and CP3 polyplexes in solution with different sodium sulfate concentrations. PAA:DNA ratio=2:1

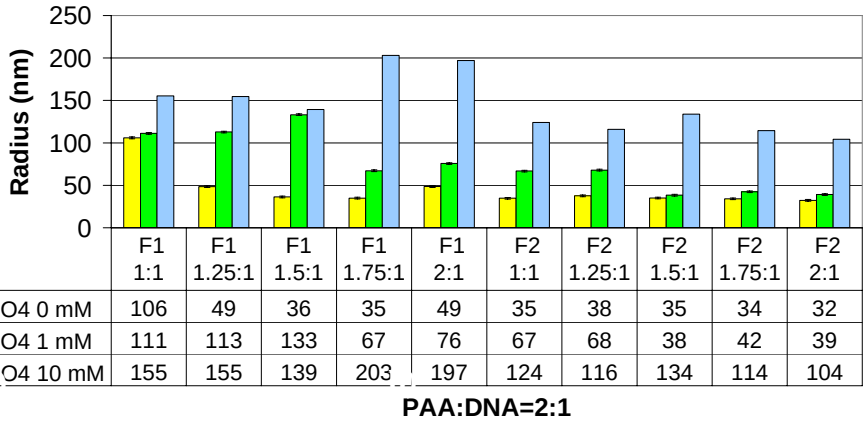

	F1 1:1	F1 1.25:1	F1 1.5:1	F1 1.75:1	F1 2:1	F2 1:1	F2 1.25:1	F2 1.5:1	F2 1.75:1	F2 2:1
Na2SO4 0 mM	106	49	36	35	49	35	38	35	34	32
Na2SO4 1 mM	111	113	133	67	76	67	68	38	42	39
Na2SO4 10 mM	155	155	139	203	197	124	116	134	114	104

Table 6.4. DLS analyses of salmon sperm DNA and CP3 polyplexes in solution with different sodium sulfate concentrations. PAA:DNA ratio=3:1.

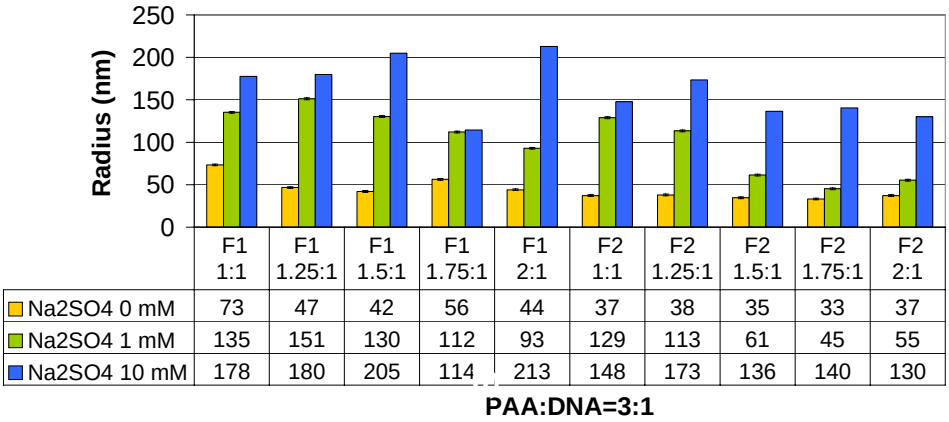

	F1 1:1	F1 1.25:1	F1 1.5:1	F1 1.75:1	F1 2:1	F2 1:1	F2 1.25:1	F2 1.5:1	F2 1.75:1	F2 2:1
Na2SO4 0 mM	73	47	42	56	44	37	38	35	33	37
Na2SO4 1 mM	135	151	130	112	93	129	113	61	45	55
Na2SO4 10 mM	178	180	205	114	213	148	173	136	140	130

DNA enzimatic degradation tests were initially performed only on the formulation with 3:1 XLP:CP3 ratio and 1.25:1 PAA:DNA ratio, in comparison with a non-cross linked formulation in which CP1 was used instead of XLP (Figure 6.10). DNA was visible only in non degraded sample, with the exception of XLP based polyplexes in which DNA was always not detectable. This could suggest that no DNA displacement occurred to this samples even in the presence of poly(styrene-4-sulfonic-*co*-maleic)acid, proving cross-linking effectiveness.

A slight DNA trace was revealed in the case of XLP based sample – F1, probably due to a non complete complex stabilization. Moreover, fluorescence in the wells could be ascribed to interaction between still complexed DNA and ethidium bromide due to a more loosened PAA-DNA interaction compared to F2 sample, therefore appearing as the best sample. Several different gel electrophoresis retardation tests were performed in different conditions but no definitive proof was obtained about complexes stability.

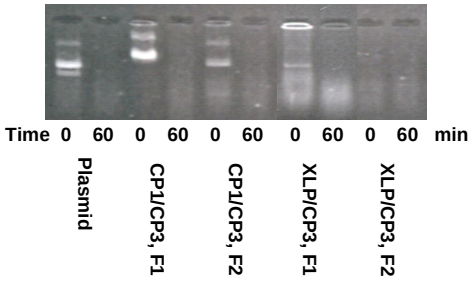

Figure 6.10. Gel electrophoretic retardation of gWIZLuc plasmid by PAA polymers, with 1.25 PAA:DNA, 3:1 XLP:CP3 or CP1:CP3 ratio. The anode and cathode are marked + and -, respectively.

On the bases of previous results and according to the best PEG-PAA ratio defined in previous research, our attention was focused on the following formulatons: 2:1 XLP:CP3 - 1.5 PAA:DNA and 3:1 XLP:CP3 - 1.25 PAA:DNA..

To obtain more reliable and reproducible results and to test complex formation procedure scalability, a semi-automatic mixing system was set up, in which polymer and/or DNA solutions were mixed in a small mixing chamber at a constant flow rate controlled by two peristaltic pumps, according to the different dilutions and compositions.

A small amount of NaCl was added to polymer and DNA solutions, up to a 5 mM final concentration, in order to increase chains mobility and to obtain more tight complexes with a better defined architecture. Nanoparticles formed in water were invariably smaller in size according to DLS analyses (e.g. complexes formed in water: 15-20 nm radius; NaCl 5mM solution: 20-30 nm radius), TEM images showed surprisingly very interesting differences. While round shaped polyplexes were formed in distilled water, in 5mM NaCl solution very regular rods or toroids were obtained (Figure 6.11)

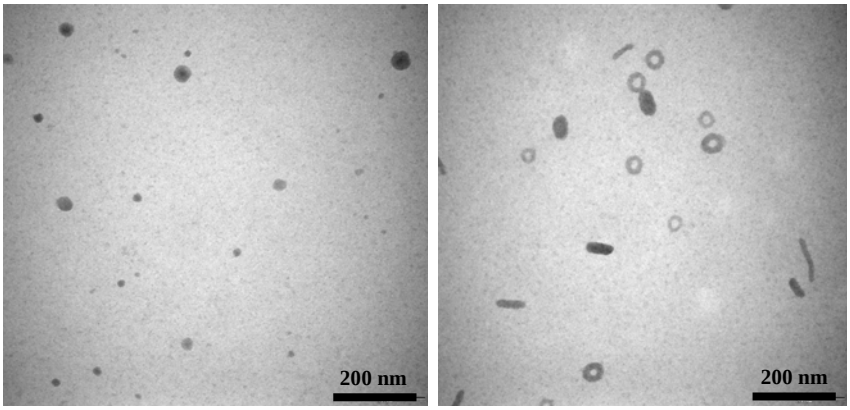

Figure 6.11. TEM images of salmon sperm DNA-CP3 polyplexes, with 1.25 PAA:DNA ratio, 2:1 XLP:CP3 ratio. obtained with a semi automatic mixing system, in distilled water (on the left) or in 5 mM NaCl solution.(right)

To definitely prove the stability of complexes in high dilution conditions, ultrafiltration tests were performed. Microcon centrifugal filters were used with a nominal cut off of 100 k, allowing free polymer and/or DNA to pass through the filter while retaining the complexe. DLS showed the presence of nanoparticles in the retained solution for both compositions, with a certain increase in nanoparticle size; anyway a slight better behaviour was observed in 2:1 XLP:CP3 - 1.5 PAA:DNA formulation, in term of size increasing and of sample recovery (see Table 6.5)

Table 6.5. DLS analyses of salmon sperm DNA and CP3 polyplexes before and after ultrafiltration

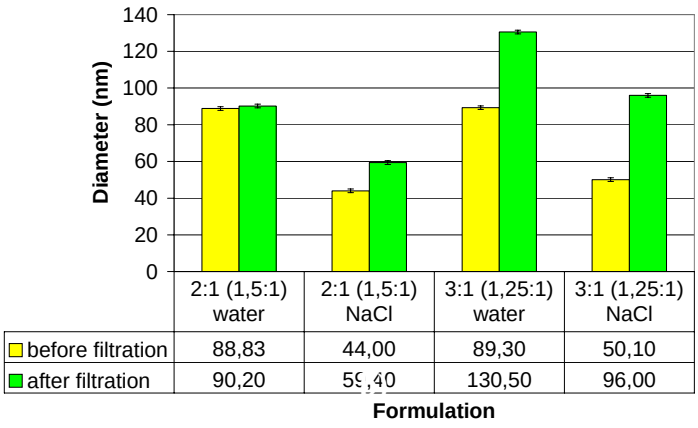

TEM images were taken on 2:1 XLP:CP3 - 1.5 PAA:DNA sample before and after ultrafiltration to observe polyplexes presence and shape. A formulation in which XLP have been substituted with CP1 was analyzed for comparison. Results are reported in Figure 6.12.

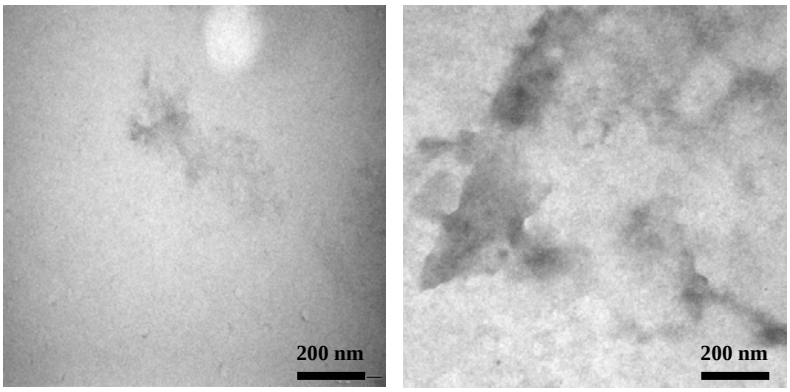

Figure 6.12. TEM images of salmon sperm DNA-CP1 polyplexes, with 5:1 PAA:DNA ratio, obtained with a semi automatic mixing system after ultrafiltration test. On the left side the retained solution, on the right the filtrate solution.

No trace of non-cross linked complexes remained in the retained solution while in the filtrate a disorganized solid mass was present almost everywhere in the sample.

On the contrary, complexes were present in the formulations with the cross linker (XLP), both in distilled water and in NaCl 5 mM solution. Moreover both samples retained the initial polyplexes shape, as discussed above. Filtrate solutions appeared both clear and free of solutes (Figure 6.13)

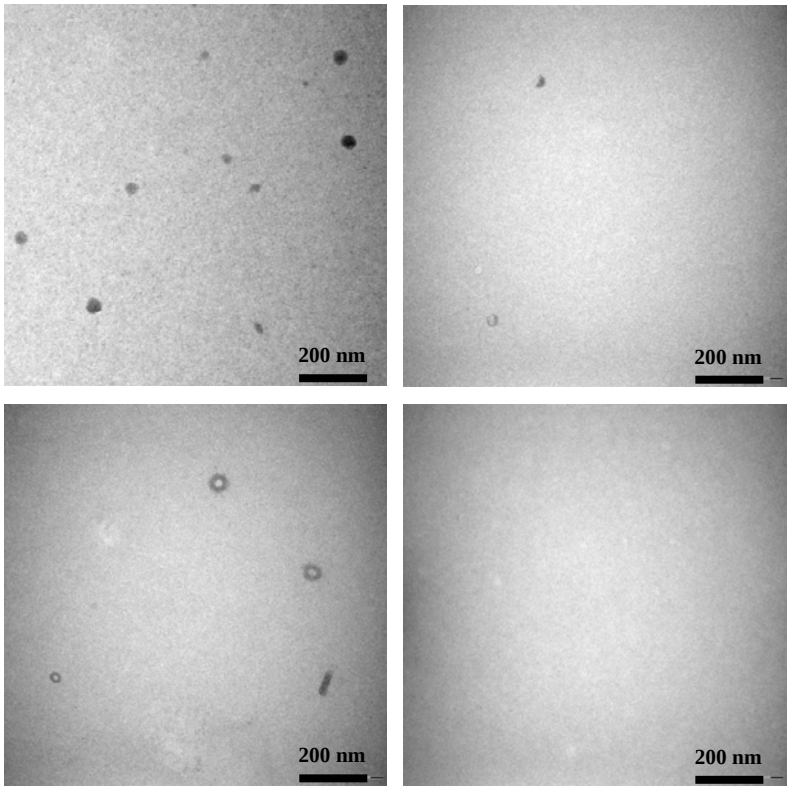

Figure 6.13. TEM images of salmon sperm DNA-CP3 polyplexes, with 1.25 PAA:DNA ratio, 2:1 XLP:CP3 ratio. obtained with a semi automatic mixing system, in distilled water (on top) or in 5 mM NaCl solution.(on bottom) after ultrafiltration test. On the left side the retained solution, on the right the filtrate solution

6.4 DISCUSSION

Cationic polymers and DNA complexes have been studied in these years as non viral vectors for gene delivery. Stability of complexes in various conditions is still one of the problematic aspect affecting in vivo application of gene therapy. For this reason we decided to perform this preliminary study on multi-components polyplexes based on PAA. The aim was to stabilize the DNA-PAA complexes by means of two strategies: creating a hydrophilic shell of PEG, well known to be stealth-like and non interactive with proteins or other biological media, and cross-linking the polyplexes through disulphide linkages, widely adopted in recent years for their stability in serum and blood but susceptible to be reduced in the cytoplasmic environment.

Previous researches, performed in Nottingham University, demonstrated the stability enhancement of polyplexes combining PEG and cationic PAA, the best PAA:PEG ratio for preventing particle coalescence being between 10:1 and 5:1.

According to this research we synthesised two different PAA-based polymers. In the first one (CP2) a semi-thelechelic approach was used and a mono-PEG functionalised polymer was obtained. A stepwise strategy was adopted to control polymer architecture, but the entire procedure was very time consuming, due to the numerous synthetic and purification steps, and results were not as expected. In fact only 2/3 of the expected thiol pendants were detected in the final product. This is probably due to incomplete MBA or cystamine-m-Boc addition to functionalised PEG chains and/or coupling reaction between two PEG chains occurring during MBA or cystamine-m-Boc addition. As a result, also the PAA:PEG ratio resulted to be higher than the one previously found (around 20:1).

Different XLP:CP2 polymer blend ratios were investigated in DNA complexing ability. The ratios were chosen as a function of the number of CP2 pending sulphydryl groups. In all cases round shaped nanoparticles with good diameters were obtained, in particular when 0.6:1 and 0.8:1 XLP:CP2 ratios were used, but all formulations showed less DNA protecting ability to enzymatic degradation than the corresponding non-cross linked polyplexes.

On the basis of these results a different polymer was synthesised with a lower PAA:PEG ratio and a higher number of sulphidryl pendants. Also the synthetic strategy was modified from a step-by-step to a block addition one, the latter not involving large excess of reagents, therefore not requiring extensive purifications.

Also in this case different XLP:CP3 blends were investigated in DNA complexing ability. XLP:CP3 ratios were higher than the previously used ones, namely 2:1 and 3:1, leading to final PAA:PEG ratios of 6.5 and 8.5 respectively. Both blends were formulated with DNA using PAA:DNA ratios between 1:1 and 2:1 and almost all formulations showed good DNA complexing

properties. Polymer addition order to DNA was also varied and some differences were found. It was already known that better performances were obtained when polymer solution was added to DNA solution in a single addition. The best approach resulted to be mixing polymers together and adding the polymer solution to DNA solution, according to a commonly adopted protocol. According to this strategy better results were obtained, not only in term of particles size (polyplexes obtained according to F2 were invariably smaller than the ones obtained with F1) but also in term of stability in the presence of salt (a smaller increase in size was observed in the case of F2 polyplexes). In gel retardation assays, CP3 based complexes formed stable complexes with DNA that were not affected by the interaction with poly(styrene sulfonic-co-maleic)acid, a polyanion used to disrupt polyplexes, thus evidencing the efficacy of cross linking. Moreover, F2 complexes resulted so tight that no interaction between ethidium bromide and DNA occurred (as evidenced by the absence of fluorescence in the loading wells).

More difficulties were encountered in finding the best composition, because electrophoresis gel retardation assays resulted to be not completely reliable. Therefore, ultrafiltration tests have been performed on the formulations that showed better results, in particular, 2:1 XLP:CP3 - 1.5 PAA:DNA and 3:1 XLP:CP3 - 1.25 PAA:DNA ratios, obtained according to F2 protocol.

Using a semi-automatic mixing system and NaCl 5mM solution as the solvent for complexes formation, we obtained very reproducible results on nanoparticles formation in terms of shape and dimensions. These sample were used in ultrafiltration test and the results obtained definitely confirmed that 2:1 XLP:CP and 1.5 PAA:DNA was the formulation with the higher stability.

6.5 CONCLUSIONS

In the present work novel PAA based multi-component polyplexes with increased stability for gene transfection purposes have been studied. The polymer mixture, combined two cross-linkable polymers: a PEG-PAA polymer bearing sulfidryl pendants and a PAA containing

ethenyldithiopyridine residues. Two different synthetic strategies were adopted and a wide screening of different compositions and formulations were performed. The composition identified as the most stable presented a very low polymer/DNA ratio compared to the commonly adopted polycationic transfection agents. The polyplexes obtained showed a remarkable stability in dilute solution even in presence of high concentration of salt; colloidal stability of polyplexes solution has also been demonstrated. Cytotoxicity and transfection assays are ongoing to definitely demonstrate the potential of these polyplexes as transfection promoters.

Moreover, this system are currently tested by a private company for applications in the field of environmental analyses, ground water tracing and pollution source recovery.

CHAPTER 7

Glass surface functionalization for AFM imaging of lipid systems

7.1 INTRODUCTION

Atomic force microscopy is one the most powerful techniques used not only for studying drugs morphology but also to better understand physicochemical properties of drugs, in particular nanostructured drug and gene delivery systems, since they are increasingly considered as the real key improvement to enhance therapies efficacy.

On the other hand, comprehension of internalization mechanisms of such kind of drug delivery systems by cells is strongly related to understanding cell membranes morphology and behaviour. Several studies have been performed in vitro on real or simulated cellular membranes constituted by lipid bilayers [1-5].

In collaboration with CIMaINa, Nanostructured Materials and Interfaces Interdisciplinary Center, we focused our attention on lipid based architecture, both small lipoproteins and lipid surfaces, within an extensive research concerning AFM characterization of reconstructed high-density

lipoproteins, used as model systems for the study of fat-hunting proteins involved in prevention of cardiovascular diseases [6-8].

In order to better understand lipid-surface interactions, different surfaces have been employed by virtue of their different interfacial chemical properties and wettability: mica (hydrophilic, negatively charged), SiO_2 and glass (hydrophilic, negative OH- groups), Highly Oriented Pyrolitic Graphite (HOPG-hydrophobic). However, these few surfaces were not sufficient to investigate thoroughly the effect of different surface chemistries on the formation mechanisms of liposome patterns or even lipid bilayer. Surface functionalization was the natural choice to succeed in investigate different conditions with greater elasticity.

Several studies are reported about engineering of surfaces in order to provide specific binding sites for lipid particles and layers [9-12]. Cholesterol is often chosen as functional group, being a omnipresent hydrophobic molecule in living organism, involved in several biological processes and naturally present in cell membranes [13]. Surface linked cholesterol proved to act as molecular binding sites for lipid layers and particles, providing a stable and specific link [9,12,14].

Based on this premises, in this part of the work the preparation of functionalized glass surfaces able to selectively bind phospholipids systems, small liposomes or extended bilayers, with tunable binding efficiency was reported. Cholesterol was chosen as functional binding molecule and a short PEG chain was inserted as hydrophilic spacer between glass and cholesterol.

In order to test the properties of this novel surface, an extensive AFM study of the interaction between phospholipid 1,2-Diphytanoyl-sn-Glycero-3-Phosphocholine (Diph-PC) with cholesterol-functionalized surfaces was carried out. Freshly cleaved mica, HOPG and PEG functionalized glass coverslips were also used in comparison to better understand the mechanism of phospholipids bilayer formation.

7.2 EXPERIMENTAL PART

7.2.1 Materials

Glass coverslips (12 mm diameter) and mica disks (10 mm diameter) were purchased from Ted Pella; HOPG square pieces (10 mm x 10 mm) were purchased from MikroMasch; PEG-1000, 1,1'-carbonyldiimidazole (CDI) (>97%) were purchased from Fluka and used as received, cholesterylchloroformate (97%) was purchased from Aldrich and used as received, (3-Aminopropyl)triethoxysilane (APTES), ethylenediamine (EDA) and triethylamine (TEA) were purchased from Fluka and distilled before use, hydrochloric acid (37%) and nitric acid (67%) were purchased from Carlo Erba Reagents and used as received, ACS grade acetone and chloroform were purchased from Fluka and used as received, water was MilliQ grade. All functionalisation and washing steps were performed in a Sonorex RK510H ultrasonic bath operating at 640W/35kHz at room temperature. Diph-PC (1,2-Diphytanoyl-sn-Glycero-3-Phosphocholine) (Avanti Polar Lipids) was a kind gift from Markus Paulmichl and Silvia Dopinto, Department of Biomolecular Sciences and Biotechnologies of the University of Milan. DiPH-PC is a synthetic lipid commonly used for reconstituting ion channels (since this lipid is not found in native membranes).

Synthesis of di-imidazolyl terminated PEG (PEG-Im_2)

PEG (5 g, 5 mmol,) was put in a two-necked round bottom flask equipped with a stirring bar, vacuum/nitrogen inlet and a glass stopper. PEG was molten under gentle warming and the equipment purged with nitrogen. After cooling down to room temperature, chloroform (15 mL) was added under nitrogen, PEG allowed dissolving and CDI (4.8 g 30 mmol) subsequently added in small portions. After 1 hour, unreacted CDI was quenched by addition of water (5 mL) and the organic phase extracted with a saturated sodium chloride aqueous solution (4 x 15 mL). The organic phase was then dried over anhydrous sodium sulphate and the solvent evaporated under reduced

pressure. A pale yellow oil was obtained almost quantitatively, with purity > 95%, according to NMR and IR analyses.

Glass coverslips functionalization

Glass coverslips were treated before functionalization with aqua regia to increase the hydroxyl group content on the surface (5 washings, 1 min each). The functionalization procedure consisted of four steps. In the first step, the glass surface was functionalized with amino groups by reaction with (3-Aminopropyl)triethoxysilane (APTES). We used a freshly prepared 5% water/acetone solution of APTES 1% v/v for 3 min and rinsed with acetone. In the second step, PEG spacers were linked to the amino groups on the surface by reaction with an imidazolyl activated PEG [15]. A large excess of di-functionalized PEG was used to link only one chain end to the surface. A 5% w/v PEG-Im_2 acetone solution was allowed to react for 15 min and rinsed with acetone. In the third step, an amino function was added to the free imidazolyl PEG terminus by reaction with a large excess of EDA, obtaining the EDA-PEG intermediate. To this purpose, coverslips were put in a 5% v/v EDA acetone solution, allowed to react for 15 min and rinsed with acetone. Finally, cholesterol was linked to the amino terminus of the PEG spacer by substitution reaction with cholestryl chloroformate. Coverslips were put in a 5% w/v cholesteryl chloroformate chloroform solution with 3% TEA v/v, allowed to react for 15 min and finally rinsed with chloroform and acetone. TEA was used as scavenger of the HCl formed during the reaction.

All functionalisation and washing steps were performed in ultrasonic bath at 30° C. Rinsing procedure consisted in three washings of 1 min in the solvent used in the previous reaction, followed by rinsing with 3 mL of running solvent.

7.2.2 Methods

Vesicles suspension preparation

50 µl of a solution of Diph-PC at 2% in chloroform were prepared. The solvent was then evaporated under a stream of nitrogen gas. The lipids were resuspended overnight in 400 µl of MilliQ water and the mixture was vortexed for 3 minutes in order to produce multilamellar vesicles.

Atomic Force Microscopy

The investigation of morphology of the samples was carried out in air using a Bioscope II AFM equipped with a Nanoscope V controller (Veeco Instruments, USA). All images were acquired in Tapping Mode using single crystal silicon tips with nominal radius of curvature of 5-10 nm and cantilever resonance frequency in the range 200-300 kHz. Scan areas were typically 5µm x 2.5µm and 50µm x 25µm, with scan rates of 1.5 Hz and 0.5 Hz, accordingly. Phase maps were recorded simultaneously to topographic maps. Phase maps report the phase lag between the cantilever free end and the driving oscillation [16]. Topographic and Phase maps at higher magnification were collected with resolution of typically 1-2 nm/pixel.

Sample preparation for AFM analysis.

The supported lipid bilayers were prepared by vesicles fusion: 10-70 µl of the vesicles solution were deposited on the substrate (mica, HOPG, amino-terminated PEG-functionalized coverslips, cholesterol-functionalized coverslips) and incubated for 5-90 minutes at room temperature. Subsequently 50 µl of HBS (150 mM KCl, 5 mM Hepes, pH 8) were added for 3 minutes to remove of weakly bound phospholipids [18]. The samples were rinsed with 3 ml of MilliQ water in order to remove the excess of vesicles, gently dried with nitrogen and eventually analyzed.

Contact angle measurements.

Advancing contact angles of water on different substrates have been measured using a FTA 1000 instrument. Droplet volume was approximately 3 microliters. Shape analysis of the droplet in

equilibrium on the surfaces has been performed using Fta32 Video v2.0 software. For each drop we have estimated the contact angle as the average of left and right contact angles. Measures was performed in triplicate and final value was calculated as average of the three results.

7.3 RESULTS AND DISCUSSION

In this work, a novel protocol to obtain cholesterol-functionalized glass surfaces suitable for AFM imaging was reported. Wettability and morphological properties of this novel substrate have been studied by advancing contact angle and AFM imaging, in comparison to other surfaces having different physical and chemical properties. Moreover, a thoroughly study concerning interaction mechanism and structure of phospholipid patches after different incubation times on the different surfaces have been performed.

7.3.1 Surface functionalization and morphology of substrates

The aim of the work was to design a new tethered binding site for lipid based systems, satisfying several requirements: specificity against lipids, high mobility in aqueous solutions, ability to stay sufficiently far-away from the substrate (about 1 nm).

We chose to modify glass surfaces for several reasons: glass coverslips are easily available and functionalizable, they satisfy smoothness requirements for AFM imaging and, due to their transparency, they can be also used for optical microscope imaging applications.

Cholesterol was chosen as binding molecule, being an omnipresent compound of biological membranes and naturally inserting into phospholipid double layers. A short PEG chain was chosen as linker between cholesterol and glass due to its amphiphilic properties and its ability not to interact with proteins [18-20]. PEG high hydration provides the desired separation of the binding site from the substrate, and keeps it from collapsing onto it.

Glass coverslips have been functionalized following an original four-step protocol described in Scheme 7.1.

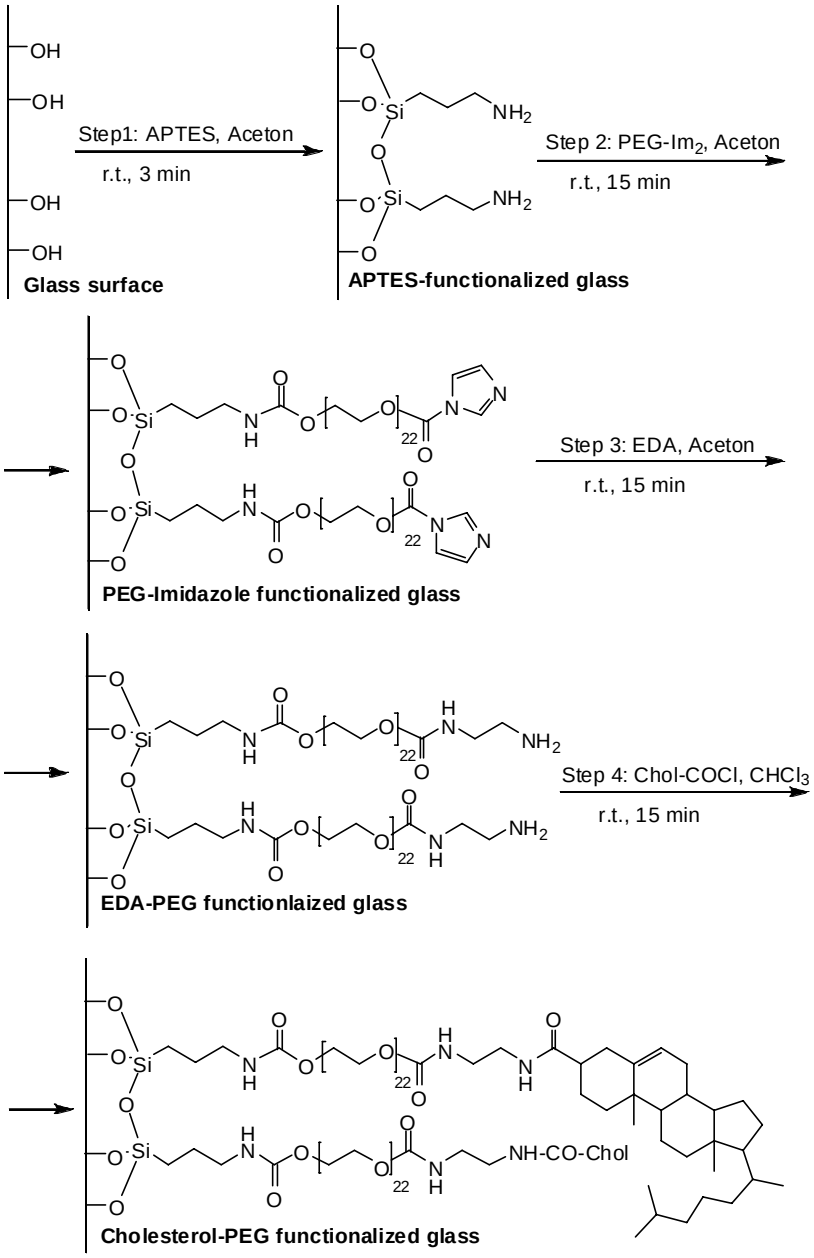

Scheme 7.1. Functionalization strategy of glass coverslips.

The protocol aims to firmly attach cholesterol groups to elastic PEG spacers, covalently attached to the glass surface. According to Scheme 1, imidazolyl-terminated PEG, obtained through an original procedure as shown in Scheme 7.2, is allowed to react with a previously amine-terminated

glass surface in order to bind PEG. Imidazolyl-terminated PEG is very reactive towards exchange with primary or secondary amines, and is also stable enough to be isolated and stored in the cool [15].

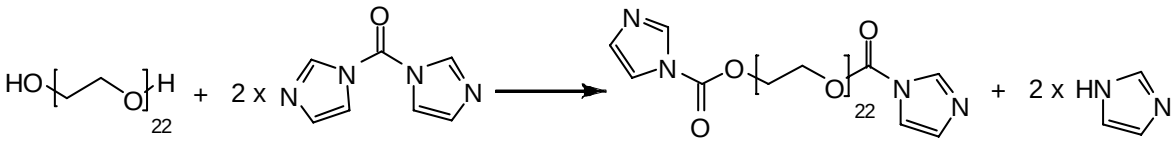

Scheme 7.2. synthesis of bis-imidazolyl PEG.

The addition of an amino function to the end of PEG chains provides the EDA-PEG intermediate surface that has been investigated in this study. Eventually, cholesterol is added. Figure 2 shows an AFM image of a cholesterol-functionalized glass coverslip (the last step of the functionalization procedure). The surface of cholesterol-functionalized glass coverslips shows the typical nano-porous, textured morphology of untreated glass coverslips (not shown). In particular, the typical nanometer-sized holes observed in clean untreated glass coverslips appear in Figure 7.1 as dark spots. These holes do not get filled upon surface functionalization, because the latter acts at the molecular level, and the functionalization density is relatively low.

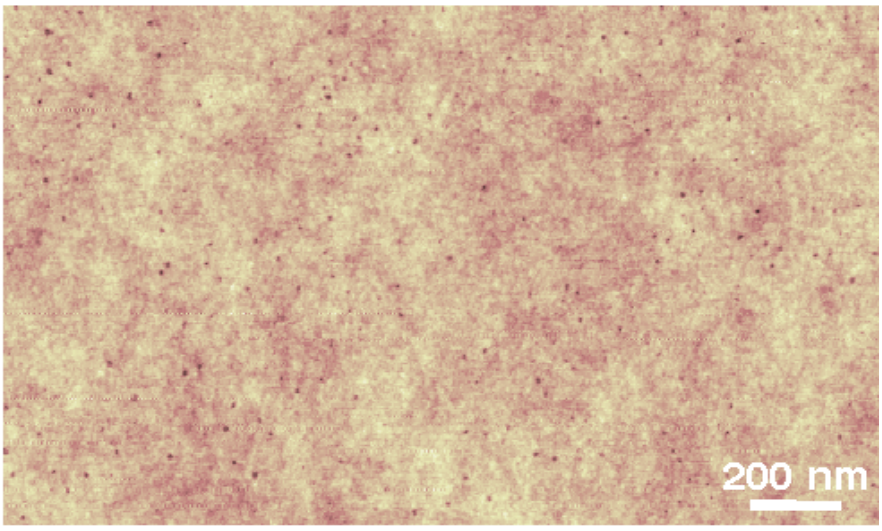

Figure 7.1. AFM topography of cholesterol functionalized glass coverslip.

The typical rms-roughness of clean glass coverslips is 0.3 nm; it remains well below 1 nm after functionalization with EDA-PEG and cholesterol. Mica and HOPG substrate were used fresh after cleavage. These substrates are atomically smooth.

Several expedients were adopted in order to obtain very clean surfaces satisfying the standard for AFM imaging of small nanoparticles. Only freshly prepared reagents were utilized and much attention was paid to materials purity grade. Reaction times were kept short, and concentrations were kept low, in order to avoid deposition of excess materials on the surface and preserve its smoothness. Each reaction and rinsing step was performed in an ultrasonic bath at 30° C, in order to improve the spatial homogeneity of the functionalization, enhance the reaction kinetics, and minimize re-deposition of desorbed excess material on the surface.

7.3.2 Contact angle measurements

Table 7.1 summarizes the advancing contact angles of water measured on cholesterol-functionlized and EDA-PEG-functionalized glass coverslips, glass coverslips freshly cleaned in aqua-regia for 15', HOPG and mica. Freshly cleaved mica is highly hydrophilic.

Table 7.1. advancing contact angles of water upon different surfaces

Surface	Contact Angle (°)
Mica	< 5
Glass coverslip (aqua regia cleaned)	32 ± 2
Amino-terminated PEG	69 ± 3
HOPG	85 ± 2
Cholesterol-functionalized	91 ± 6

We measured a contact angle of less than 5°, corresponding to complete wetting. As reference, we have measured the contact angle of a clean glass coverslip surface (32 ± 2°), because this is the basic substrate for all the functionalized surfaces considered in this study. Amino-termination of

PEG molecules led to a surface with a contact angle of 69 ± 3°. On cholesterol-functionalized coverslips we measured a contact angle of 91 ± 6°, while that measured on HOPG is 85 ± 2°. According to these values, cholesterol functionalized glass appear as the most hydrophobic surface.

We can estimate approximately the effective coverage of amino and cholesterol groups on glass coverslips. The binding efficiency of imidazolyl-PEG to silane is very high, and the incubation times allow for a complete saturation of silane sites by PEG. This is also true for the binding affinity of EDA to imidazolyl-PEG and of cholesterol to EDA terminals. We assume therefore that all the sites where silane attached are also successfully functionalized with EDA and/or cholesterol. As a consequence, the glass/PEG/cholesterol surfaces consist in uncovered glass domains and in cholesterol- or EDA-PEG-functionalized regions. According to Cassie & Baxter [21,22], the relation between the measured contact angle $cos\theta_{Glass/Chol}$ and those of homogeneous glass and cholesterol surfaces is:

$$\cos\theta_{Glass/Chol} = (1 - f_{Chol})\cos\theta_{Glass} + f_{Chol}\cos\theta_{Chol} \qquad \text{Eq(7.1)}$$

where f_{Chol} is the fraction of the surface occupied by the cholesterol molecules. From the plot of $cos\theta$ vs. cholesterol coverage shown in Figure 2 of ref. 14, assuming that the maximum effective coverage of cholesterol on a gold surface is 65% [24], and recalibrating the curve accordingly, we calculate a value of $\theta_{Chol} = 141°$ for a surface with a 100% cholesterol coverage. Using our data for $\theta_{Glass/Chol}$ and θ_{Glass}, we obtain $f_{Chol} \approx 55\%$. According to our hypotheses, this value represents also the fractional degree of functionalization of EDA-PEG on glass coverslips. Sheikh et al. found a similar functionalization density of cholesterol on self-assembled monolayers on gold [12].

7.3.3 AFM imaging of phospholipids layers.

Diph-PC multilamellar vescicles preparation and deposition onto the different surfaces were performed according to standard procedures. Lipid patches, both layers and particles, are firmly

attached to all the substrates. Despite the fact that samples are (gently) washed with water and a liposolvent agent, HBS, and dried before AFM imaging, lipid domains neither detach, nor loose their structural order, when present. Images of each sample are collected after different incubation times, from 10 to 90 minutes in order to appreciate deposition kinetics. Anyway after only ten minutes from deposition, relevant differences among the different samples are revealed.

On mica phospholipids tend to form circular islands with a quite regular shape (Figure 7.3). These circular islands have different heights, all consistent with an integer multiple of the bilayer basic thickness (around 6 nm) and very steep sidewalls, even when their thickness is more than that of a single bilayer. The almost perfect circular shape suggests that the bilayers, generated by adhesion and flattening of lipid vescicles, have high lateral mobility and can easily undergo changes of shape on mica in order to minimize the line tension. Moreover, The growth of lipid patches seemed to be more three-dimensional (up to 15 stacked bilayers are observed) than two-dimensional, suggesting that phospholipids interact more likely among themselves that with mica surface. After time, surface covering increase and wider lipid patches formed as a consequence of island coalescence.

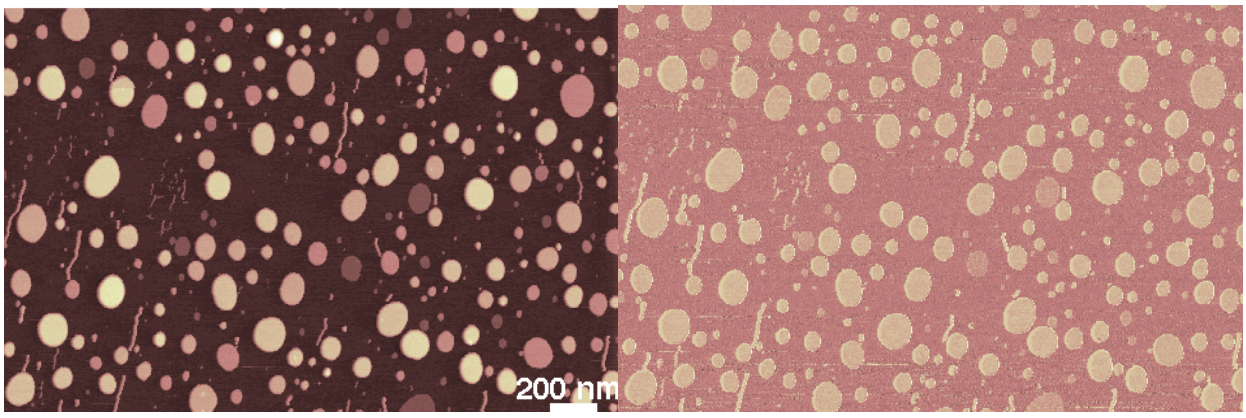

Figure 7.3: AFM topographic (left) and phase (right) maps of supported phospholipid bilayers on mica after an incubation time of 10 minutes (vertical scale 50 nm)

HOPG showed not surprisingly a completely different behavior. Only small lipids domains can form on the surface, with a thickness around 2 nm, compatible with single Diph-PC layer (Figure 7.4). In the case of hydrophobic HOPG, in fact, liposomes can interact only after a severe structure modification, since hydrophilic phospholipids head is initially exposed in the aqueous solution. Once the liposome is disrupted, small mono-layers initially form, in which interaction between phospholipids hydrophobic tails and the surface occurred.

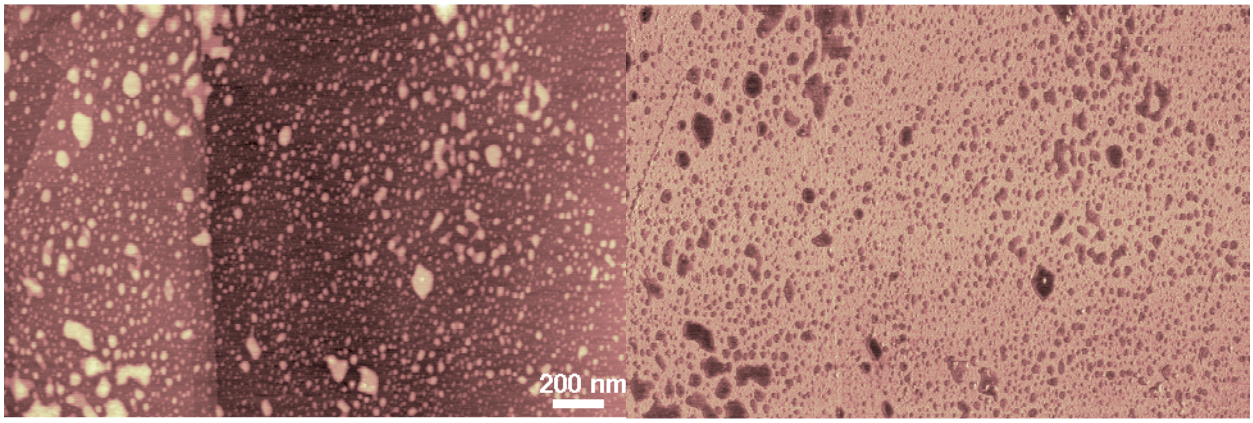

Figure 7.4: AFM topographic (left) and phase (right) maps of supported phospholipid bilayers on HOPG after an incubation time of 10 minutes (vertical scale 50 nm)

The behavior of liposomes upon glass surface functionalized with amino terminating PEG chains was also analyzed, in order to better understand the behavior of liposomes on cholesterol functionalized glass obtained by reaction of cholesteryl chloroformate with EDA-PEG glass.

The morphology is similar to that of mica after a much longer time. Regular, extended bilayers are already formed after only 10 minutes, although less stratification is observed with respect to mica and no circular islands are visible (Figure 7.5). EDA-PEG terminated surfaces evidently favor the rapid adsorption of negatively charged vesicles and the binding of phospholipids, thus accelerating the formation of extended bilayers

Bilayers appear to be less thick than on mica (around 5 nm). This behavior is not well understood. It can be possibly ascribed to a direct interaction between weakly basic amine PEG terminus with the anionic part of Diph-PC, causing a distortion in phospholipids arrangement and/or to a thinner water interlayer between glass and lipid bilayer induced by a backdrawing PEG effect. EDA-PEG terminated surfaces favor the rapid adsorption of negatively charged vesicles and the binding of phospholipids, thus accelerating the formation of extended bilayers.

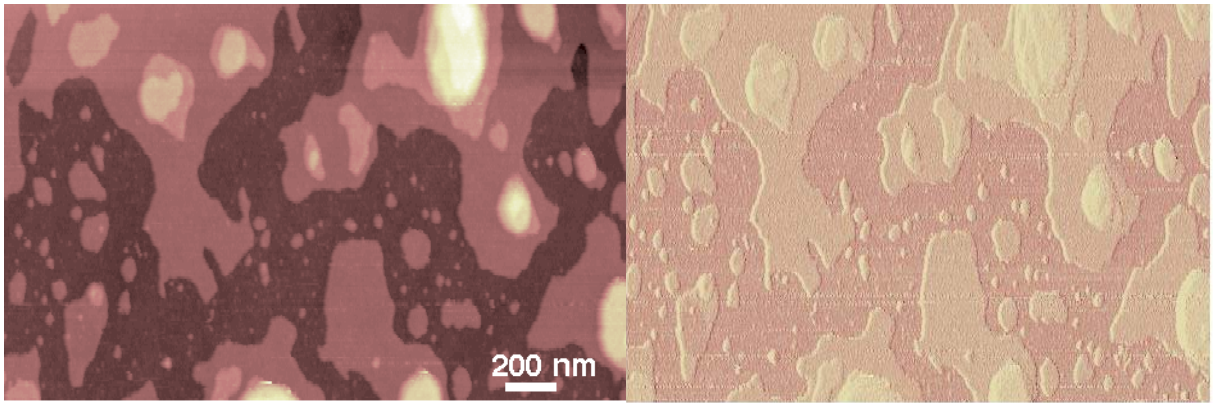

Figure 7.5: AFM topographic (left) and phase (right) maps of supported phospholipid bilayers on EDA-PEG fuctionalized glass surface after an incubation time of 10 minutes (vertical scale 50 nm)

The case of cholesterol-PEG functionalized glass surface is, as expected, much different. Despite the hydrophobicity was very similar to (or even higher than) HOPG, only after 10 minutes from deposition, very uniform and extended bilayers was formed, covering almost completely the surface with a few exceptions (Figure 7.6).

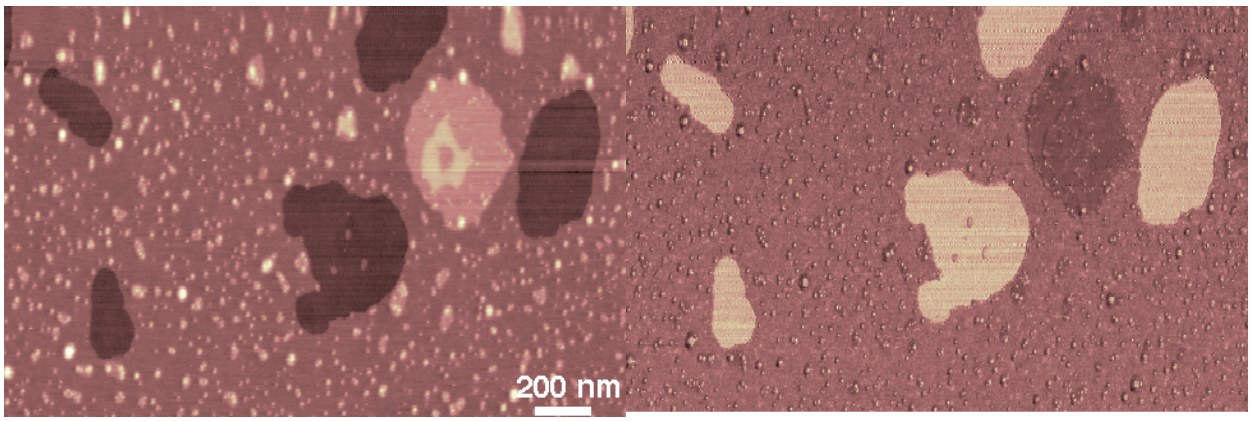

Figure 7.6: AFM topographic (left) and phase (right) maps of supported phospholipid bilayers on cholesterol fuctionalized glass surface after an incubation time of 10 minutes (vertical scale 50 nm)

Small lipid particles are decorating the top of the first bilayer. Rare second and third bilayer can also be seen, representing the early stages of the formation of a second bilayer. The measured thickness of the first bilayer appeared to be smaller than on mica and EDA-PEG coverslip (around 4.5 nm). We though that cholesterol mobile residues tethered by PEG to the glass surface can intercalate lipids bilayers disrupting the regularly phospholipids arrangement, thus accelerating single bilayer assembly on top of the surface. A schematic representations of the already discussed different lipids-surfaces interaction is reported in Figure 7.7.

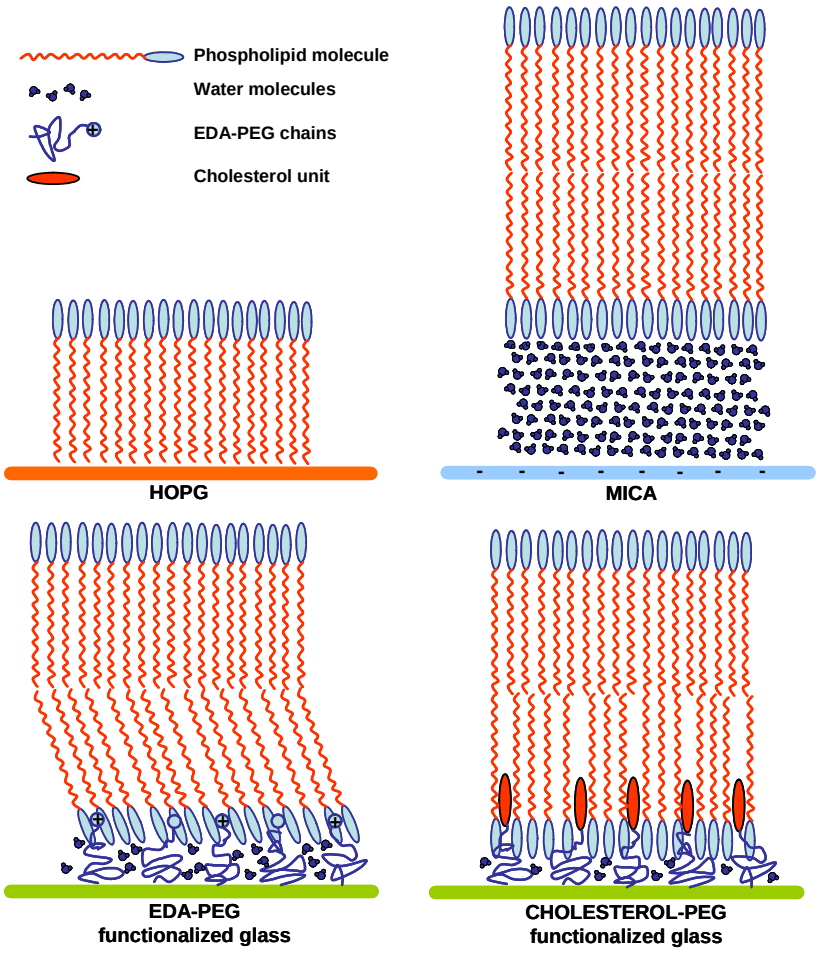

Figure 7.7: Schematic representation of the first phospholipid layers on different surfaces considered in this study. *HOPG*: DiPH-PC forms a phospholipid monolayer by the hydrophobic interaction of the lipophilic chains with HOPG surface. *Mica*: several water layers arrange between the negatively charged surface and the phospholipid bilayer. *EDA-PEG:* positively charged EDA-PEG

macromolecules grafted on the glass surface directly interact with the negative charges of DiPh-PC molecules, inducing a bending on the double layer assembly. In this case only the PEG-solvating water molecules are positioned between the double layer and the surface. *Cholesterol-PEG*: when cholesterol is bound to a PEG chain, lipophilic interactions between cholesterol and liposomes take place, causing cholesterol intercalation in the double layer. The presence of a small water layer solvating PEG chains prevents from the direct interaction of the lipophilic tails of DiPh-PC with the substrate's surface.

As already stated, a cholesterol coverage around 55 % can be estimated for the cholesterol-functionalized glass studied in this work. It is noticeable that the degree of functionalization can be easily modified by tuning of the first glass functionalization step, for example controlling silanization reaction time or silane concentration.. We expect that a lower density of cholesterol group allows to obtain single lipid nanoparticles binding instead of extended bilayers, as suggested by preliminary studies.

7.4 CONCLUSIONS

Structure and morphology of DiPh-PC phospholipid domains on different surfaces have been thoroughly investigated by atomic force microscopy. In particular, a new functionalization strategy based on the attachment of cholesterol residues to glass coverslips surface for the firm binding of phospholipid layers and nanoparticles have been developed, providing ultra-clean, smooth substrate suitable for single-particle studies by AFM. Modified glass surfaces obtained according the stated protocol can be also useful in optical microscopy studies, being glass transparency not affected by the functionalization. In particular by AFM –fluoresecnce microscopy coupling, further possibilities of studying proteins interaction with lipid bilayers are opened.

APPENDIX 1:

References

1. Akiyama E., Morimoto N., Kujawa P., Ozawa Y., Winnik F. M., Akiyoshi K., *Biomacromolecules* **2007**, 8, 2366.
2. Akiyoshi K., Deguchi S., Moriguchi N., Yamaguchi S., Sunamoto J., *Macromolecules* **1993**, 26, 3062.
3. Akiyoshi K., Deguchi S., Tajima H., Nishikawa T., Sunamoto J., *Macromolecules* **1997**, 30, 857.
4. Alberts B., Johnson A., Lewis J., Raff M., Roberts K., Walter P., *Molecular biology of The Cell* **2002**, published by Garland Publishing, fourth edition, chapter 10, 583.
5. Annunziata R., Franchini J., Ranucci E., Ferruti P., *Magn. Res. Chem.* **2007**, 45, 51.
6. Appfel C.A., *Cancer Res.* **1976**, 36, 1527
7. Arpicco S., Dosio F., Brusa P., Crosasso P., Cattel L., *Bioconjugate Chem.* **1997**, 8, 327.
8. Atanasov V., Knorr N., Duran R.S., Ingebrandt S., Offenhauser A., Knoll W., Koper I., *Biophysical Journal* **2005**, 89 1780.
9. Bencini M., Ranucci E., Ferruti P., Manfredi A., *Macrom Rapid Commun* **2006**, 27, 1060.
10. Bignotti F., Ranucci E., Ferruti P., *Macromol. Rapid Commun.* 15 (**1994**) 659–667.
11. Bonomini F., Tengattini S., Fabiano A., Bianchi R., Rezzani R.. *Histol Histopathol*. **2008**, 23, 381.
12. Boussif O., Lezoualc'h F., Zanta M.A., Mergny M.D., Scherman D., Demeneix B., Behr J.-P., *Proc. Natl. Acad. Sci. U. S. A.* **1995**, 92, 7297.
13. Bulmus V., Woodward M., Lin L., Murthy N., Stayton P., Hoffman A., *Journal of Controlled Release,* **2003**, 93, 105.
14. Carlson J.W., Jonas A., Sligar S.G., *Biophysical Journal* **1997**, 73 1184.

15. Cassie A.B.D., Baxter S. *Trans. Farad. Soc.* **1944**, 40, 546.

16. Choi J.S., Lee E.J., Choi Y.H., Jeong Y.J., Park J.S., *Bioconjug. Chem.* **1999**, 10, 62.

17. Christensen L.V., Chang C.-W., Kim W. J., Kim S. W., Zhong Z., Lin C., Engbersen J. F. J., Feijen J., *Bioconjugate Chem.* **2006**, 17, 1233.

18. Culot C., Durant F., Lazarescu S., Thiry P.A., Vanloo B., Rosseneu M.Y.,Lins L., Brasseur R., *Appl. Surf. Sci* **2004**, 230, 151.

19. Danieli B., Giardini A., Lesma G., Passarella D., Peretto B., Sacchetti A., Silvani A., Pratesi G., Zumino F., *J Org Chem.* **2006,** 71,2848.

20. Danusso F., Ferruti P., *Polymer* **1970**, 11, 88.

21. Dash P.R., Read M.L., Fisher K.D., Howard K.A., Wolfert M., Oupicky D., Subr V., Strohalm J., Ulbrich K., Seymour L.W., *J. Biol. Chem.* **2000**, 275, 3793.

22. Davis F.F. Adv *Drug Del Rev* **2002**, 54, 457.

23. Devalapally H., Chakilam A., Amiji M.M., *J Pharm Sci.* **2007**, 96, 2547

24. Duncan R. Polymer-drug conjugates. In: Budman D, Calvert H, Rowinsky E (eds) Book of anticancer drug development, Lippincott, Williams & Wilkins **2003**, Philadelphia, 239.

25. Duncan R., *Nat. Rev.* **2003**, 2, 347.

26. Duncan R., *Nat. Rev.* **2006**, 6, 688.

27. Duncan R., Ringsdorf H., Satchi-Fainaro R. *Adv. Polym.Sci*, **2006** 192.

28. Emilitri E., Ferruti P., Annunziata R., Ranucci E., Rossi M., Falciola L., Mussini P., Chiellini F., Bartoli C., *Macromolecules* **2007**, 40, 4785.

29. Emilitri E., Ranucci E., Ferruti P., *J. Polym. Sci., Part A: Polym. Chem.***2005**, 43, 1404.

30. Feng M., Morales A. B., Beugeling T., Bantjes A., van der Werf K., Gosselink G., de Grooth B., Greve J., *J Colloid Interf Sci* **1996**, 177, 364.

31. Ferruti P. *Macromol. Synth.*, **1985**, 9, 25.

32. Ferruti P., Bianchi S., Ranucci E., Chiellini F., Caruso V., *Macromol Biosci* **2005**, 5, 613.

33. Ferruti P., Bianchi S., Ranucci E., Chiellini F., Piras A.M., *Biomacromolecules* **2005**, 6, 2229.

34. Ferruti P., Franchini J., Bencini M., Ranucci E., Zara G.P., Serpe L., Primo L., Cavalli R., *Biomacromolecules* **2007**, 8, 1498.

35. Ferruti P., Knobloch S., Ranucci E., Duncan R., Gianasi E., *Macromol. Chem. Phys.* **1998**, 199, 2565.

36. Ferruti P., *Macromol. Syntheses* **1985**, 9, 25.

37. Ferruti P., Manzoni S., Richardson S.C.W., Duncan R., Pattrick N.G., Mendichi, R., Casolaro, M., *Macromolecules* **2000**, 33, 7793-7800.

38. Ferruti P., Marchisio M.A., Barbucci R., *Polymer*, **1985**, 26, 9, 1336.

39. Ferruti P., Marchisio M.A., Duncan R., *Macromol. Rapid Commun*. **2002**, 23, 332.

40. Ferruti P., Ranucci E., Bigotti F., Sartore L., Bianciardi P., Marchisio M.A., *J. Biomater. Sci. Polym. Ed.* **1994**, 6, 833.

41. Ferruti P., Ranucci E., Trotta F., Gianasi E., Evagorou E.G., Wasil M., Wilson G., Duncan R., *Macromol. Chem. Phys*., **1999**, 200, 1644.

42. Franchini J., Ranucci E., Ferruti P., Rossi M., Cavalli R., *Biomacromolecules* **2006**, 7, 1215.

43. Garavaglia M, Dopinto S., Ritter M., Furst J., Saino S., Guizzardi F., Jakab M., Bazzini C., Vezzoli V., Dossena S., Rodighiero S., Sironi C., Botta G., Meyer G., Henderson R.M., Paulmichl M., *Cellular Physiology and Biochemistry* **2004**, 14 231.

44. Gosselin M.A., Guo W., Lee R.J., *Bioconj. Chem.* **2001**, 12, 989.

45. Grandbois M., Clausen-Schaumann H., Gaub H., *Biophysical Journal* **1998**, 74, 2398.

46. Green J.D., et al., *J. Mol. Biol.* **2004**, 342, 877.

47. Gref R., Minamitake Y., Peracchia M.T., Trubetskoy V., Torchilin V., R. Langer, *Science* **1994**, 263, 1600.

48. Griffiths P.C., Paul A., Khayat Z., Wan K.W., King S.M., Grillo I., Schweins R., Ferruti P., Franchini J., Duncan R. *Biomacromolecules*, **2004**, *5*, 1422.

49. Groll J., Amirgoulova E.V., Amiringer T., Heyes C.D., Rocker C., Nienhaus G.U., Moller G.U., *J Am Chem Soc* **2004**, 126, 4234.
50. Haag R., Kratz F. *Angev. Chem. Int. Ed* **2006**, 45,1198.
51. Harder P., Grunze M., Dahint R., Whitesides G.M., Laibinis P.E., *J Phys Chem B* **1998**, 102, 426.
52. Hill I. R., Garnett M.C., Bignotti F., Davis S.S., *Biochim. Biophys. Acta* **1999**, 1427, 161.
53. Hill I.R., Garnett M.C., Bignotti F., Davis S.S., *Anal. Biochem.* **2001**, 291, 62.
54. Huang S.Y., Pooyan S., Wang J., Choudhury I., Leibowitz M.J., Stein S., *Bioconjugate Chem.* **1998**, 9, 612.
55. Huber W.W., Parzefall W., *Curr Opin Pharmacol.* **2007,** 7,404.
56. Ishida T., Kirchmeier M.J., Moasea E.H., Zalipsky S., Allen T.M., *Biochim. Biophys. Acta* **2001**, 1515, 144.
57. Iwasaki Y., Akiyoshi K., *Biomacromol*. **2006**, 7, 1433.
58. Jatzkewitz H. Z., *Naturforsch*. **1955**,.10, 27.
59. Jin S., Ye K., *Biotechnol. Prog.* **2007**, 23, 32.
60. Jones N.A., Hill I.R., Stolnik S., Bignotti F., Davis S.S., Garnett M.C., *Biochim. Biophys. Acta* **2000**, 1517, 1.
61. Jordan P.A., Gibbins J.M., *Antioxid Redox Signal*.**2006**, 8, 312.
62. Katz E., Willner I., *Angev. Chem. Int. Ed* **2004**, 43, 6042.
63. Kosuke I., Properties of Solvents and Solvent Classifications, in *Electrochemistry in nonaqueous solutions*, Wiley-VCH **2002**, Verleg GmbH, Weinheim, 5 and *Ibidem,* Potentiometry in Non-Aqueous Solutions, 182.
64. Kukowska-Latallo J.F., Bielinska A.U., Johnson J., Spindler R., Tomalia D.A., Baker J.R., *Proc. Natl. Acad. Sci. U. S. A.* **1996**, 93, 4897.

65. Kwoh D.Y., Coffin C.C., Lollo C.P., Jovenal J., Banaszczyk M.G., Mullen P., Phillips A., Amini A., Fabrycki J., Bartholomew R.M., Brostoff S.W., Carlo D.J., *Biochim. Biophys. Acta* **1999**, 1444, 171.

66. Kwok K.Y., Y. Park, Y. Yang, McKenzie D.L., Liu Y., Rice K.G., *J. Pharm. Sci.* **2003**, 92, 1174.

67. Lavignac N., Lazenby M., Franchini J., Ferruti P., Duncan R., Int. *J. Pharm*. **2005**, 300, 102.

68. Lavignac N., Lazenby M., P. Foka, B. Malgesini, I. Verpilio, P. Ferruti, R. Duncan R. *Macromol Biosci.* **2004**, 4, 922.

69. Lee J. H., Lee H.B., Andrade J.D., *Prog Polym Sci* **1995**, 20, 1043.

70. Li Y.Q., Zhang H.Z., Davidovits P., Jayne J.T., Kolb C.E., Worsnop D.R., *J. Phys. Chem. A* **2002**, 106, 1220.

71. Lin C, Blaauboer C.J., Timoneda M.M., Lok M.C., Van Steenbergen M., Hennink W.E., Z. Zhong, Feijen J., Engbersen J.F.J., *J. Contr. Rel* **2008**, 126, 166.

72. Lin C., Zhong Z., Lok M.C., Jiang X., Hennink W.E., Feijen J., Engbersen J.F.J. *J. Contr. Rel.* **2007**, 123, 67.

73. Lin C., Zhong Z., Lok M.C., Jiang X., Hennink W.E., Feijen J., Engbersen J.F.J., *Bioconjugate Chem.* **2007**, 18, 138-145.

74. Lin C., Zhong Z.Y., Lok M.C., Jiang X.L., Hennink W.E., Feijen J., Engbersen J.F.J., *J. Control. Release* **2006**, 116, 130.

75. Maeda H., Polymer conjugated macromolecular tumour-drugs for specific targeting. In *Polymeric site specific pharmacotherapy*, Doumb, A. J., Ed., John Wiley **1994**, New York.

76. Maeda H., Wu J., Sawa T., Matsumura Y., Hori K., *J. Controlled Release* **2000**, 65, 271.

77. Malgesini B., Verpilio I., Duncan R., Ferruti P. *Macromol. Biosci.* **2003**, 3, 59.

78. Mandeville W.H., Goldberg D.I. *Curr. Pharm. Des.* **1997**, 3, 15.

79. Masuho Y., Kishida K., Saito M., Umemoto N., Hara T., *J. Biochem.* **1982**, 91, 1583.

80. Matsumura Y., Maeda H., *Cancer Res.* **1986**, 46, 6387.

81. Matsusaki M., Fuchida T., Kaneko T., Akashi M., *Biomacromol*. **2005**, 6, 2374.

82. Mecke, et al., *Chem. and Phys. of Lipids* **2004**, 132, 3.

83. Meister A., Anderson M.E., *Annu. Rev. Biochem* **1983**, 52, 711.

84. Miyata K., Kakizawa Y., Nishiyama N., Harada A., Yamasaki Y., Koyama H., Kataoka K., *J. Am. Chem. Soc.* **2004**, 126, 2355.

85. Miyata K., Kakizawa Y., Nishiyama N., Yamasaki Y., Watanabe T., Kohara M., Kataoka K., *J. Contr. Release* **2005**, 109, 15.

86. Morimoto N., Endo T., Iwasaki Y., Akiyoshi K., *Biomacromolecules* **2005**, 6, 1829.

87. Nguyen H.K., Lemieux P., Vinogradov S.V., Gebhart C.L., Guerin N., Paradis G., Bronich T.K., Alakhov V.Y., Kabanov A.V., *Gene Ther.* **2000**, 7, 126.

88. Oupicky D., Parker A.L., Seymour L.W., *J. Am. Chem. Soc.* **2002**, 124, 8.

89. Pack D.W., Hoffman A.S., Pun S., Stayton P.S. *Nat. Rev. Drug Discov.* **2005**, 4, 581.

90. Pattrick N.G., Richardson S.C.W., Casolaro M., Ferruti P., Duncan R., Journal *J. Contr. Rel.* **2001**, 77, 225.

91. Pesen D., Hoh J.H., *Biophysical Journal* **2005**, 88, 670.

92. Plank C., Mechtler K., Szoka F.C., Wagner E., *Hum. Gene Ther.* **1996**, 7, 1437.

93. Pouton C.W., Seymour L.W., *Adv. Drug Deliv. Rev.* **1998**, 34, 3.

94. Rackstraw B.J., Stolnik S., Bignotti F., Garnett M.C., *Biochim. Biophys. Acta* **2002**, 1576, 269.

95. Ranucci E., Ferruti P., *Macromolecules* 24 (**1991**) 3747– 3752.

96. Ranucci E., Ferruti P., *Polymer* **1991**, 32, 2876.

97. Ranucci E., Ferruti P., Suardi M.A., Manfredi A., *Macrom. Rap. Com.*, **2007**, 28, 1243.

98. Ranucci E., Ferruti P., *Synthetic Communications* **1990**, *20(19)*, 2951.

99. Read M.L., Singh S., Ahmed Z., Stevenson M., Briggs S.S., Oupicky D., Barrett L.B., Spice R., Kendall M., Berry M., Preece J.A., Logan A., Seymour L.W., *Nucleic Acids Res.* **2005**, 33, e86

100. Reynolds A., Laurie C., Mosley R.L., Gendelman H.E., *Int Rev Neurobiol.* **2007,** 82, 297.

101. Richardson S., Ferruti P., Duncan R., *J. Drug Targeting* **1999**, 6, 391-404.

102. Richardson S.C.W., Pattrick N.G., Man Y.K.S., Ferruti P., Duncan R., *Biomacromolecules*, **2001**, *2*, 1023.

103. Ringsdorf H. Polym *J Polym. Sci, Polymer Symp* **1975**, 51, 135.

104. Saito G., Swanson J.A., . Lee KD., *Adv Drug Deliv Rev.* **2003,** 55,199

105. Schaffer D.V., Fidelman N.A., Dan N., Lauffenburger D.A., *Biotechnol. Bioeng*. **2000**, 67, 598.

106. Sheikh K.H., Christenson H.K., Bushby R.J., Evans S.D., *J Phys Chem B* **2007**, 111, 379.

107. Stolnik S., Dunn S.E., Garnett M.C., Davies M.C., Coombes A.G.A., Taylor D.C., Irving M.P., Purkiss S.C., Tadros T.F., Davis S.S., Illum L., *Pharm. Res.* **1994**, 11, 1800.

108. Sugimoto H., Nakanishi E., Yamauchi F., Yasumura T., Inomata K., *Polymer* **2005**, 46, 10800.

109. Teitlebaum M.S.D., Arnon R., Sela, M. *Cell Biol. Life Sci.* **1997**, 53, 24.

110. Tero R., Takizawa M., Li Y.-J., Yamazaki M., Urisu T., *Langmuir* **2004**, 20, 7526.

111. Toby A, Jenkins A., Boden N., Bushby R.J., Evans S.D., Knowles P.F., Miles R.E., Ogier S.D., Schonherr H., Vansco G.J., *J Am Chem Soc* **1999**, 121, 5274.

112. Toncheva V., Wolfert M.A., Dash P.R., Oupicky D., Ulbrich K., Seymour L.W., Schacht E.H., *Biochim. Biophys. Acta* **1998**, 1380, 354.

113. Torchilin V.P., *AAPS Journ.* **2007**, 9, 128.

114. Torchilin V.P., *Annu. Rev. Biomed. Eng.* **2006**, 8, 343.

115. Torchilin V.P., *Nat. Rev. Drug Discov.* **2005**, 4, 145.

116. Turner Y.T., Roberts C.J., Davies M.C., *Adv Drug Deliv Rev.* **2007**, 59, 1453

117. Van de Wetering P., Cherng J.-Y., Talsma H., Hennink W.E., *J. Control. Release* **1997**, 49, 59.

118. Vliet K.J.V., Hinterdorfer P., *Nano Today* **2006**, 1, 18.

119. Wang D., Wang L., Goh S.H., Yang Y., *Biomacromol*. **2007***,* 8*,* 1028-1037.

120. Wang Y., Gao S., Ye W.H., Yoon H.S., Yang Y.Y., *Nat. Mat.* **2006**, 5, 791.

121. Watson J.D., Crick F.H. *Nature* **1953**, 171, 737.

122. Whangbo M-H, Bar G., Brandsch R., *Surface Science* **1998**, 1-2, L794.

123. Williams L.M., Evans S. D., Flynn T. M., Marsch A., Knowles P. F., Bushby R. J., Boden N., *Langmuir* **1997**, 13, 751.

124. Woghiren C., Sharma B., Stein S., *Bioconjugate Chem.* **1993**, 4, 314.

125. Wu G., Fang Y.Z., Yang S., Lupton J.R., Turner N.D., *J Nutr.* **2004,** 134*,* 489.

126. Wu G.Y., Zhan P., Sze L.L., Rosenberg A.R., Wu C.H., *J. Biol. Chem.* **1994**, 269, 11542.

127. Xu J.P., Ji J., Chen W.D., Shen J.C., *Macromol. Biosci.* **2005**, 5, 164.

128. Yang, Z.P., Engquist, I, Kauffmann, J.M., Liedberg, B. *Langmuir* **1996**, 12, 1704.

129. Yusa S.I., Kamachi M., Morishima Y. *Macromol*. **2000**, 33, 1224.

130. Zhou X., Huang L., *Biochim. Biophys. Acta* **1994**,1189, 195.

131. Zhou X.B., De Hosson, J.Th.M. *J. Mater. Res.* **1995**, 10, 1984.

APPENDIX 2:

Common materials and methods

Materials.

1,4-Dithio-DL-threitol (DTT) (99%), carbonyl di-imidazole (>97%), cystamine dihydrochloride (>98%), lithium hydroxide monohydrate (>98%), morpholine (>99%), N,N'-dimethylethylenediamine (>98%) (DMEDA), piperazine (>99%), poly(ethylene glycol) (PEG) 1000, poly(ethylene glycol) methyl ether 750, poly(ethylene glycol) methyl ether 2000, tri-etyl amine (TEA), tris(hydroxymethyl)aminomethane (TRIS) (>99.8%), were purchased from Fluka and used as received; 2,2'-dipyridyl disulfide (98%), 2-mercaptopyridine (>95%), azobenzene (>98%), cholesteryl chloroformate (97%), di-tert-butyl-dicarbonate (>98%), estradiol (97%), N,N'-methylenebis(acrylamide) (MBA) (>98%), thiocholesterol (98%), were purchased from Aldrich and used as received; ethylene diamine (EDA) was purchased from Fluka and distilled before use, 2-Methylpiperazine were purchased from Fluka and used after sublimation, purity controlled by acidimetric titration; 2,2-Bis(acrylamido)acetic acid (BAC) (Ferruti, Ranucci et al., 1999) and bis(acryloyl)piperazine (BP) (Ferruti, 1985) were synthesized according to a procedure reported elsewhere. $CDCl_3$ (99.8%) stabilized over silver coil, D_2O (99.9%), d6-DMSO (99.8%), MeOD (99.8), DCl 35% in D_2O solution and NaOD 30% in D_2O solution were purchased from Aldrich. Organic solvents used were all analytical grade and were purchased from Fluka. Water was bidistilled.

Instruments and Methods.

(a) ^{1}H and ^{13}C NMR spectra were run on a Brüker Advance 400 spectrometer operating at 400.132 MHz (1H) and 100.623 (13C).

(b) Size exclusion chromatography (SEC) traces of polymers soluble in organic solvents (polystyrene standards) were obtained with Phenomenex Phenogel 500, 103, and 104 A columns,

connected in series, UV detector operating at 254 nm, mobile phase 9/1 (v/v) $CHCl_3/CH_3OH$. SEC traces of water soluble polymer (pullulan standards) were obtained using a WATERS 515 HPLC PUMP instrument, with Toso-Haas 486 columns, using 0.1 M TRIS buffer pH 8.0 ± 0.1 as mobile phase, UV detector operating at 230 nm.

(c) UV-VIS spectra were run on a Perkin-Elmer Lambda EZ210 spectrometer. For all measurements, quartz cells with a 1 cm path length were used.

(d) IR spectra were recorded with a Jasco FT/IR-4100 spectrometer.

(e) Elemental analyses were performed with a Fison EA 1108 CHNS apparatus.

(f) Specific optical rotations were measured with a Jasco P-1030 polarimeter.

(g) Transmission electron microscopy analyses were performed with Zeiss LEO 912AB (EFTEM). One drop of 0.1 mg/mL nanoparticle dispersion was placed on a polymer coated sample grid after filtration on 0.45 μm HPLC syringe filter, the excess dried out and the sample stained with uranyl acetate.

(h) Particle size distributions were measured using a Viscotek 802 Dynamic Light Scattering analyzer. Samples were prepared dispersing 1 mg of lyophilized nanoparticles in 1 mL of distilled water in ultrasonic bath for 15 min, then diluting with a three fold amount of water or phosphate buffer solution and filtering on 1 μm HPLC syringe filter. Samples were analyzed with a Viscotek 802 DLS, data analized with Omnisize 2.0 software, Correlator resolution 256 channel.

(i) AFM imaging was performed using a Bioscope II AFM equipped with a Nanoscope V controller (Veeco Instruments, USA). All images were acquired in Tapping Mode using single crystal silicon tips with nominal radius of curvature of 5-10 nm and cantilever resonance frequency in the range 200-300 kHz. Scan areas were typically 5μm x 2.5μm and 50μm x 25μm, with scan rates of 1.5 Hz and 0.5 Hz, accordingly.

APPENDIX 3:

Poster and oral presentations:

EPF 3rd Summer School

22-27 May 2005 - Saint Die des Vosges, France

Poster:

1. Marco Suardi, Amedea Manfredi, Jade Wu, Elisabetta Ranucci, Paolo Ferruti.

   Kinetic analysis of polymerization of poly(amidoamine)s in organic solvents.

2. Marco Suardi*, Sabrina Bianchi*, Federica Chiellini**, Elisabetta Ranucci*, Paolo Ferruti*.

   Novel poly(amidoamine)-based hydrogels as scaffold for tissue engineering.

33rd Annual Meeting of the Controlled Release Society

July 22-26, 2006 - Wien, Austria

Poster:

Suardi Marco, Franchini Jacopo, Cavalli Roberta, Ranucci Elisabetta, Ferruti Paolo

Transfection efficiency and preliminary pharmacokinetics study of amphoteric agmatine-based poly(amidoamine)

1° Forum Nazionale dei Giovani Ricercatori su Materiali Polimerici e Biomteriali

September 18-20, 2006 - Modena, Italy

Member of the scientific committee.

7th International Symposium on Frontiers in Biomedical Polymers

June 24-27, 2007 - Ghent, Belgium

Oral presentation:

Marco A. Suardi, Elisabetta Ranucci, Paolo Ferruti

New stimuli-responsive polymeric nanoparticles based on cholesterol-poly(amidoamine) conjugates.

3rd IUPAC International Symposium on Novel Materials and their Synthesis (NMS-III) & 17th International Symposium on Fine Chemistry and Functional Polymers (FCFP-XVIII)

October 17-21, 2007- Shanghai, China

Oral presentation:

M.A. Suardi, E. Ranucci P. Ferruti, E. Emilitri, F. Martello, E. Lattanzio, F. Fenili.

Biocompatible and Bioeliminable Hydrophilic Polymers

International Congress on Biohydrogels

November 14-18, 2007- Viareggio, Italy

Oral Presentation:

Marco Suardi, Elisabetta Ranucci, Paolo Ferruti, Federica Chiellini.

Novel poly(amidoamine)-based hydrogels as scaffold for tissue engineering.

APPENDIX 4:

Publications:

1. Amedea Manfredi, Elisabetta Ranucci, Marco Suardi, Paolo Ferruti, "Polymerization Kinetics of Poly(amidoamine)s in Different Solvents", *J. Bioact. Comp. Polym*. **2007**, 22, 1-14.

2. Elisabetta Ranucci, Paolo Ferruti, Marco Alessandro Suardi, Amedea Manfredi, "Poly(amidoamine)s with 2-Dithiopyridine Side Substituents as Intermediates to Peptide–Polymer Conjugates", *Macrom. Rapid. Commun*. **2007**, 28, 1243-1250

3. Elisa Emilitri, Fabiana Guizzardi, Cristina Lenardi, Marco Suardi, Elisabetta Ranucci, Paolo. Ferruti, "Novel Poly(amidoamine)-based Hydrogels as Scaffolds for Tissue Engineering", *Macromolecular Symposia*, accepted **January 2008**

4. Marco Indrieri, Marco Suardi, Alessandro Podestà, Elisaebtta Ranucci, Paolo Ferruti, Paolo Milani, "Quantitative investigation by atomic force microscopy of supported phospholipid layers and nanostructures on cholesterol-functionalized glass surfaces", *Langmuir*, accepted **January 2008**.

5. Elisabetta Ranucci, Marco Aalessandro Suardi, Rita Annunziata, Paolo Ferruti, Federica Chiellini, Cristina Bartoli, "Nanostructured self-assembling poly(amidoamine) conjugates bearing disulphide linked cholesterol pendants", *Biomacromolecules*, submitted **January 2008**.

Polymerization Kinetics of Poly(amidoamine)s in Different Solvents

AMEDEA MANFREDI, ELISABETTA RANUCCI*, MARCO SUARDI, AND PAOLO FERRUTI
Dipartimento di Chimica Organica e Industriale, Università di Milano, via Venezian 21, 20133 Milano, Italy and CIMAINA, Centro Interdisciplinare Materiali e Interfacce Nanostrutturate, via Golgi 19, 20133 Milano, Italy

ABSTRACT: The polyaddition kinetics of 2-methylpiperazine to 1,4-bis-acryloylpiperazine was determined in water, methanol, ethylene glycol, formamide, and dimethylformamide, respectively. In the protic solvents, the polyaddition proceeded through a two-step mechanism, each step involved one of the two different secondary amino groups; the difference in amine reactivity was ascribed to the different steric hindrance by the neighbouring groups. Each step followed pseudo-second-order kinetics; the kinetic constants included the catalytic protonic species. In the case of dimethylformamide, the polyaddition proceeded through third-order kinetics; this accounted for the autocatalytic activity of the amino groups. The apparent kinetic constants in the protic solvents increased with the increase in the autoprotolysis constant values and decreased with the increase of the dipole moment.

KEY WORDS: poly(amidoamine)s, polymerization kinetics, stepwise polyaddition in organic solvents.

INTRODUCTION

Poly(amidoamine)s (PAAs) are biodegradable and biocompatible synthetic polymers characterized by the presence of *tert*-amino

Q1 *Author to whom correspondence should be addressed.
Colour figures information.

0883-9115/07/04 001–13 $10.00/0 DOI: 10.1177/0883911507076453

groups in the main chain [1–5]. Besides being endowed with interesting properties as polymeric bases and metal ion complexing agents [6–9], PAAs have important biomedical properties, such as heparin-complexing ability [9,10]. Water-soluble PAAs have been extensively studied by Duncan *et al.* as drug carriers and endosomolytic polymers [11–16]. In cross-linked form, hydrophilic PAAs give rise to hydrogels, some of which exhibit excellent biocompatibility and are currently being studied as scaffolds for tissue engineering [17,18].

PAAs are usually obtained by hydrogen-transfer polyaddition of primary or secondary amines to bis-acrylamides (Scheme 1). The reaction conditions involve room temperature (15–30°C) conditions with no added catalysts.

One of the advantages of PAAs as specialty polymers is that they are amenable to further functionalization. PAAs containing other chemical functions as side-substituents can be obtained by using suitably functionalized monomers. In fact, only a few groups are able to interfere in the polyaddition reaction and, in principle, nearly every aliphatic amine and bis-acrylamide can be used as a monomer.

For some purposes, PAAs containing hydrophobic moieties can be obtained. This involves the use of water-insoluble monomers and, therefore, organic reaction solvents are needed [19]. Pioneering studies performed by the authors showed, not surprisingly, that high molecular weight polymers can only be obtained in organic solvents bearing mobile hydrogens, such as alcohols. Aprotic solvents gave poor results irrespective of their polarity [1].

Since systematic comparison studies of the polymerization kinetics of PAAs in water and alcohols were lacking, a comparative study of the kinetics was performed in water, methanol, and ethylene glycol of a typical polyaddition reaction, namely that of 2-methylpiperazine (MP) to 1,4-bis-acryloylpiperazine (BP). Formamide, was also studied, together with a typical dipolar aprotic solvent, dimethylformamide.

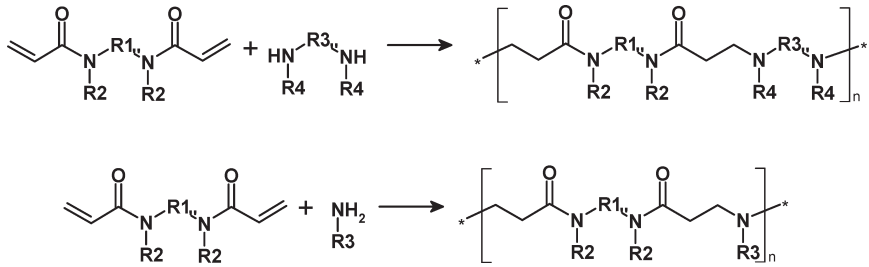

Scheme 1. Synthesis and genera molecular structure of PAAs.

EXPERIMENTAL

Materials and Methods

BP was prepared as previously described [20]; 2,5-dimethylpiperazine (DMP) was commercially available (Aldrich) and was used without further purification. The MP was purchased from Fluka and recrystallized from n-heptane (1 g MP in 20 mL solvent) before use. Its purity was checked just before use by potentiometric titration. The organic solvents were anhydrous analytical grade, freshly purchased from Fluka. They were transferred under dry nitrogen by means of syringes. The bottles were opened just before use and their content leftover molecular sieve. 0.1 M hydrochloric acid solution was purchased from Riedel-de Haen. Water was doubly distilled.

Measurements

UV-VIS spectra were run on a Perkin-Elmer Lambda EZ210 spectrometer connected to a PC for data transfer. For all measurements, quartz cells with a 1 cm path length were used. The calibration curves were obtained for each solvent in the analysis of BP at nine different concentrations; the absorbance at 250 nm fell within the range 0.04–0.9. The solutions were prepared using as solvent 0.1 M hydrochloric acid containing 0.05% v/v of the organic solvent used. The data were processed by means of the least square fitting.

Model Polymerization Reactions

A 0.4 M solution of BP in the appropriate solvent (25 mL) and a 0.4 M solution of MP (or DMP) in the same solvent (25 mL) were introduced by means of syringes into a 100 mL one-necked flask, equipped with a silicon rubber stopper and thermostated at 25°C. The reaction mixture was flushed with dry nitrogen and then kept at 25°C without stirring. Aliquots (10 μL) were withdrawn at specific reaction times, and the final volume of each was adjusted to 20 mL with 0.1 M hydrochloric acid. The UV absorption of each solution was measured against the appropriate blank solution, that is, 0.1 M hydrochloric acid containing 0.05% v/v of organic solvent; the experiments were performed in duplicate.

RESULTS AND DISCUSSION

The aim of this work was to study the kinetics in different solvents (water, methanol, ethylene glycol, formamide, and dimethylformamide)

of a typical polyaddition reaction leading to a PAA. The model reaction adopted in this study was the polyaddition of MP to BP (Scheme 2).

This reaction was chosen as model PAA preparation, because both the monomers involved, as well as the resultant polymer, are easily soluble in water, lower alcohols, and formamide. Perhaps plain piperazine would have been an even better model, because it bears two perfectly identical amino groups. Piperazine, however, was discarded because its polymer with BP is soluble only in water [2–4] and, therefore, in organic solvents precipitation would occur after a short reaction time. Moreover, MP is the amine used as the monomer in the PAAs with particular biomedical interest, some of which also employ BP as a co-monomer (4). In addition, to investigate the effect of the different steric hindrance of the substituents in the α-position to the reactive secondary amine groups on the polyaddition reaction with bis-acrylamides, MP and, in the case of aqueous solutions, DMP were chosen as monomers.

The reactions were carried out at 25°C (close to the room temperature for the PAA syntheses). The reaction progress was monitored by UV spectroscopy, preferred to other methods for its sensitivity, fastness, and cheapness, measuring the decrease in the intensity of the absorption band of the conjugated double bonds of BP. The following procedure was invariably adopted. The polymerization reactions were carried out at a 0.2 M concentration in the selected solvent (see Experimental Section), that is, approximately 1/10 of the reaction concentrations commonly adopted in PAA syntheses. Aliquots (10 μL) of the polymerization solutions were taken at specific time intervals and diluted in 20 mL 0.1 M aqueous hydrochloric acid, in order to stop the polymerization reaction and to reach a suitable concentration for UV measurements. The UV spectra of MP, BP and their polyaddition product were, therefore, preliminarily studied in 0.1 M aqueous hydrochloric acid containing 0.05% v/v of organic solvent, in order to verify the influence of the residual solvent on the absorption spectra of reagents and products. The absorption spectra in 0.1 M aqueous hydrochloric acid + 0.05% (v/v) methanol are shown in Figure 1. In all the aqueous mixtures, the absorption spectrum of BP showed a peculiar absorption band with a maximum at 240 nm due to the π–π*

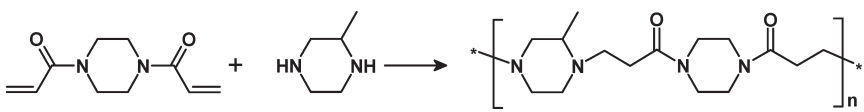

Scheme 2. Polyaddition reaction of BP to MP.

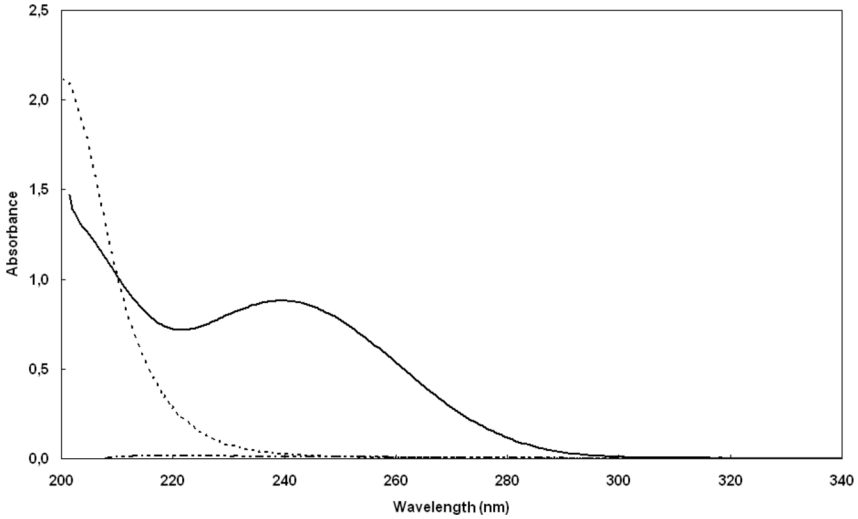

Figure 1. Absorption spectra of BP (—), MP (—·—) and the the polyaddition products (- - -) in 0.1 M aqueous hydrochloric acid + 0.05% (v/v) methanol.

transition of the BP conjugate double bond. In this range, BP spectrum partially interferes with the tail of polymer absorption bands. For this reason, a different wavelength, 250 nm, was chosen for measuring the decrease in BP concentration. The molar extinction coefficients curves obtained in the different aqueous hydrochloric acid/solvent mixtures, ε, are reported in Table 1. The experimentally determined values of ε show slight differences in different aqueous/solvent mixtures, reflecting the different interactions between solvent and BP.

*Table 1. Molar extinction coefficients ε for bis-acryloylpiperaizine.**

Solvent	Molar Extinction Coefficient (1/M cm)
Water	10 600
Ethylene glycol	12 200
Methanol	11 400
Formamide	11 700
Dimethylformamide	12 400

*In 0.1 M hydrochloric acid with 0.05% of different organic solvents at 250 nm.

Kinetic Features and Determination of Rate Constants

The conversion curves obtained in the polyaddition reaction of BP with MP in the series of solvents listed in Table 1 are shown in Figure 2. It is apparent that the reaction proceeds much faster in water and glycol than in methanol, formamide, and dimethylformamide, the latter solvents gave the poorest performance.

To investigate the kinetic features of the polymerization reactions of BP with MP in different protic solvents, we referred to our previous studies on hydrogen transfer addition and polyaddition reactions involving acrylamides, bis-acrylamides, and/or bis-acrylic esters [21–23]. These reactions exhibited pseudo-second-order kinetics, with the kinetic constants that included the concentration of the catalytic protonic species, when performed in the presence of hydroxyl solvents. On the basis of this premise, the current data was substituted in the following equation:

$$\frac{\mathrm{d}\left[\mathrm{BP}\right]}{\mathrm{d}t} = -k\left[\mathrm{BP}\right]\left[\mathrm{MP}\right] \tag{1}$$

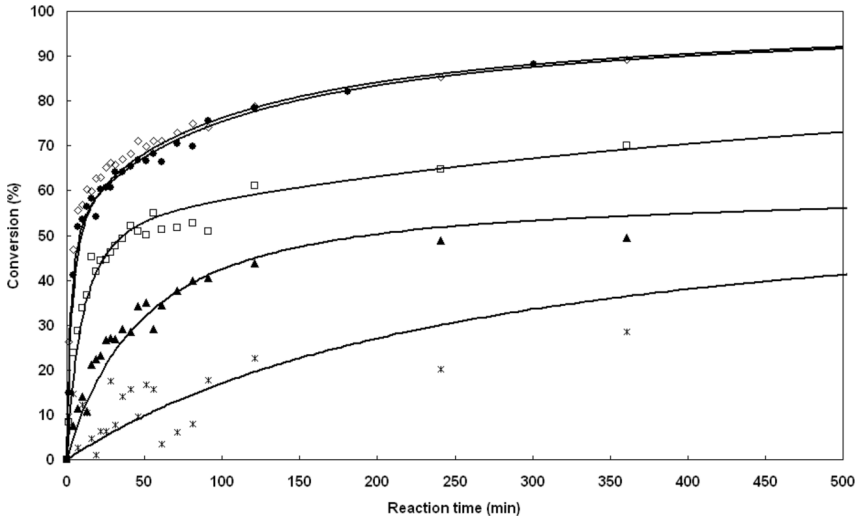

Figure 2. Conversion curves of the polyaddition reaction of BP with MP in different solvents: water (●), glycol (♫), methanol (□), formamide (π) and dimethylformamide (☂) **Q3** [the best fitting curves were obtained using Equation (3) and for dimethylformamide Equation (4)].

on integration, if the initial reagent concentrations, $[BP]_o$ and $[MP]_o$, are equal, Equation (2) is obtained:

$$\frac{1}{[BP]} = \frac{1}{[BP]_o} + kt \tag{2}$$

The results obtained from the experimental data using Equation (2) are reported in Figure 3(a)–(d). Unexpectedly, the 1/[BP] versus t curves obtained were not linear, but they all diverged at ~50% conversion. These facts suggested that the amine groups on MP may not be equivalent, due to the different steric hindrances by the neighbouring groups. To confirm this hypothesis, polymerization reactions were performed in water using DMP with two equivalent amine groups. A typical conversion curve was obtained (Figure 4). The results obtained from these experimental data using Equation (2) are reported in Figure 5. In this case, the relationship of 1/[BP] versus t curve was approximately linear with some deviation in the lower conversion region. This was ascribed to a small decrease in reactivity, affecting the second amino group of DMP after the first addition step had occurred. The pseudo-second-order kinetic constants, k_{DMP}, are reported in Table 2.

These findings indicate that the polyaddition reaction of MP with BP proceeds through two distinct reaction steps, each characterized by a different rate. The first relatively fast step corresponds to the addition of the least hindered amine, whereas the second to the addition of the most hindered amine.

In the case of protic solvents, the kinetic constants of the two reaction steps were obtained by determining the slopes of the very initial and the very final segments of the 1/[BP] versus t curves (Figure 3), with the assumption that in either regions the reaction of one amino group of MP prevails over the other. Specifically, the faster step, with kinetic constant k_1, occurs in the initial phase of the reaction, whereas the slower step, with kinetic constant k_2, occurs in the final reaction phase.

The values of the k_1 and k_2 kinetic constants obtained for the different protic solvents are reported in Table 2. These values were used to simulate the theoretical conversion curves by numerically integrating the differential Equation (3),

$$\frac{d[BP]}{dt} = -k_1[BP][MP_1] - k_2[BP][MP_2] \tag{3}$$

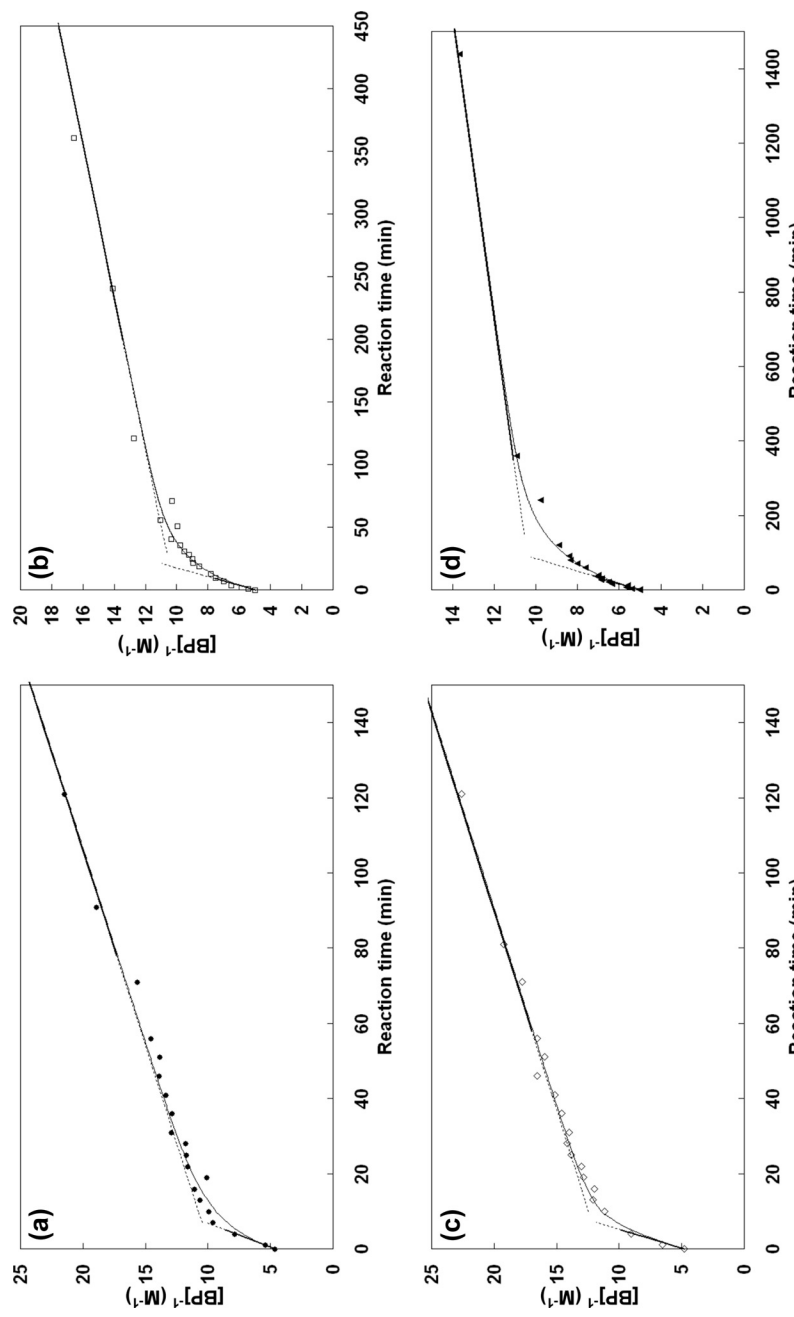

Figure 3. Calculated kinetic data using Equation (2). Panels (a)–(d): polyaddition reaction of MP to BP in (a) water, (b) methanol, (c) ethylene glycol and (d) formamide [the best fitting curves were obtained using Equation (3)].

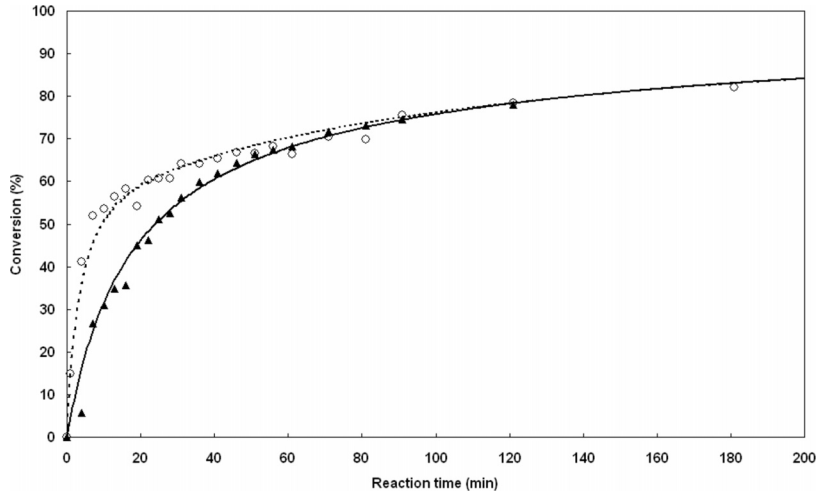

Figure 4. Conversion curves of the polyaddition reaction of BP with MP (O) and DMP (π) in water. **Q3**

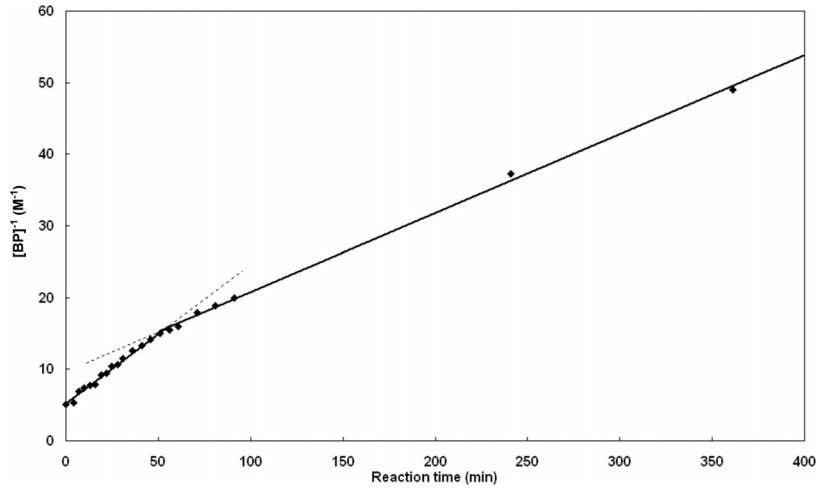

Figure 5. Calculated kinetic data using Equation (2) for the polyaddition reaction of BP with DMP in water [the best fitting curve was obtained using Equation (3)].

where $[MP_1]$ is the concentration of the least hindered amino group and $[MP_2]$ the concentration of the most hindered amino group. The results, reported in Figure 3, fit the experimental data. Moreover, a comparison of the k_2-value relative to the MP reaction in water with

Table 2. Kinetic constants for the polyaddition reaction with DMP.*

Solvent	k_1 (1/min M)	k_2 (1/min M)
Water	0.804	0.0961
Methanol	0.143	0.0158
Etylene glycol	1.013	0.0946
Formamide	0.042	0.0030
Water – DMP	/	0.0972

*In 0.1 M Hydrochloric acid with 0.05% of different organic solvents at 250 nm.

the k_{DMP}, value (Table 2) in the same solvent shows that they are very close to each other, thus confirming that steric hindrance influences the second MP reaction step.

A different case was represented by MP reaction in dimethylformamide, where the best fitting curve was obtained by assuming a third-order kinetics (Equation 4), which accounts for the autocatalytic effect of the aminic functions in aprotic solvents. Because the reaction rate in dimethylformamide under the conditions adopted is very slow, it was not possible to reach more than 50% conversion and, consequently, to determine the kinetics of the second step. The kinetic constant determined was 0.0142 min/M^2.

$$\frac{\mathrm{d}[\mathrm{BP}]}{\mathrm{d}t} = -k[\mathrm{BP}][\mathrm{MP}]^2 \tag{4}$$

A comparison of the kinetic constants obtained in the different solvent systems allowed us to confirm that the proton concentration and solvent polarity are the main factors affecting the reactivity of the system. The pK_a and dipole moment, μ, values for all solvents employed are reported in Table 3. It was observed that, in general, the reactivity increased with increasing proton concentration and decreasing solvent polarity. In the case of formamide, a dipolar solvent with an autoprotolysis constant (pK_a = 16.80), which is similar to that for methanol (16.71), the reaction rate is remarkably low. It appears that in the case of formamide, which has a very high dipole moment, the establishing of dipole–dipole interactions between solvents and reactants largely overshadowed the positive effect of proton availability on the reaction rate. In particular, the polarizable acrylic moiety of BP, stabilized by the dipolar solvent, showed a decrease in addition reactivity. The same stabilizing effect may be responsible for the very low reaction rate

Table 3. Solvent pKa and the dipole moment, μ, values used in the BP/MP polymerization†.

Solvent	pK_a	μ (D)
Water	14.00	1.85
Ethylene glycol	15.84	2.2‡
Methanol	16.71	2.87
Formamide	16.80	3.37
Dimethylformamide	>30	3.24

†From reference [24, 25].
‡From reference [26].

observed in dimethylformamide, a classical aprotic dipolar solvent, which also had a very low autoprotolysis constant ($pK_a > 30$).

CONCLUSIONS

The kinetic constants, hence the polymerization rates for typical Michael-type stepwise polyadditions leading to PAA have been studied in different solvents. It was found that the solvent's nature is the key factor governing the reactivity of the system, and general correlations were established. In particular, the reaction is of second order in solvents carrying mobile hydrogens and, in solvents of comparable polarity, the kinetic constants are roughly proportional to the autoprotolysis constants. Solvent polarity has a negative effect on the reaction rate, as demonstrated by the remarkable sluggishness of the reaction in formamide, a solvent with high polarity and high autoprotolysis constant. In polar solvents with low autoprotolysis constant, the reaction constant is extremely low.

Until now, the preferred reaction solvent for PAA preparation was water. It would appear that lower alcohols and glycols may be suitable alternatives as reaction media. From a practical standpoint, this may extend the scope of PAA synthesis to water-insoluble amines and bis-acrylamides.

ACKNOWLEDGEMENTS

The Authors gratefully acknowledge support from the Italian Ministry for Scientific and Technological Research, COFIN project 2004–06.

REFERENCES

1. Danusso, F. and Ferruti, P. (1970). Synthesis of tertiary amine polymers, *Polymer*, **11**(2): 88–113.

2. Ferruti, P., Marchisio, M.A., and Barbucci, R. (1985). Synthesis, physico-chemical properties and biomedical applications of poly(amido-amine)s, *Polymer*, **26**(9): 1336–1348.
3. Ferruti, P. (1996). Ion-Chelating Polymers for Medical Applications. In: *Polymeric Materials Encyclopedia*, volume 5, Salamone, J.C. (ed.), pp. 3334–3359, CRC Press Inc., Boca Raton, Florida.
4. Ferruti, P., Marchisio, M.A., and Duncan, R. (2002). Poly(amido-amine)s: biomedical applications, *Macromol. Rapid Commun.*, **23**(5/6): 332–355.
5. Barbucci, R., Barone, V., Ferruti, P., and Oliva, L. (1981). Thermodynamics of protonation of polymeric bases whose repeating units behave independently, *J. Polym. Sci., Polymer Symp.*, **69**: 49–66.
6. Barbucci, R., Casolaro, M., Ferruti, P., and Barone, V. (1982). Macroinorganics. 8. Chelation of copper(II) ion with some new poly (amido-amines), *Polymer*, **23**(1): 148–151.
7. Ferruti, P., Bertoglio Riolo, C., Soldi, T., and Pesavento, M. (1982). Applied macroinorganics. II. Protonation and heavy metal ions complex-formation behavior of three crosslinked resins of poly(amido-amine) structure, *J. Appl. Polymer Sci.*, **27**(6): 2239–2248.
8. Pesavento, M., Soldi, T., Ferruti, P., Barbucci, R., and Benvenuti, M. (1983). Applied macroinorganics. IV. Effect of the crosslinking agent on resins with poly(amido-amine) structure, *J. Appl. Polymer Sci.*, **28**(11): 3361–3368.
9. Marchisio, M.A., Ferruti, P., Longo, T., and Danusso, F. (1975). Method to Form Stable Complexes of Polyanions Occurring in Biological Liquids, US Patent 3.865.723.
10. Marchisio, M.A., Ferruti, P., Bertoli, S., Barbiano di Belgiojoso, G., Samour, C.M., and Wolter, K.D. (1988) A Novel Approach to the Problems of Heparin in Haemodialysis: The Use of a De-Heparinizing Filter. In: *Polymers in Medicine II*, Migliaresi, C., and Chiellini, E. (eds.), pp. 111–118, Elsevier Science Publishers B.V., Amsterdam.
11. Schacht, E., Ferruti, P., and Duncan, R. (1994). Drug Delivery Agents Incorporating Mitomycin, PCT Internat. Pat. Appln. No. PCT/IB94/00259 to the Commission of the European Communities.
12. Ferruti, P., Ranucci, E., Trotta, F., Gianasi, E., Evagorou, E.G., Wasil, M., Wilson, G., and Duncan, R. (1999). Synthesis, characterization, and anti-tumor activity of platinum(II) complexes of novel functionalised poly(amido amine)s, *Macromol. Chem. Phys.*, **200**(7): 1644–1654.
13. Richardson, S., Ferruti, P., and Duncan, R. (1999). Poly(amidoamine)s as potential endosomolytic polymers: evaluation in vitro and body distribution in normal and tumor-bearing animals, *J. Drug Targeting*, **6**(6): 391–404.
14. Pattrick, N.G., Richardson, S.C.W., Casolaro, M., Ferruti, P., and Duncan, R. (2001). Poly(amidoamine)-mediated intracytoplasmic delivery of ricin a-chain and gelonin, *J. Controlled Release*, **77**(3): 225–232.

15. Richardson, S.C.W., Pattrick, N.G., Man, Y.K.S., Ferruti, P., and Duncan, R. (2001). Poly(amidoamine)s as potential nonviral vectors: ability to form interpolyelectrolyte complexes and to mediate transfection in vitro, *Biomacromolecules*, **2**(3): 1023–1028.
16. Ferruti, P., Manzoni, S., Richardson, S.C.W., Duncan, R., Pattrick, N.G., Mendichi, R., and Casolaro, M. (2000). Amphoteric linear poly(amidoamine)s as endosomolytic polymers: correlation between physicochemical and biological properties, *Macromolecules*, **33**(21): 7793–7800.
17. Ferruti, P, Bianchi, S., Ranucci, E., Chiellini, F., and Caruso, V. (2005). Novel poly(amido-amine)-based hydrogels as scaffolds for tissue engineering, *Macromol. Biosci.*, **5**(7): 613–622.
18. Ferruti, P., Bianchi, S., Ranucci, E., Chiellini, F., and Piras, A.M. (2005). Novel Agmatine-containing poly(Amidoamine) hydrogels as scaffolds for tissue engineering, *Biomacromolecules*, **6**(4): 2229–2235.
19. Malgesini, B., Verpilio, I., Duncan, R., and Ferruti, P. (2003). Poly(amidoamines) carrying primary amino groups as side substituents, *Macromol. Biosci.*, **3**(1): 59–66.
20. Ferruti, P. (1985). Poly(amido-amines). Poly[1,4-piperazinediyl(4,7-dimethyl-1,10-dioxo-4,7-diazadecamethylene)], *Macromol. Syntheses*, **9**: 25–29.
21. Ranucci, E. and Ferruti, P. (1991). New Basic multifunctional polymers: 5. Poly(ester thioether amines) by polyaddition of 2,2′-alkylenediimino diethanethiols to bisacrylic and bismethacrylic esters, *Polymer*, 32(15): 2876–2879.
22. Ferruti, P., Knobloch, S., Ranucci, E., Duncan, R., and Gianasi, E. (1998). A novel modification of poly(L-lysine) leading to a soluble cationic polymer with reduced toxicity and with potential as a transfection agent, *Macromol. Chem. Phys.*, **199**(11): 2565–2575.
23. Emilitri, E., Ranucci, E., and Ferruti, P. (2005). New poly(amidoamine)s containing disulfide linkages in their main chain, *J. Polym. Sci., Part A: Polym. Chem.*, **43**(7): 1404–1416.
24. Kosuke, I. (2002). Properties of Solvents and Solvent Classifications. In: *Electrochemistry in Nonaqueous Solutions*, pp. 5–8, Wiley-VCH, Verleg GmbH, Weinheim.
25. Kosuke, I. (2002). Potentiometry in Non-Aqueous Solutions. In: *Electrochemistry in Nonaqueous Solutions*, pp. 182, Wiley-VCH, Verleg GmbH, Weinheim.
26. Li, Y.Q., Zhang, H.Z., Davidovits, P., Jayne, J.T., Kolb, C.E., and Worsnop, D.R. (2002). Uptake of HCl(g) and HBr(g) on ethylene glycol surfaces as a function of relative humidity and temperature, *J. Phys. Chem. A*, **106**: 1220–1227.

Q2

AUTHOR QUERIES **JBC076453**

Q1 Please provide e-mail address, telephone no. and fax no. for the corresponding author "Elisabetta Ranucci".

Q2 Since the style for "ibid" is not provided, the reference 24b has been set as a separate ref. 25. Please check.

Q3 The symbols given in the figure is different from the corresponding symbols explained in their captions for Figures 2 and 4. Please verify and provide the correct the symbols.

Poly(amidoamine)s with 2-Dithiopyridine Side Substituents as Intermediates to Peptide–Polymer Conjugates

Elisabetta Ranucci,* Paolo Ferruti, Marco Alessandro Suardi, Amedea Manfredi

Cystamine, when employed as a cross-linking agent, leads to poly(amidoamine) networks, which on reaction with 2,2′-dithiodipyridine turn into linear poly(amidoamine)s with side dithiopyridyl groups that easily undergo exchange reactions with reduced L-glutathione, a model thiol-containing biologically active peptide. The resultant products represent the first examples of soluble poly(amidoamine)–peptide conjugates in which the peptide moieties are linked to the polymer chain by S–S bonds stable in blood, but cleavable inside cells.

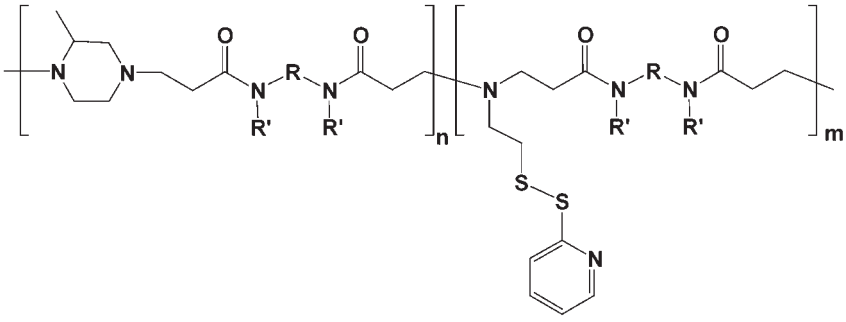

Introduction

Biocompatible polymers that bear disulfide linkages in their structure can be regarded as stimuli-sensitive systems stable in the blood but apt to intracellular release of active substances triggered by disulfide reduction.[1,2] In particular, significant interest has been focused on disulfide cross-linked non-viral gene delivery systems designed to mediate the intracellular release of DNA.[3–8]

Poly(amidoamine)s (PAAs) are a family of synthetic functional polymers developed for use as polymer therapeutics.[9] Linear PAAs are commonly prepared by the polyaddition of primary mono-amines or bis-*sec*-amines to bis-acrylamides. Primary bis-amines usually lead to cross-linked PAAs.[9–12] PAAs are normally degradable in aqueous media[13] and many of them are only moderately toxic in spite of their polycationic nature.[12,14] Amphoteric PAAs that carry pendant carboxy groups are approximately as biocompatible as dextran, and when injected in animals they are endowed with 'stealth-like' properties and passively concentrate in solid tumors by the EPR (enhanced permeation and retention) effect.[14] These PAAs are pH-dependent membrane responsive and have been examined as anticancer drug carriers and endosomolytic vectors for gene and toxin delivery.[12–16] Recently, 'smart' PAAs that bear disulfide linkages regularly arranged along the backbone, and are therefore amenable to both hydrolytic and reductive degradation, have been reported.[17–19]

Based on this premise, we describe here a synthetic route to novel linear PAAs that bear pendant 2-ethenyldithiopyridine moieties (PAA-SSPy), which involves the disulfide–disulfide exchange reaction of cystamine cross-linked PAAs with 2,2′-dithiodipyridine. These polymers are intermediates for the synthesis of new bioactive macromolecular conjugates amenable to exchange reaction with thiol-containing active molecules. 2-Ethenyldithiopyridine-

E. Ranucci, P. Ferruti, M. A. Suardi, A. Manfredi
Dipartimento di Chimica Organica e Industriale and Centro Interdipartimentale Materiali ed Interfacce Nanostrutturati (CIMAINA), Università degli Studi di Milano, via Venezian 21, 20133 Milano, Italy
Fax: +39-02-50314129; E-mail: elisabetta.ranucci@unimi.it

DOI: 10.1002/marc.200700139

derived disulfides are, in fact, extremely active towards these reactions, the driving force of which is the production of 2-mercaptopyridine which, upon predominantly forming the tautomeric 2-thiopyridone, is an excellent leaving group.[20]

Experimental Part

Instruments and Methods

^{1}H and ^{13}C NMR spectra were run on a Bruker Advance 400 spectrometer operating at 400.132 (^{1}H) and 100.623 (^{13}C) MHz.

Size exclusion chromatography (SEC) traces of water-soluble polymers (pullulan standards) were obtained with Toso-Haas 486 columns using 0.1 M Tris buffer pH 8.00 ± 0.05 as a mobile phase, with a UV detector operating at 230 nm. SEC traces of polymers insoluble in the above buffer (polystyrene standards) were obtained with Phenomenex Phenogel 500, 103, and 104 A columns, with a UV detector operating at 254 nm, and a 9/1 (v/v) dichloromethane/methanol mobile phase.

Swelling Tests

The tests were carried out on sheets with dimensions 10 × 20 × 1 mm^3. The average weight, in the dry state, was 21.2 ± 0.6 mg. Each specimen of initial mass M_0 was placed inside a 10 mL test-tube that contained 5 mL of solvent at 37 °C. After 12 h the specimen was taken out of the test-tube and weighed after wiping off any visible surface moisture. The percentage water absorbed was calculated using Equation (1):

$$\text{abs}\% = \frac{M_t}{M_0} \times 100 \quad (1)$$

where M_t is the water mass absorbed at time t and M_0 is the mass of the sample at time zero.

UV spectra were run on a Perkin–Elmer Lambda EZ210 spectrometer. 2-Mercaptopyridine was determined at 343 nm in 0.1 M TRIS buffer pH 8.5 (ε = 8 070 mol^{-1} · cm^{-1}). Specific optical rotations were measured with a Jasco P-1030 polarimeter.

Materials

Where not otherwise specified all materials and analytical grade HPLC solvents were purchased from Fluka and used as received, apart from 2-methylpiperazine (MeP), which was re-crystallized from heptane. D_2O (99.9%), CD_3OD (99.8%), and 2,2′-dithiodipyridine were purchased from Aldrich. 2,2-Bis(acrylamido)acetic acid (BAC)[21] and bis(acryloyl)piperazine (BP)[22] were synthesized as previously described.

Synthesis

HG-BP30: BP (1.960 g, 10.0 mmol), cystamine di-hydrochloride (0.338 g, 1.5 mmol), and lithium hydroxide monohydrate (0.126 g, 3.0 mmol) were dissolved in water (3.5 mL) under nitrogen and MeP (0.701 g, 7.0 mmol) was added under stirring. The homogeneous solution settled into a hydrogel. After 120 h the hydrogel was finely ground, extensively extracted with water and acetone, and dried at 37 °C and 0.1 Torr. Yield = 2.46 g (84%.)

HG-BP20, HG-BP10, HG-BAC30, HG-BAC20 and HG-BAC10 were prepared following the same procedure as described for HG-BP30 (see Table 1 for the kind and the amount of reagents). The HG-BAC series was treated with ethanol in place of acetone before drying.

BP30-SSPy: HG-BP30 (5.00 g, 1.13 mmol disulfide) was soaked in ethanol (30 mL) and 2,2′-dipyridyldisulfide (0.750 g, 3.4 mmol) and a catalytic amount of 2-mercaptopyridine were added. The gel dissolved in a few hours. The resultant solution was stirred for a further 24 h at room temperature, and then diluted to 100 mL with water. Excess 2,2′-dipyridyldisulfide precipitated out. The mixture was then filtered through a HPLC filter (0.45 μm), and then ultrafiltered through a membrane with a nominal molecular weight cut-off of 3 000 after adjusting the pH to 2.5 (HCl). The product was recovered by freeze drying. Yield = 4.28 g (81%).

BP20-SSPy and BP10-SSPy were prepared as for BP30-SSPy, using a three-fold molar excess of 2,2′-dipyridyldisulfide over disulfide units.

BAC10-SSPy, BAC20-SSPy and BAC30-SSPy were prepared by following the same procedure, using a 2 : 1 (v/v) water/ethanol mixture as reaction medium.

NMR of BP–SSPy series (as hydrochlorides): ^{1}H NMR (CD_3OD): δ = 1.38 (d, CH_3), 2.88–3.65 (m, br, CO–CH_2, N–CH, N–CH_2, S–CH_2), 7.35 (m, pyridine, N–C–CH), 7.84–7.87 (m, pyridine, N–C–*CH*–*CH*), 8.43 (m, pyridine, N–CH–C). ^{13}C NMR (CD_3OD): δ = 14.18 (CH_3), 26.94–28.34 (*C*–CO), 41.46–56.48 (*C*–N, *C*–S), 122.14 (pyridine, N–C–*C*H), 122.82 (m, pyridine, N–CH–*C*), 139.24 (pyridine, N–C–C–*C*), 149.76 (pyridine, N–C), 156.86 (pyridine, N–C), 170.59–171.11 (C=O).

NMR of BAC-SSPy series (as hydrochlorides): ^{1}H NMR (CD_3OD): δ = 1.38 (CH_3), 2.70–2.74 (m, br, CO–CH_2), 2.85–3.62 (m, br, N–CH, N–CH_2, S–CH_2), 5.56 (m, br, CH–COO), 7.35 (m, pyridine, N–C–CH), 7.79–7.87 (m, pyridine, N–C–*CH*–*CH*), 8.44 (m, pyridine, N–CH–C). ^{13}C NMR (CD_3OD): δ = 13.93 (CH_3), 28.74–31.60 (*C*–CO), 48.37–58.21 (C–N, C–S), 122.14 (pyridine, N–C–*C*H), 122.78 (m, pyridine, N–C–*C*H), 139.27 (pyridine, N–C–C–*C*H), 149.62 (pyridine, N–CH), 156.86 (pyridine, N–C), 171.36–172.91 (C=O).

BP30-SSG: BP30-SSPy hydrochloride (0.3 g, 0.149 mmol SSPy units) was dissolved under nitrogen in 20 mL of 0.1 mol TRIS buffer pH 8.50 (20 mL) and reduced L-glutathione (0.0458 g, 0.149 mmol) was added. The solution immediately turned intensely yellow. The reaction went to completion in a matter of minutes, as ascertained by UV determination of the amount of 2-mercaptopyridine evolved. The solution was then diluted with water (300 mL), ultrafiltered through a membrane with a nominal molecular weight cut-off of 3 000, and freeze-dried. Yield = 0.266 g (82.8%.)

$[\alpha]_D^{25} = -7.4$ deg · dm^{-1} · g^{-1} · cm^3 (c = 1 in H_2O). For comparison purposes, reduced L-glutathione had $[\alpha]_D^{25} = -17.2$ deg · dm^{-1} · g · $^{-1}$ · cm^3 (c = 2 in H_2O).

^{1}H NMR (D_2O): δ = 1.29 (d, CH_3), 2.15 (glutamic acid residue, H_2N–C–*CH*$_2$), 2.51 (glutamic acid residue, H_2N–C–C–*CH*$_2$), 2.55–2.70 (m, br, CO–CH_2), 2.70–3.65 (m, br, N–CH, N–CH_2, S–CH_2), 3.77 (glycine residue, HO–CO–*CH*$_2$–NH), 5.50 (m, br, CHCOO). ^{13}C NMR (D_2O): δ = 14.18 (CH_3), 26.28 (glutamic acid residue, H_2N–CH–*CH*$_2$),

Macromolecular Journals
DOI: 10.1002/marc.200700139

Table 1. Preparation of cystamine cross-linked PAA networks.

Code[a]	BP	BAC	Cystamine · 2HCl	$LiOH \cdot H_2O$	MeP	Yield	Swelling degree	Elemental analysis			
	mmol	mmol	mmol	mmol	mmol	%	%	%			
								C	H	N	S
								found (calcd)	found (calcd)	found (calcd)	found (calcd)
HG-BP30[b]	10.0	–	1.5	3.0	7.0	84	170[d]	58.53 (59.97)	8.78 (8.49)	17.15 (18.05)	3.43 (3.34)
							80[e]				
							140[f]				
HG-BP20[b]	10.0	–	1.0	2.0	8.0	82	270[d]	59.93 (59.73)	8.82 (8.63)	17.32 (18.38)	2.42 (2.21)
							130[e]				
							290[f]				
HG-BP10[b]	10.0	–	0.5	1.0	9.0	87	320[d]	59.57 (60.47)	8.93 (8.78)	17.86 (18.71)	1.29 (1.10)
							210[e]				
							560[f]				
HG-BAC30[c]	–	10.0	1.5	13.0	7.0	88	950[d]	48.72 (47.68)	7.33 (7.56)	15.98 (15.10)	3.23 (3.17)
HG-BAC20[c]	–	10.0	1.0	12.0	8.0	82	1 140[d]	48.65 (49.73)	7.39 (6.66)	16.96 (17.77)	2.39 (2.32)
HG-BAC10[c]	–	10.0	0.5	11.0	9.0	83	3 180[d]	49.59 (50.53)	7.18 (6.81)	17.36 (18.09)	1.24 (1.06)

[a] All samples were prepared in 3.5 mL water; [b] $(C_{15}H_{26}N_4O_2)_n(C_{12}H_{20}N_3O_2S)_m$: $n/m = 7:3$ (BP30), 8: 2 (BP20), and 9: 1 (BP10); [c] $(C_{13}H_{20}N_4O_4Li)_n(C_{10}H_{16}N_3O_4SLi)_m$: $n/m = 7:3$ (BAC30), 8: 2 (BAC20), and 9: 1 (BAC10); [d] In water; [e] In ethanol; [f] In dichloromethane.

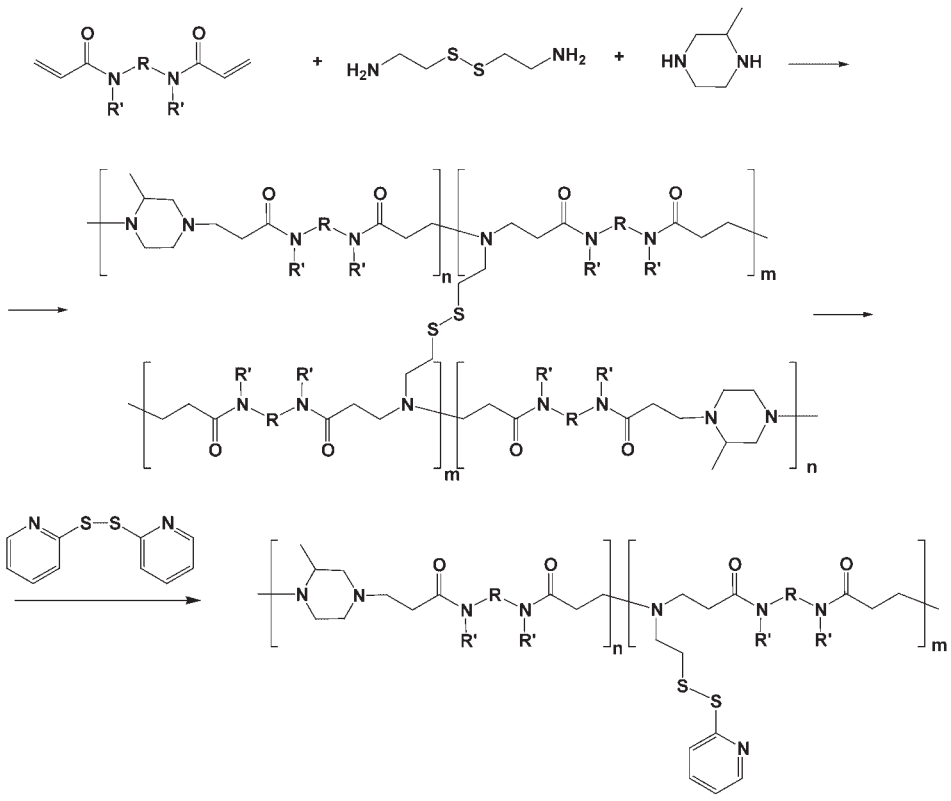

Scheme 1. Polyaddition reaction leading to cystamine-cross-linked PAAs and subsequent disulfide–disulfide exchange reaction. In the BP series: R = CH_2–CH_2 and R′ = CH_2. In the BAC series: R = CH–COOH and R′ = H.

26.94–28.34 (*C*–CO), 31.59 (glutamic acid residues, H_2N–C–C–*C*H_2), 43.33 (glycine residue, HO–CO–*C*–NH), 41.46–56.48 (C–N, C–S), 170.59–171.11 (C=O).

BAC30-SSG was prepared by a similar procedure. Yield = 78.2%. $[\alpha]_D^{25} = -5.4$ deg · dm^{-1} · g^{-1} · cm^3 · (*c* = 1 in H_2O).

^{1}H NMR (D_2O): δ = 1.38 (d, CH*C*H_3), 2.09 (glutamic acid residue, H_2N–C–*C*H_2), 2.51 (glutamic acid residue, H_2N–C–C–*C*H_2), 2.88–3.65 (m, br, CO–CH_2, N–CH, N–CH_2, S–CH_2), 3.77 (glycine residue, HO–CO–*C*H_2–NH). ^{13}C NMR (D_2O): δ = 14.18 (CH_3), 26.28 (glutamic acid residue, H_2N–C–*C*H_2), 28.30–28.93, 30.8 (*C*–CO), 31.59 (glutamic acid residues, H_2N–C–C–*C*H_2), 43.33 (glycine residue, HO–CO–*C*H_2–NH), 48.1–55.9 (C–N, C–S), 58.25 (*C*COO), 170.93–173.02 (C=O).

Results and Discussion

The aim of this work was to obtain a new family of PAAs with pendant 2-ethenyldithiopyridine moieties, to be used for the preparation of smart soluble polymer conjugates sensitive to reductive cleavage. The synthetic approach involved two steps: the preparation of cross-linked PAA networks using cystamine as a tetrafunctional cross-linking agent, and their conversion into linear soluble PAAs that bear activated disulfide pendants by disulfide–disulfide exchange reaction with 2,2′-dithiodipyridine (Scheme 1). Disulfide–disulfide exchange reactions have been previously reported and their mechanism described.[23]

Six different cross-linked PAA samples were obtained by reacting BP (HG-BP10, HG-BP20, and HG-BP30) or BAC (HG-BAC10, HG-BAC20, and HG-BAC30) with MeP as co-monomer and three different amounts of cystamine as cross-linker (Table 1). More precisely, in HG-BP10 and HG-BAC10 the amount of the amine hydrogens of cystamine over the total number of amine hydrogens was 10%, whereas in HG-BP20 and HG-BAC20 this amount was 20%, and in HG-BP30 and HG-BAC30 30%. The molar ratios of the reagents used in each preparation are reported in Table 1. It may be observed that the composition of the cystamine cross-linked PAA networks are in good agreement with the feed ratios.

The exchange reactions were performed on finely ground PAA gels swollen in ethanol (HG-BP series) or in a 2:1 (v/v) water/ethanol mixture (HG-BAC series) under slightly alkaline conditions (pH of the swelling liquors after dilution with water ≈8.5). The exchange reaction is triggered by catalytic amounts of 2-mercaptopyridine (see Scheme 2). A 3:1 excess of 2,2′-dipirydyldisulfide with respect to cystamine moieties was employed to force the reaction to completion. The reaction mixture turned into a clear homogeneous solution in a few hours, the dissolution

Macromolecular Journals
DOI: 10.1002/marc.200700139

Table 2. Characterization of the products.

Code[a]	$\overline{M}_n$	$\overline{M}_w$	n/m[b]	Yield	C/S ratio	Elemental analysis				
	10^{-3} g · mol^{-1}	10^{-3} g · mol^{-1}		%	found (calcd)	%				
						C	H	N	S	Cl
						found (calcd)	found (calcd)	found (calcd)	found (calcd)	found (calcd)
BP30-SSPy	9.5	32	3.5	81	12.1 (12.9)	48.6 (50.9)	7.96 (7.45)	14.6 (15.4)	4.02 (3.94)	13.9 (13.5)
BP20-SSPy	47	190	6.7	83	13.7 (13.6)	47.1 (51.2)	7.96 (7.65)	14.1 (15.6)	3.10 (2.33)	14.9 (14.2)
BP10-SSPy	40	130	11.9	84	13.7 (13.8)	49.8 (51.4)	8.49 (7.77)	15.1 (15.8)	1.68 (1.40)	15.1 (14.6)
BAC30-SSPy	20	36	4.5	80	13.7 (13.8)	44.7 (45.9)	7.32 (6.24)	15.6 (16.0)	3.26 (3.33)	9.51 (10.1)
BAC20-SSPy	44	93	5.6	84	15.2 (16.4)	41.7 (46.1)	6.71 (6.30)	14.6 (16.1)	2.74 (2.81)	11.3 (10.2)
BAC10-SSPy	26	52	12.3	82	28.9 (32.7)	45.4 (46.4)	7.29 (6.47)	15.8 (16.5)	1.57 (1.41)	10.8 (10.4)
BP30-SSG	8.5	31	3.5	85	13.78 (13.98)	50.01 (50.64)	7.64 (7.22)	15.39 (15.86)	3.63 (3.62)	9.29 (9.04)
BAC30-SSG	17	34	4.5	81	14.22 (14.73)	44.10 (44.78)	7.01 (6.39)	15.52 (15.97)	3.10 (3.04)	9.38 (9.28)

[a] BP-SSPy: $(C_{15}H_{26}N_4O_2 \cdot 1.5HCl)_n(C_{17}H_{24}N_4O_2S_2 \cdot HCl)_m$, BAC-SSPy: $(C_{13}H_{22}N_4O_4 \cdot HCl)_n(C_{15}H_{20}N_4O_4S_2 \cdot HCl)_m$, BP-SSG: $(C_{15}H_{26}N_4O_2 \cdot HCl)_n(C_{22}H_{32}N_6O_8S_2 \cdot HCl)_m$, BAC-SSG: $(C_{13}H_{22}N_4O_4 \cdot HCl)_n(C_{20}H_{30}N_6O_9S_2 \cdot HCl)_m$; [b] Compositional data from ^{1}H NMR spectra.

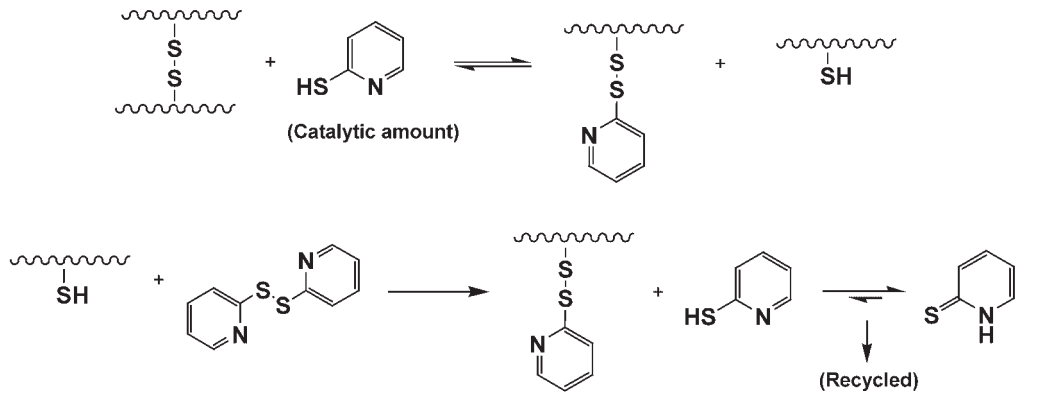

Scheme 2. Mechanism of the thiol-disulfide exchange reaction between PAA hydrogels and 2,2′-dithiodipyridine.

time largely dependant on the particle size of the gels. The mixtures were then allowed to react for a further 24 h, filtered through an HPLC filter, and ultrafiltered. The resultant products (Table 2) were finally recovered by freeze drying the retained portion. The elemental analyses of the products reported in the same table are in good agreement with the expected composition from NMR data.

Similar results were obtained by substituting 5,5′-dithiobis(2-nitrobenzoic acid) (Ellman's reagent) for 2,2′-dipyridyldisulfide (data not reported). The chemical reactivity of the resultant products was approximately the same.

An alternative synthetic route was also tried based on the polyaddition of commercial 2-(2-pyridyl)dithioethylamine, by its primary amine group, to bis-acrylamides. However, most of the pendant disulfide groups decomposed under the conditions of PAA synthesis.

The molecular weights of the linear PAAs obtained, BP10-SSPy, BP20-SSPy, BP30-SSPy BAC10-SSPy BAC20-SSPy and BAC30-SSPy, were of the same order as those of most PAAs described so far.[10–12] Moreover, their NMR spectra revealed that no terminal double bonds were present. These results prove that all the four amine hydrogens of cystamine participate in the polyaddition reaction notwithstanding the chemical constrains of a cross-linked network, in agreement with a previous HR-MAS NMR study on ethylenediamine-crosslinked PAA networks.[24]

Polymers of the BP series, as hydrochlorides, were soluble in water, methanol, dimethyl sulfoxide (DMSO), and *N*,*N*-dimethylformamide (DMF), but insoluble in chloroform, acetone, toluene, ether and ethyl acetate. As

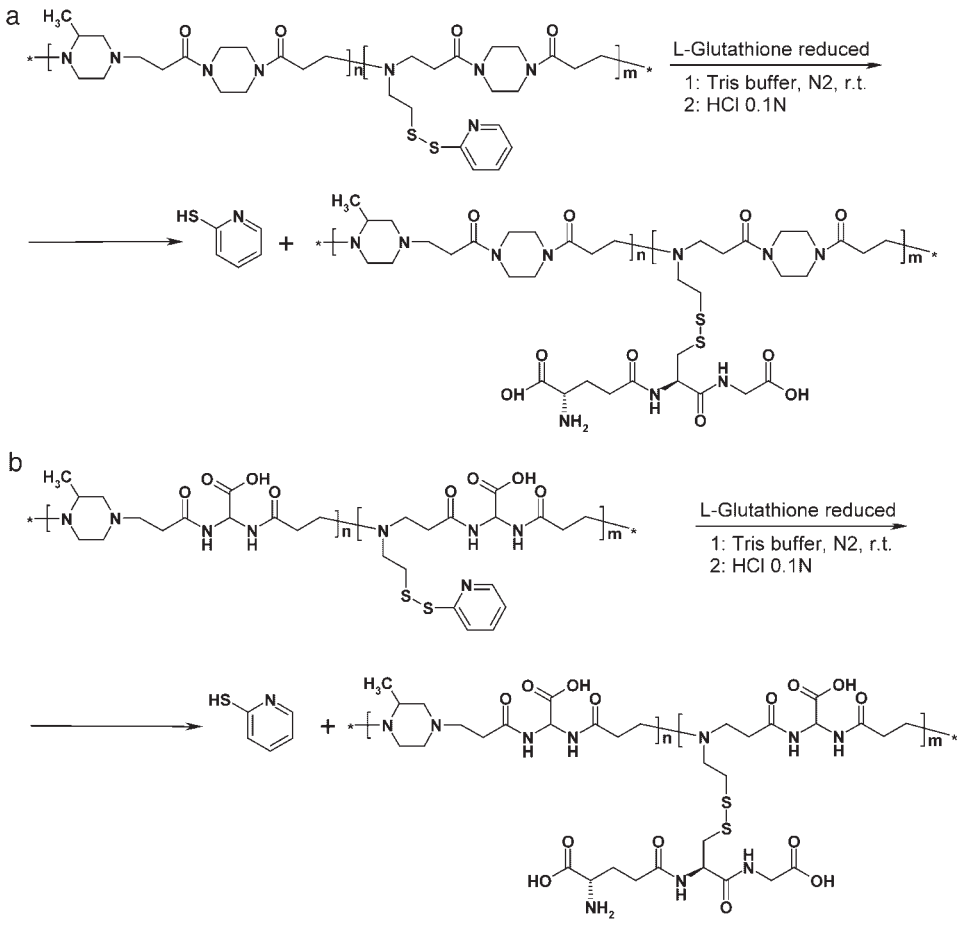

Scheme 3. Exchange reaction of reduced L-glutathione with BP-SSPy (a) and BAC-SSPy (b).

Macromol. Rapid Commun. **2007**, *28*, 1243–1250

DOI: 10.1002/marc.200700139

free bases they were soluble in DMSO, DMF, chloroform, and methanol, but insoluble in water, acetone, toluene, ether, and ethyl acetate. Polymers of the BAC series, both as hydrochlorides and free bases, were soluble in water and methanol, but insoluble in DMSO, DMF, chloroform, acetone, toluene, ether, and ethyl acetate. Moreover, the solubility properties of both BP-SSPy and BAC-SSPy polymer series were somewhat different from those of the corresponding PAAs derived from 2-methylpiperazine and BP (MeP-BP) or BAC (ISA23), which have similar main backbones, but are devoid of dithiopyridine side substituents. In particular, the PAAs of the BP-SSPy series, as free bases, were insoluble in water, whereas MeP-BP was,[9,10] and those of the BAC-SSPy series, both as hydrochlorides and free bases, were soluble in methanol, whereas ISA 23 was not.[9,25]

All dithiopyridyl-containing linear PAAs were fully characterized by ^{1}H and ^{13}C NMR spectroscopy. The n/m ratio between the MeP units and the 2-(2-aminoethyl)-dithiopyridyl units was calculated from the integral ratio of the signals at 1.38 and 7.35, assigned to the methyl group of MeP and to the H-5 of the pyridyl residue, respectively (Table 2).

The ability of PAA-SSPy of both series to undergo fast exchange reactions with thiols, according to a general and well-established mechanism,[26] was ascertained for BP30-SSPy and BAC30-SSPy with reduced L-glutathione as a model thiol-containing peptide (Scheme 3). After purification, the NMR spectra of the resultant products (BP30-SSG and BAC30-SSG) showed L-glutathione diagnostic peaks at 2.09, 2.51, and 3.77, whereas the diagnostic peaks of pyridine at 7.35, 7.85, and 8.43 ppm were absent. As expected, both BP30-SSG and its BAC-deriving counterpart BAC30-SSG showed optical rotation power. The measured $[\alpha]_D^{25}$ values ($c = 1$ in H_2O) were -7.4 ($deg \cdot dm^{-1} \cdot g^{-1} \cdot cm^{3)}$ and -5.4 ($deg \cdot dm^{-1} \cdot g^{-1} \cdot cm^3$), respectively, to be compared with the $[\alpha]_D^{25}$ of reduced glutathione (-17.2 $deg \cdot dm^{-1} \cdot g^{-1} \cdot cm^3$, $c = 2$ in H_2O).

Conclusion

Cystamine was used as a cross-linking agent to obtain PAA networks with various amounts of S–S interchain linkages. These networks reacted with 2,2′-dipyridyl disulfide to yield linear PAAs that carry activated disulfide moieties as side substituents, which under remarkably mild conditions underwent exchange reactions with reduced L-glutathione, chosen here as a model thiol-containing peptide. Therefore, it may be reasonably concluded that the results reported in this preliminary Communication open a general and facile synthetic route to PAA conjugates of biologically active peptides and proteins that contain SH groups. The bond between the two components of these hybrid materials is expected to be stable in the bloodstream, but amenable to reductive cleavage inside cells.

As a minor remark, the molecular weights of the linear PAAs obtained in this work were in the range of those of most PAAs obtained by direct polyaddition of bis-amines to bis-acrylamides,[9–12] and no evidence of terminal double bonds is present in their NMR spectra. Therefore, all the amine hydrogens of cystamine participated in the polyaddition reaction.

Received: February 23, 2007; Revised: March 28, 2007; Accepted: April 4, 2007; DOI: 10.1002/marc.200700139

Keywords: biocompatibility; biodegradable; disulfide-containing polymers; functionalization of polymers; poly(amidoamine)s; polymer–peptide conjugates

[1] S. Arpicco, F. Dosio, P. Brusa, P. Crosasso, L. Cattel, *Bioconjugate Chem.* **1997**, *8*, 327.
[2] Y. Masuho, K. Kishida, M. Saito, N. Umemoto, T. Hara, *J. Biochem.* **1982**, *91*, 1583.
[3] K. Miyata, Y. Kakizawa, N. Nishiyama, Y. Yamasaki, T. Watanabe, M. Kohara, K. Kataoka, *J. Controlled Release* **2005**, *109*, 15.
[4] K. Y. Kwok, Y. Park, Y. Yang, D. L. McKenzie, Y. Liu, K. G. Rice, *J. Pharm. Sci.* **2003**, *92*, 1174.
[5] D. Oupicky, M. Ogris, L. W. Seymour, *J. Drug Targeting* **2002**, *10*, 93.
[6] M. L. Read, S. Singh, Z. Ahmed, M. Stevenson, S. S. Briggs, D. Oupicky, L. B. Barrett, R. Spice, M. Kendall, M. Berry, J. A. Preece, A. Logan, L. W. Seymour, *Nucleic Acids Res.* **2005**, *33*, 386.
[7] M. A. Gosselin, W. Guo, R. J. Lee, *Bioconjugate Chem.* **2001**, *12*, 989.
[8] M. A. Gosselin, W. Guo, R. J. Lee, *Bioconjugate Chem.* **2002**, *13*, 1044.
[9] P. Ferruti, M. A. Marchisio, R. Duncan, *Macromol. Rapid Commun.* **2002**, *23*, 332.
[10] F. Danusso, P. Ferruti, *Polymer* **1970**, *11*, 88.
[11] P. Ferruti, M. A. Marchisio, R. Barbucci, *Polymer* **1985**, *26*, 9, 1353.
[12] P. Ferruti, "Ion-Chelating Polymers (Medical Applications)", in: *Polymeric Materials Encyclopedia*, Vol. 5, J. C. Salamone, Ed., CRC Press INC, Boca Raton, Florida 1996, pp. 3334-3359.
[13] P. Ferruti, E. Ranucci, L. Sartore, F. Bignotti, M. A. Marchisio, P. Bianciardi, F. M. Veronese, *Biomaterials* **1994**, *15*, 1235.
[14] S. Richardson, P. Ferruti, R. Duncan, *J. Drug Targeting* **1999**, *6*, 3.
[15] N. G. Patrick, S. C. W. Richardson, M. Casolaro, P. Ferruti, R. Duncan, *J. Controlled Release* **2001**, *77*, 225.
[16] S. C. W. Richardson, N. G. Patrick, Y. K. S. Man, P. Ferruti, R. Duncan, *Biomacromolecules* **2001**, *2*, 1023.
[17] E. Emilitri, E. Ranucci, P. Ferruti, *J. Polym. Sci., Part A: Polym. Chem.* **2005**, *43*, 1404.
[18] C. Lin, Z. Zhong, M. C. Lok, X. Xulin Jiang, W. E. Hennink, J. Feijen, J. F. C. Engbersen, *J. Controlled Release* **2006**, *116*, 130.

[19] C. Lin, Z. Zhong, M. C. Lok, X. Xulin Jiang, W. E. Hennink, J. Feijen, J. F. C. Engbersen, *J. Bioconjugate Chem.* **2007**, *18*, 138.
[20] V. Bulmus, M. Woodward, L. Lin, N. Murthy, P. Stayton, A. Hoffman, *J. Controlled Release* **2003**, *93*, 105.
[21] P. Ferruti, E. Ranucci, F. Trotta, E. Gianasi, E. G. Evagorou, M. Wasil, G. Wilson, R. Duncan, *Macromol. Chem. Phys.* **1999**, *200*, 1644.
[22] P. Ferruti, *Macromol. Synth.* **1985**, *9*, 25.
[23] B. Danieli, A. Giardini, G. Lesma, D. Passarella, B. Peretto, A. Sacchetti, A. Silvani, G. Pratesi, F. Zunino, *J. Org. Chem.* **2006**, *71*, 2848.
[24] R. Annunziata, J. Franchini, E. Ranucci, P. Ferruti, *Magn. Reson. Chem.* **2007**, *45*, 51.
[25] P. Ferruti, S. Manzoni, S. C. W. Richardson, R. Duncan, N. G. Pattrick, R. Mendichi, M. Casolaro, *Macromolecules* **2000**, *33*, 7793.
[26] D. R. Grassetti, J. F. Murray, *Arc. Biochem. Biophys.* **1967**, *119*, 41.

DOI: 10.1002/marc.200700139

Novel Poly(amidoamine)-based Hydrogels as Scaffolds for Tissue Engineering

Elisa Emilitri[1,2], Fabiana Guizzardi[2], Cristina Lenardi[2], Marco Suardi[1], Elisabetta Ranucci[1,2], Paolo. Ferruti[1,2].*

[1] Dipartimento di Chimica Organica e Industriale, Università di Milano, via Venezian 21, 20133 Milano, Italy.
[2] CIMAINA, Centro Interdisciplinare Materiali e Interfacce NAnostrutturati, Università di Milano, via Celoria 16, 20133 Milano, Italy.
* Corresponding author e-mail: paolo.ferruti@unimi.it

Summary: Poly(amidoamine)s are biocompatible biodegradable polymers, which can be easily functionalized with a number of bioactive and biomimetic compounds. Co-polymerization of these polymers with 4-aminobutyl guanidine (agmatine) leads to an RGD mimicking structure. Hydrogels based on this structure showed an enhanced cell adhesion and could be chemically linked to a glass substrate to create a bioadhesive support for cell growth. Preliminary optimization and cell adhesion tests on Madin-Darby Canine Kidney cells were performed, both on functionalized and non-functionalized structures, with promising results.

Keywords: Hydrogels, Poly(amidoamine), biocompatible surfaces, agmatine, RGD mimic.

Introduction

The advancement of biological sciences and biomaterials has given a fundamental contribution to the development of techniques for dealing with proteins, cells and tissues both in vitro and in vivo. These technologies require reliable support materials with good biocompatibility and cell adhesion, and would greatly profit from new materials that are reliable, disposable and simple to use.[1, 2] Among synthetic materials, hydrogels present unrivalled tissue-like properties for interactions with living cells,[3] such as similar water content and permeability to oxygen and metabolites. In principle, synthetic hydrogels, as opposed to naturally derived materials (e.g. gelatin, chitosan etc.) should be most advantageous, giving the possibility of a complete control over hydrogel composition, surface properties and other key parameters such as water absorption and (bio)degradation time. Moreover, hydrogel structures could be used to encapsulate cells, proteins and signaling factors, as well as bioactive moieties to be slowly released during cell growth. Provided cell adhesion is effective, supported or free standing micro-and nano-structured

hydrogels could be advantageously exploited for tissue engineering, as matrixes for in vitro cell screening, and for microarray technology.[4]

Cell adhesion on synthetic hydrogels, however, is still an issue for many of these materials, such as poly(hydroxyethyl)metacrylate (PHEMA) or crosslinked poly(ethyleneoxide) (PEG) derivatives.[5,6] A number of chemical and physical modifications have been proposed to overcome this problem, often relying on modification of the synthetic surface with biological or biomimetic moieties, peptides or proteins.[7,8]

Cell adhesion is a complex process, mediated by specific interactions between surface ligands and cell receptors;[9] several studies have shown that the arginin-glycin-aspartic acid (RGD) tripeptide and some of its analogues can interact with adhesion regulating proteins of the integrin family, and promote cell adhesion and spreading.[10-12] Modifications of chemical structures in order to include an RGD or RGD-like groups have been proposed for a number of applications where interaction with cells was desired, to enhance adhesion or recognition by cellular receptors.[13-14]

Research in our group has been for several years focused on biomaterials based on poly(amidoamine)s (PAAs). PAAs are synthetic polymers endowed with many biologically interesting properties, being highly biocompatible, non toxic and biodegradable.[15,16] They are obtained by Michael-type addition of bis-acrylamides to primary amines and/or secondary diamines, under mild conditions. Several structures including biologic, biomimetic and bioactive compounds, can be incorporated in the PAA backbone by covalent attachment during the synthetic process.[17-19] Hydrogels based on PAAs besides having both the properties of hydrogels and PAAs, can be easily modified by the introduction of functional co-monomers.[20,21] These extremely versatile materials are especially interesting when carrying carboxylic groups as well as amino groups, since amphoteric PAAs have been demonstrated to have very low toxicity and “stealth” properties in vivo.[22]

In the last years, PAA polymers containing RGD mimic units have been prepared. They are obtained by the introduction of 4-aminobutylguanidine (agmatine), used as co-monomer, to build a functional amphoteric repeating unit that is structurally similar to RGD. The soluble polymers carrying these functionalities have extremely low toxicity even if they are polycationic at physiologic pH[23] and have shown potential as transfection agents.[24] Introducing this structure in a crosslinked amphoteric PAA hydrogel resulted in an enhancement of adhesion for fibroblasts.[25] In this work, a similar adhesion promoting

material was used to prepare a thin film supported on glass, as a model device for cell screening. Comparative tests of cell adhesion and growth of RGD-binding $\alpha_V\beta_3$ integrin expressing epithelial Madin-Darby canine kidney (MDCK) cells were performed to assess its efficiency, with promising results.[26]

Materials and Methods

Ethanol, hydrochloric acid (37%), nitric acid (65%), 3-aminopropyltrimethoxy silane, 1,2-diaminoethane (EDA), 4-aminobutylguanidine sulfate (agmatine sulfate), purity 97%, cystamine di-hidrochloride (Fluka, > 98%,), and GRGD peptide were purchased from Sigma-Aldrich and used as received. 2-Methylpiperazine was purchased from Fluka and used after sublimation. Its final purity (96,8 %) was determined with acidimetric titration. N,N'-Bis (acrylamido)acetic acid (BAC) was prepared as reported in the literature[27] and purity (97,5%) determined by NMR and titration. Phosphate buffer solution (PBS) 10 mM was prepared using Sigma Aldrich tablets according to manufacturer's instructions. All chemicals used in the biological tests were purchased from Sigma-Aldrich. TCPS (tissue culture plate surfaces), multiwells, and tissue culture flasks were purchased from Zellkultur und Labortechnologie, Switzerland; round glass coverslips as support for hydrogels (13 mm in diameter, 0.7 mm thickness) from Zeus super.
Spin coating was performed using a Laurell WS-400B-6NPP –Lite spin coater.
1H and 13CNMRspectra were obtained using a Brüker Avance400 spectrometer operating at 400.132 MHz (1H) and 100.623(13C), and using Brüker software.

Preparation procedure for AGMA1-75 hydrogel: in a 10 ml round bottomed flask BAC (1099 mg, 5.4 mmol) was added under nitrogen atmosphere and stirring to an aqueous lithium hydroxide solution (LiOH*H2O, 226.26 mg 5.4 mmol in 1.8 ml). After complete dissolution, agmatine sulfate (308.17 mg, 1.35 mmol) and more lithium hydroxide monohydrate (81.9 mg, 2.7 mmol) were added and dissolved. This mixture was allowed to react for 24 hr at room temperature (20 ± 5°C) in the dark, and then EDA (121.7 mg, 2.05 mmol) was added. The solution was stirred for 2 minutes, retrieved with a syringe and injected in a square mould made of two silanized 10x10 cm glass plates separated by a 0.3 mm silicone spacer. The hydrogel was allowed to crosslink at room temperature for 72 hr, and retrieved as a pliant solid film. The sample was purified by extracting with excess

ethanol and then with doubly distilled water. To avoid ruptures caused by osmotic shock, water was not added at once to the ethanol-swollen hydrogel; instead, the sample was exposed to water/ethanol mixtures with increasing water concentrations, until pure water was used. The extraction time was at least 30 min for each step.

ISA23-75 was prepared and purified using the same procedure, and the following reagents: BAC (1099 mg, 5.4 mmol), lithium hydroxide monohydrate (226.26 mg 5.4 mmol), 2-methylpiperazine (135.3 mg, 1.35 mmol), doubly distilled water (1.8 ml), and EDA (121.7 mg, 2.05 mmol). Structure was confirmed by IR spectroscopy in KBr.

Soluble AGMA1 was prepared as reported in literature,[23] its structure confirmed by NMR and GPC. Molecular weight of the sample used: $\overline{M}_n$ = 5500 and $\overline{M}_w$ = 6500, polydispersity =1.25; its NMR was consistent with those reported in the literature.

Glass amino silane functionalization: Round glass coverslips, 13 mm in diameter, were treated as previously reported.[28] They were soaked in aqua regia at room temperature for 5 hr (20 coverslips were laid out in a glass dish 100 mm in diameter and covered with 12 ml of the acid mixture), washed several times in doubly distilled water and then in ethanol before being soaked in a 10% v/v ethanol solution of 3-aminopropyltrimethoxy silane (15 ml) overnight. The samples were recovered and washed in ethanol (2 x 20 ml), doubly distilled water (3 x 20 ml), and then sonicated in doubly distilled water. They were finally dried with soft paper and used within 24 hr.

Supported hydrogel layer preparation: AGMA1-75: BAC (39 mg 0.197 mmol) was dissolved in doubly distilled water (66 µl) together with lithium hydroxide monohydrate (14.5 mg, 0.30 mmol). After the solution cleared, agmatine sulfate (11.20 mg 0.05 mmol) was added and dissolved. The mixture was allowed to react, in the dark and under nitrogen, for 24 hr at room temperature (20±5°C), then EDA (6.4 mg 0.09 mmol) was added just before casting. About 20 µl of the solution were cast on each pre-treated glass coverslip, using a Pasteur pipette, before spin coating them.

After deposition, samples were kept in a closed sterile container for 3 days at room temperature, to allow the cross linking reaction to proceed. Then they were retrieved, put each in a well of a multiwell plate and washed as described for the free hydrogels, each sample being soaked in 1 ml solution. 30 min after the last addition of water/ethanol mixture, the solution was removed, and replaced with 1 ml of doubly distilled sterile water. Samples were kept in water at 37°C overnight, rinsed in doubly distilled water and sterilized with UV-rays for ten minutes before use.

ISA23-75: The procedure was the same as reported above for AGMA1-75, using the following quantities: BAC (39 mg, 0.197 mmol) doubly distilled water (66 μl), lithium hydroxide monohydrate (8.25mg, 0.197 mmol), 2-methylpiperazine (5.0 mg 0.05, mmol), EDA (4.2 mg, 0.68 mmol).

Cell culture condition: Immortalized MDCK cells were cultured in Dulbecco's Modified Eagle's Medium, supplemented with 10% Fetal Bovine Serum, 2 mM L-Glutamine, 0.1 mM non essential amino acids, 1.5 g/l sodium bicarbonate, 1 mM sodium pyruvate, 100 units/ml penicillin and 100 μg/ml streptomycin. Cells were grown in tissue culture flasks at 37°C in controlled atmosphere (5% CO2). After achieving 70% of confluence into the flask, the cells were passed using Trypsin-EDTA solution and seeded at a concentration of 104 cells/well to 13 mm diameter round glass coverslips coated with AGMA1-75, ISA23-75 and to TCPS.

Cell adhesion, proliferation and morphology: We measured MDCK adhesion on AGMA1-75, ISA23-75 and TCPS and compared the results. The seeded cells were stored into a humidified incubator at 37°C. They were monitored every 30 min during the first four hours after cell plating, then every hour for the next 2 or 3 hr. Afterwards they were observed once a day until cells achieved confluence. Images from each sample were collected with a Power Shot G6 Canon digital camera mounted on a Zeiss Axiovert 40CFL inverted optical microscope using 10X objective lens. Four random fields from each sample were photographed and the number of cells both adhered and not adhered was counted to determine the percentage of adhesion, defined as:

Adhesion (%) = (number of adhered cells / total number of cells) x 100.

For the cell adhesion experiments in the presence of soluble AGMA1 or GRGD peptide, cells were seeded in culture medium supplemented with 1 mM AGMA1 (calculated on the repeating unit concentration), 10 mM AGMA1 or 1 mM GRGD. After 4 hr we calculated the inhibition of adhesion defined as:

Inhibition (%) = [1-(Adhesion (%)/Adhesion (%) in control condition)] x 100,

where Adhesion (%) in control condition is the result of cell adhesion on each substrate (TCPS, AGMA1-75 and ISA23-75) in medium without soluble AGMA1 or GRGD.

Results and Discussion

Previous papers had reported on the effect of agmatine-functionalized hydrogels on the adhesion of fibroblasts (Figure 1).

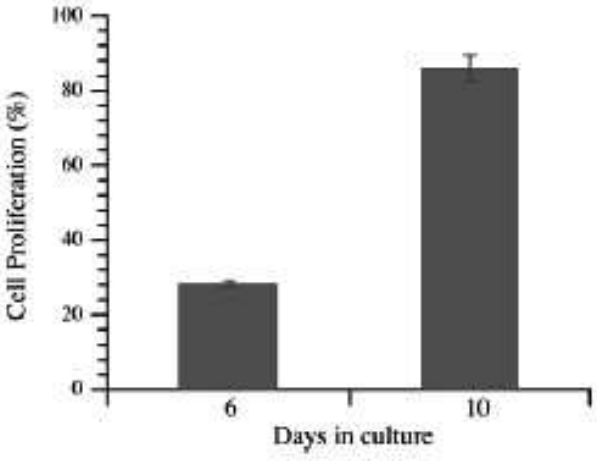

Figure 1. Effect of Agmatine functionalization on cell adhesion and proliferation for fibroblasts.

In our case, we decided to exploit the same functionalization to enhance the hydrogel adhesion of MDCK epithelial cells, in order to prepare a prototype supported device. The presence of a glass support would greatly enhance the hydrogel usefulness in the field of cell screening and molecular diagnostics.

For this reason we have designed, prepared and tested a new bi-layered system. This new system is composed by a glass support covered with a functional hydrogel layer. The glass substrate provides mechanically robust support and easier handling while the functionalized hydrogel layer interacts with the cells. Both glass support and hydrogel are optically transparent, as required for several cell characterization techniques, including optical microscopy.

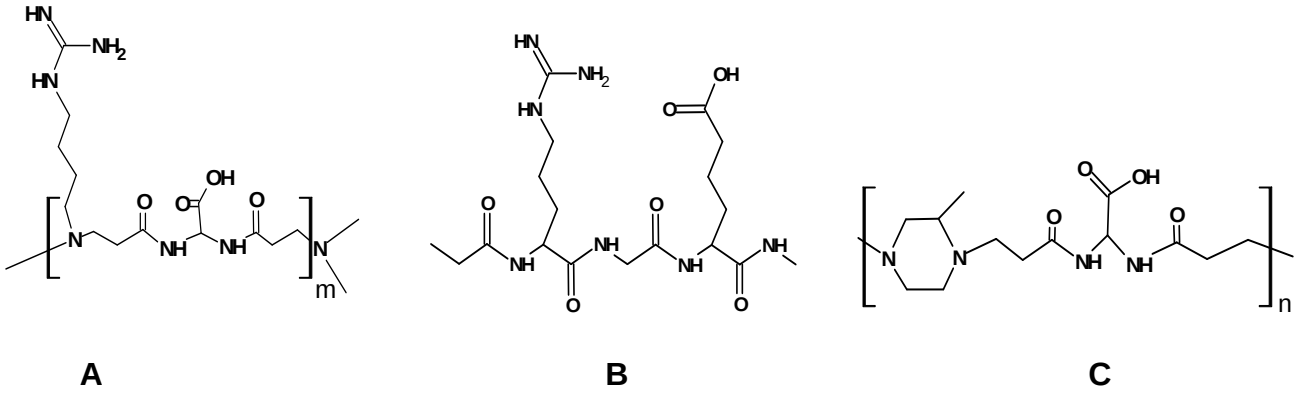

Figure 2. Structure of AGMA1 (A) and ISA23 (C) and the RGD peptide (B)

As pointed out in the introduction, in this study we chose to compare hydrogels based on two amphoteric PAA structures, AGMA1 and ISA23, both known in the literature as

highly biocompatible structures. The AGMA1 repeating units are very similar to the well known adhesion-modulating RGD peptide sequence. Figure 2 shows the repeating unit of AGMA1 polymers (A) and the structure of the RGD peptide (B). ISA23, not carrying any guanidine pendant group (structure reported in Figure 2C), can be used as a non-functional model, to rule out the effect of mechanical properties and overall surface morphology. Linear ISA23 polymers are known to be biocompatible[21,22] and their hydrogels show no significant cell adhesion properties.[29]

A semi-quantitative evaluation of the cell adhesion properties of these systems, in order to evaluate the best composition for cell adhesion was performed with different compositions. Results are reported in Figure 3.

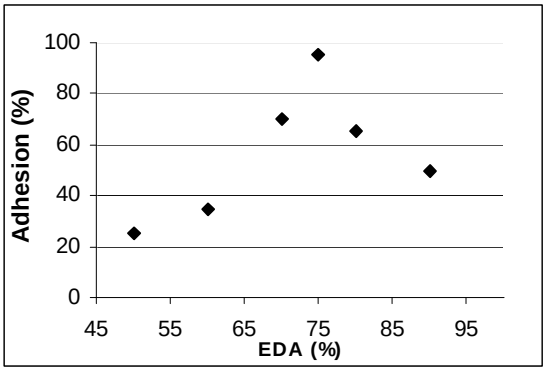

Figure 3. Cell adhesion behavior (normalized against TCPS) versus crosslinker content, given as moles ratio, that is (moles of EDA aminic hydrogens /moles of overall aminic hydrogens) x 100.

Interestingly, the best composition, which had 19% mol/mol crosslinker, and 12,5% mol/mol agmatine content has a composition similar to that of the samples found to be effective in the fibroblast tests (16,5 % mol/mol crosslinker content, 8,3 % agmatine).

Cell adhesion: After seeding 10000 cells in each well, the optical microscope showed round and pearly cells until they began to attach to the substrates. Up to 2 hr, cell adhesion on AGMA1-75 and ISA23-75 was not markedly different and adherent cells on both substrates are much less than on TCPS. At 4 hr cells on ISA23-75 were still few and showed the same morphology, whereas on AGMA1-75 the number of cells adhered to the substrate was similar to that on TCPS. At longer times, cells on TCPS start to proliferate and form clusters. On AGMA1-75, instead, cells proliferated slowly. This behavior becomes even more evident at 72 hr when cells seeded on TCPS have achieved confluence and begin to die. On AGMA1-75, instead, we still observe cell clusters without

confluence. This effect may be explained considering that despite the fact that PAA hydrogel layer were supported by a rigid material, cells probably experienced a more compliant substrate than TCPS. It generally recognized that focal contact formation and cytoskeletal assembly may be relatively more difficult on hydrogel surface, retarding cell growth.[30]

MDCK cells grown on ISA23-75 exhibited lower adhesion and slower proliferation than the AGMA1-75 and TCPS grown cells. However, after 48 hr, cells attached to some extent also on this substrate. This effect might be explained by the partial absorption of adhesive proteins from serum on to the hydrogel.

A quantitative evaluation of MDCK adhesion on substrates as a function of time showed that the adhesion had a quadratic trend on TCPS and AGMA1-75 whereas a linear trend on ISA23-75, as reported in Figure 4. The histogram shows that, up to 2 hr after seeding, cell adhesion on TCPS is higher than on hydrogels, while between 2 and 4 hr MDCK adhesion on AGMA1-75 increases remarkably compared to ISA23-75 until reaching an adhesion percentage similar to that on TCPS.

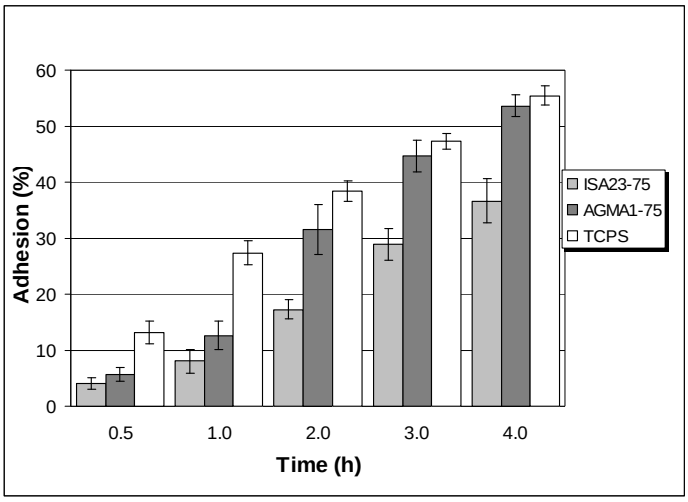

Figure 4. Cell adhesion vs time on the substrates examined: ISA23-75, AGMA1-75 and TCPS. The percentage of cell adhesion on ISA23-75 and AGMA1-75, is comparable in the first hour, and much lower than the adhesion on TCPS. After two hrs cell adhesion percentage on AGMA1-75 is higher than on ISA23-75 and similar to the value on TCPS.

Soluble AGMA-1 and GRGD similarly prevent cell-substrate adhesion: In order to confirm that the difference in cell adhesion on the Agmatine-functionalized hydrogels is due to its composition and not to other factors, such as non-specific serum protein adsorption, we tested the adhesion-inhibiting effect of soluble AGMA1 polymers and GRGD peptides.

The presence in the medium of a soluble polymer obtained by copolymerization of BAC and agmatine[23] up to a concentration of 1 mM in repeating units, proved to prevent cell adhesion on all the substrates (Figure 5).

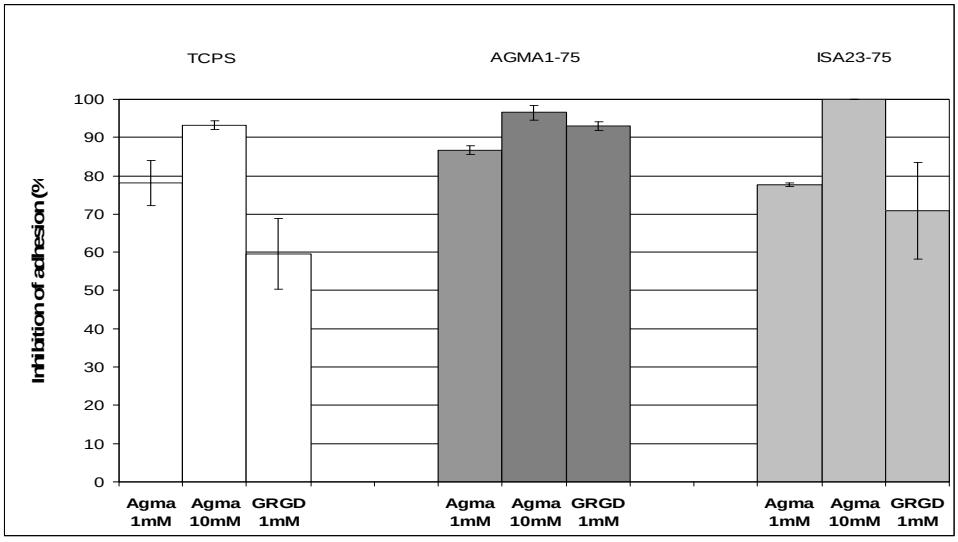

Figure 5. The presence of a soluble polymer bearing the agmatine-BAC sequence is able to prevent cell adhesion on all the substrates. 1 mM GRGD peptide and 1 mM AGMA1 (calculated on repeating unit concentration) have the same effect on cell adhesion inhibition; increasing the soluble polymer concentration to 10 mM does not increase significantly the inhibition of cell adhesion.

Increasing the AGMA1 concentration up to 10 mM did not significantly increase the inhibition of cell adhesion, suggesting that the interested receptors are already almost completely saturated at 1 mM AGMA1. Since 1 mM GRGD peptide and 1 mM AGMA1 (calculated on repeating unit concentration) have the same effect on cell adhesion inhibition, it can be reasonably concluded that both compounds bind the same integrin receptors.

Conclusions

Several possible applications can be envisioned for agmatine-functionalized PAA hydrogels. These results are a further step in this direction, showing how the cell-polymer interaction can be controlled by a simple chemical modification. Interaction with the cell receptors was confirmed, as well as biocompatibility, and a cell adhesion as good as that on TCPS for the epithelial MDCK cells.

Extending of these results on to other cell lines as well as further studies in the mechanics of the cell-AGMA1 interactions are ongoing. The growth retarding effect of the hydrogel

surface can also be interesting in order to apply these substrates to conservation and proliferation of stem cells.

Acknowledgements

This work was funded by the Italian MIUR, Cofin 2005 project. The grants of Elisa Emilitri and fabiana Guizzardi were funded by the Ingenio program of the Regione Lombardia and the European Social Found (Fondo Sociale Europeo).

References

[1] H. Shin, S. Jo, A.G. Mikos, *Biomaterials* **2003,** *24*, 4353.
[2] G. Tourniaire, J. Collins, S. Campbell, H. Mizomoto, S. Ogawa, J.F. Thabureta¸ M. Bradley, *Chem. Commun.* **2006**, 2118.
[3] C. Alexander, K.M. Shakesheff, *Adv Mater* **2006**, *18*, 3321.
[4] **G.** Krenning, P.Y.W. Dankers, D. Jovanovic, M.J.A. Van Luyn, M.C. Harmsen, *Biomaterials* **2007**, *28*, 1470.
[5] P. Krsko, M. Libera, *Materials Today* **2005**, *8*, 36.
[6] N. Satish, L.A. Lyon, *Angew. Chem. Int. Ed.* **2005**, *44*, 7686.
[7] U. Hersel, C. Dahmen, H. Kessler, *Biomaterials*. **2003**, *24*, 4385.
[8] T.G. Kim, T.G. Park, *Tissue Eng* **2006**, *12*, 221.
[9] T. Fumiko, N. Eisuke, *EMBO J*. **2007**, *26*, 1487.
[10] E. Ruoslahti, *Annu. Rev. Cell. Dev. Bi.* **1996**, *12*, 697.
[11] P.M.D.Watson, M.J. Humphries, J. Relton, N.J. Rothwell, A. Verkhratsky, R. Gibson, *Mol. Cell. Neurosci.* **2007**, *34*, 147.
[12] H.J. Kong, S. Hsiong, D.J. Mooney, *Nano Letters* **2007**, *7*, 161.
[13] S. Xu, C. Wang, X. Gu, Y. Duan, *PMSE Preprints* **2006**, *95*, 404.
[14] J.T. Connelly, A.J. Garcia, M.E. Levenston, *Biomaterials* **2007**, *28*, 1071.
[15] P. Ferruti, E. Ranucci, L. Sartore, F. Bignotti, M.A. Marchisio, P. Bianciardi, F.M. Veronese, *Biomaterials* **1994**, *15*, 1235.
[16] P. Ferruti, E. Ranucci, F. Bignotti, L. Sartore, P. Bianciardi, M.A. Marchisio, *J Biomat. Sci.-Polym. Ed.* **1995**, *6*, 833.
[17] R. Jain, S.M. Standley, M. Jean, J. Frechet, *Macromolecules* **2007,** *40*, 452.
[18] E. Emilitri, E. Ranucci, P. Ferruti, *J. Polym. Sci.–Pol. Chem.* **2005**, *43*, 1404.
[19] N. Lavignac, M. Lazenby, J. Franchini, P. Ferruti, R. Duncan, *Int. J. Pharm.* **2005**, *300*, 102.
[20] R. Annunziata, J. Franchini, E. Ranucci, P. Ferruti, *Magn. Res. Chem.* **2007**, *45*, 51.
[21] J. Franchini, P. Ferruti, *J. Bioact. Comp. Pol.* **2004**, *19*, 221.
[22] P. Ferruti, M.A. Marchisio, R. Duncan, *Macromol. Rapid Commun.* **2002,** *23*, 332.
[23] J. Franchini, E. Ranucci, P. Ferruti, M. Rossi, R. Cavalli, *Biomacromolecules* **2006**, *7*, 1215.
[24] P. Ferruti, J. Franchini, M. Bencini, E. Ranucci, G.P. Zara, L. Serpe, L. Primo, R. Cavalli, *Biomacromolecules* **2007**, *8*, 1498.
[25] P. Ferruti, S. Bianchi, E. Ranucci, F. Chiellini, A.M. Piras, *Biomacromolecules* **2005**, *6*, 2229.
[26] C.A. Shoenenberg, A. Zuk, G.M. Zinkl, D. Kendall, K.S. Martin, *J. Cell. Sci*. **1994**, *107*, 527.
[27] P. Ferruti, E. Ranucci, F. Trotta, E. Gianasi, G.E. Evagorou, M. Wasil, G. Wilson, R. Duncan, *Macromol. Chem. Phys.* **1999**, *200*, 1644.
[28] W. Lin, M.C. Garnett, M.C. Davies, F. Bignotti, P. Ferruti, S.S. Davis, L. Illum, *Biomaterials* **1997**, *18*, 559.
[29] P. Ferruti, S. Bianchi, E. Ranucci, F. Chiellini, V. Caruso, *Macromol Biosci* **2005**, *5*, 613.
[30] R.J. Pelham, Y.L. Wang, *P. Natl. Acad. Sci. USA* **1997**, *94*, 13661.

Quantitative investigation by atomic force microscopy of supported phospholipid layers and nanostructures on cholesterol-functionalized glass surfaces

Marco Indrieri[1,3], *Marco Suardi*[2,3], *Alessandro Podestà*[1,3,*], *Elisabetta Ranucci*[2,3], *Paolo Ferruti*[2,3], *Paolo Milani*[1,3]

1. Dipartimento di Fisica, Università di Milano, via Celoria 16, 20133 Milano, Italy.

2. Dipartimento di Chimica Organica e Industriale, Università di Milano, via Venezian 21, 20133 Milano, Italy.

3. CIMAINA, Centro Interdisciplinare Materiali e Interfacce Nanostrutturati, Università di Milano, via Celoria 16, 20133 Milano, Italy.

Title running head: Phospholipids on cholesterol-terminated surfaces.

Abstract

* To whom correspondence should be addressed. E-mail: alessandro.podesta@mi.infn.it.

Understanding the interaction mechanisms of phospholipids with surfaces is crucial for the exploitation of lipid bilayers as models of the cell membrane, as well as templates for biosensors. Moreover, controlling and manipulating single lipid nanoparticles for the investigation of their properties by means of single-particle sensitive surface techniques require the ability to tailor the chemical properties of surfaces in order to achieve stable and sparse binding of lipid particles, while keeping them from aggregating, or denaturing. Here we present a quantitative morphological and structural investigation by Atomic Force Microscopy of supported phospholipid layers and nanostructures on cholesterol-functionalized glass surfaces, in comparison with other surfaces with different interfacial properties. We show that functionalization of glass coverslips with cholesterol groups is a viable route for the production of optically transparent, scanning probe microscopy - compatible clean substrates, for the effective immobilization of both extended single lipid bilayers, and lipid nanoparticles.

Nanostructured self-assembling poly(amidoamine) conjugates bearing disulphide linked cholesterol pendants

Elisabetta Ranucci, [†‡]* *Marco A. Suardi,* [†‡] *Rita Annunziata,* [†] *Paolo Ferruti* [†‡], *Federica Chiellini*[§], *Cristina Bartoli*[§]

[†]Dipartimento di Chimica Organica e Industriale, Università di Milano, via Venezian 21, 20133 Milano, Italy

[‡]CIMAINA, Centro Interdisciplinare Materiali e Interfacce Nanostrutturate, via Golgi 19, 20133 Milano, Italy.

[§]Laboratorio di Materiali Polimerici Bioattivi per Applicazioni Biomediche ed Ambientali (BIOlab) – UdR INSTM – Dipartimento di Chimica e Chimica Industriale Universita' di Pisa– Via Vecchia Livornese 1291, 56122 S. Piero a Grado (Pisa), Italy

* Corresponding author. E-mail: elisabetta.ranucci@unimi.it Telephone: 0039 02 50614132. Fax: 0039 02 50314129. Postal Address: Prof. Elisabetta Ranucci, c/o Dipartimento di Chimica Organica e Industriale, Università di Milano, via Venezian, 21, 20133 – Milano, Italy

ABSTRACT

Poly(amidoamine) (PAA) networks obtained using cystamine as cross-linking agent on reaction with 2,2'-dithiodipyridine turn into linear PAAs with side dithiopyridyl groups that easily undergo exchange reaction with thiocholesterol. The resultant products represent the first examples of amphiphilic PAA–cholesterol conjugates in which lipophilic cholesterol moieties are linked to the hydrophilic PAA chain by S–S bonds stable in blood, but cleavable inside cells. These conjugates self-assemble in aqueous media into nanoaggregates whose inner core consists of lipophilic cholesterol domains. A series of PAA-cholesterol conjugates deriving from two different bis-acrylamides, namely 2,2-bis(acrylamido)acetic acid and 1,4-bis(acryloyl)piperazine, and with different cholesterol content were obtained. All products were characterized by ^{1}H and ^{13}C NMR spectroscopy and the average molecular weights of the soluble polymers determined by size exclusion chromatography. In all instances, the segregation of cholesterol residues from the aqueous medium was revealed by the comparison of their NMR spectra in $CDCl_3$ and D_2O, respectively. The TEM analysis of the PAA-cholesterol aggregates in aqueous buffers revealed homogeneous round-shaped nanospheres, whose average dimensions and dimensions distribution were determined by DLS. Preliminary cytocompatibility tests demonstrated that all prepared PAA–cholesterol samples are cytobiocompatible, thus showing potential for biotechnological applications.

Keywords: poly(amidoamine)s, cholesterol, bioactive and biocompatible polymers, disulfides, nanostructured polymers, amphiphilic polymers